The Journal of the Indian Association of Sedimentologists

Volume 36 No. 1 2019

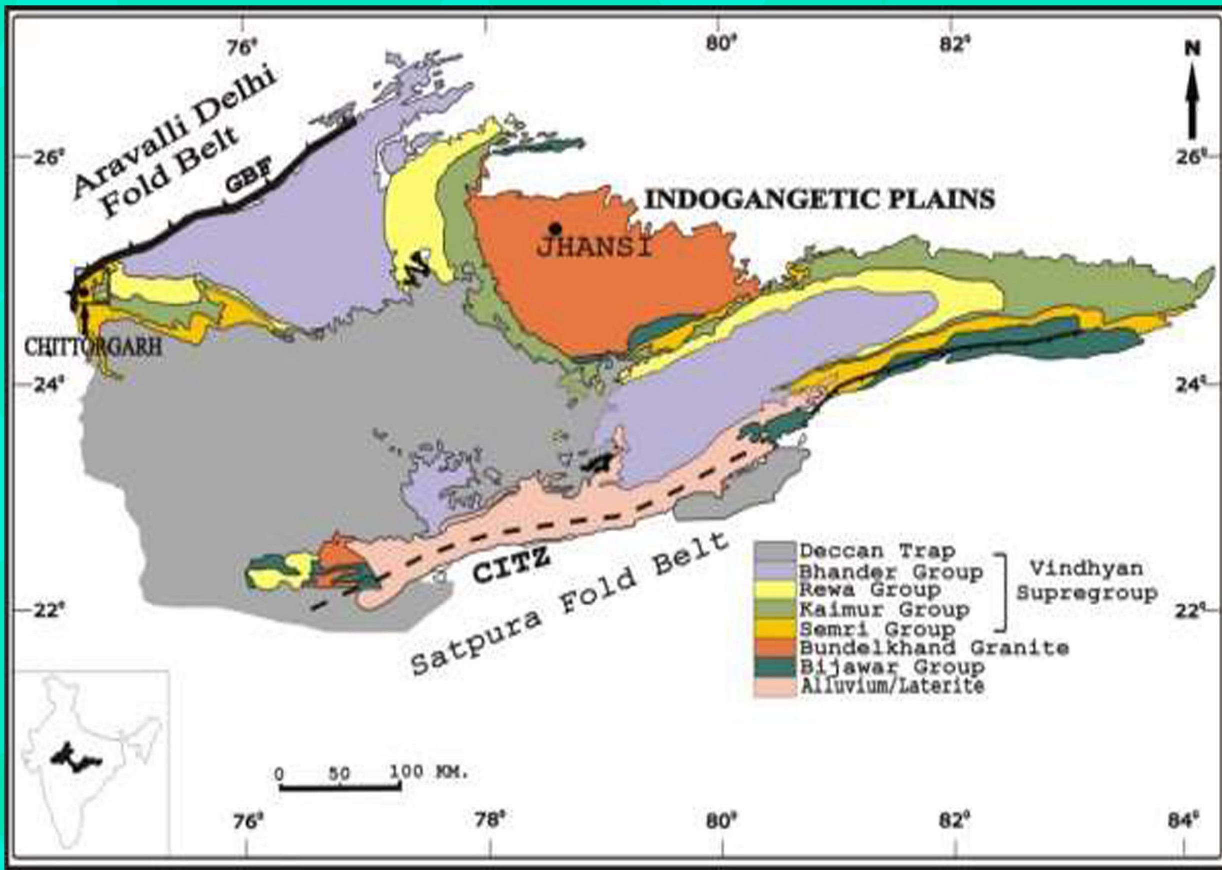

Geological Map of the Vindhyan Basin, modified after Prasad and Rao (2006)

Jour. Indian Association of Sedimentologists, Vol. 36, No. 1 & 2 (2019), pp.3-18
ISSN Online 2582 – 2020
ISSN Print 0970 – 3268

Facies variation in a half graben tectonic model: case study from Kolhan Basin, Jharkhand-Orissa

Rohini Das[1] and Subhashish Das[2]
Department of Geology and Geophysics, IIT Kharagpur, PIN: 721302, India
Rohini Das, Department of Geology and Geophysics, IIT Kharagpur, PIN: 721302, India.
E-mail romiyadas@gmail.com

Abstract: The pear shaped Kolhan Group in the studied sub-basins of Chaibasa–Noamundi and Chamakpur-Keonjhar is usually represented by a sequence of thin and discontinuous patches of basal conglomerates with sandstone and shale (±carbonate). Six lithofacies have been observed in the area. This fining upward sequence alongwith the vertical and lateral facies variation in the Kolhan implies superimposition of retrograding shorelines on an earlier prograding alluvial fan sand complex. The variations in the size parameters are indicative of changes in the water depth and the velocity at the time of sediment deposition. The basin is thought to evolve as a half-graben under the influence of an extensional stress regime. This assumption of a tectonic setting for the NE-SW trending Kolhan basin can be related to the basin opening as a consequence of E-W extensional stress system that prevailed during the development of the Newer Dolerite dyke. The half-graben development and fault growth evolve differently through time and produce different basin-filling patterns. In the initial stage the basin evolution can be explained by detachment type half-graben filling model that incorporates a basin-bounding fault soling into a sub-horizontal detachment fault. Two types of genetic sequences reflecting variations in the generated accommodation space have been recognized within the sub-basins of Chamakpur-Keonjhar and Chaibasa-Noamundi. The lower sequence in Chamakpur-Keonjhar is characterised by shallow braided river deposits that lack repetitive facies patterns and were deposited during a period of the slower rate of fault growth and generated accommodation space. During the fault growth stage the Kolhan basin grew both wider and longer through time as the basin-bounding faults lengthen and displacement accumulated as evident in the sub-basin of Chaibasa –Noamundi. Younger strata consistently pinch out against older syn-rift strata rather than pre-rift rocks in the later fault-growth stage. The basin fill thus commonly forms a fanning wedge during fluvial sedimentation, whereas lacustrine strata tend to pinch out against older syn-rift strata. The fluvial strata progressively onlap the hanging wall block, whereas the lacustrine strata pinch out against older fluvial strata at the centre of the basin but onlap along the lateral edges. The transition from fluvial to lacustrine deposition and hanging wall overlap relationships are thoroughly observed in the sub-basins of Kolhans.

Keywords: half-graben, fan-delta lacustrine, braided-ephemeral

Introduction:

It covers an area around 800 sq. km along the western margin of Singhbhum Granite. It intervenes the Singhbhum granite to the east and the Iron Ore Group of rocks (IOG) to the west (Saha, 1994). It is one of the youngest and the least studied Precambrian stratigraphic unit in Singhbhum geology (Mukhopadhyay, 2001; Saha, 1994). The Kolhan basin is a time transgressive shale dominated supracrustal succession (shallow epicontinental) set in a passive continental rift setting, and caused due to the fragmentation of the Columbia supercontinent. The succession is represented by a sequence of subarkose-quartz arenite with lenses of conglomerate overlain by extensive thick shale-limestone package and show a non-cyclicity in the sedimentation history.

The depositional environment of the Kolhans varied from braided fluvial-ephemeral pattern to a fan-delta-lacustrine type. Previously, no such inference about the tectonic evolution of the basin has been drawn. Few workers from Geological Survey of India like Mazumdar(1996) has suggested the half-graben model for Kolhan supported by Acharya,1984; Bandhopadhaya and Sengupta,2004; Roy and Bhattacharya,2012. Half-graben has certain unique sedimentation pattern (Schlische 1991). The aim of the present paper is to fit the sedimentation pattern with a half-graben tectonic model of Kolhan (Roy and Bhattacharya, 2012).

Geological Setting of Kolhan Basin

Jones (1934) stated the members of the Kolhan Group as part of his Iron Ore Series. Dunn (1940) coined the term ‘Kolhan Group’ for a sequence of un-metamorphosed sedimentary formation overlying the Singhbhum granite. The geological map of the Kolhan basin Fig. 1 shows various lithologic units of the Singhbhum craton with the Kolhan Group being the younger. The various stratigraphic units according to Saha (1994)are (a) Older Metamorphic Group (OMG) (b) Older Metamorphic Tonalite-gneiss (OMTG) (c) Singhbhum granite Phase II and Phase III (d) Iron Ore Group {shales, tuffs, phyllites, banded iron formation (BIF), banded hematite jasper (BHJ), banded hematite quartzite (BHQ), sandstone, and conglomerate} (e) Jagannathpur and Malangtoli lavas, and (f) Kolhan Group. The structure of the Kolhan basin is controlled by the trend of the Iron Ore synclinorium (Saha, 1994). There is also a strong asymmetry in the basin architecture that has given rise to lithofacies variations within the Kolhans.

The area of study is concentrated in the two sub-basins of Chamakpur - Keonjharh and Chaibasa-Noamundi respectively. The two sub-basins have a general NE-SW trend with a faulted contact with the Iron ore Group and to the west and unconformity with Singhbum Granite. The Chaibasa-Noamundi basin extends from Chaibasa (85^0 48' – 22^0 33') in the north to Noamundi (85^0 28′ – 22^0 09′) in the south (length: 60-80 km; width: 8-10 km). The Chamakpur - Keonjhargarh (Long. 85°20'-85°35' E ; Lat. 21°35'-22°10' N) on other hand covers an area approximately 375 km2 (length : 50-55 km ; width : 6-8 km).

Materials and Methods

Fieldworks were carried out to describe and characterize the lithounits of the Kolhan basin from Chaiabasa to Chamakpur. At each exposure, the different lithounits were studied and were identified on the basis of their bed geometries, gross lithologies, and sedimentary structures. Fence diagram

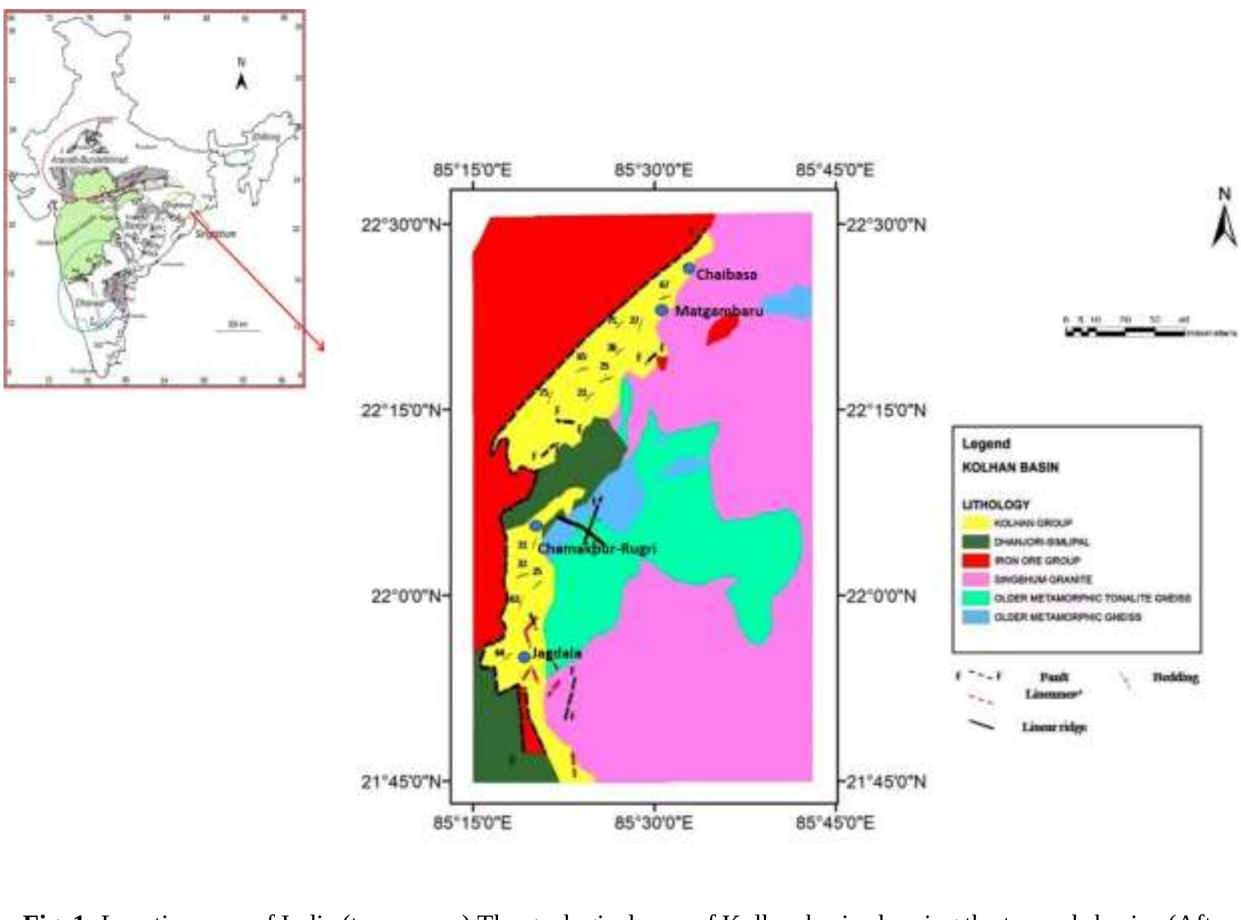

Fig. 1: Location map of India (top-corner).The geological map of Kolhan basin showing the two sub-basins (After Saha, 1994).

was prepared based on the litho-log data using ROCKWORKS16 for the two-sub-basins. The sedimentation pattern of the Kolhan basin was correlated with a half graben model. A predicted Depositional Model correlating the two sub-basins sedimentation history was prepared based on this using CANVAS 8 software.

RESULTS

Lithofacies analysis of Kolhan sandstone

The lithofacies analysis based on the field descriptions has been done for assessing the sediment depositional framework and the environment of deposition. The detailed examination of outcrop patterns along with the variations in the sedimentary structures appears to be the most effective means for analyzing and interpreting the stratal geometries and the depositional history. The architectural elements used in the present study are the field stratal characteristics, primary sedimentary structures, textures, fabrics of the lithofacies and their geometrical relationships (Miall, 1985, 1996).

Granular lag facies (GLA)

Granular lag facies, overlying the Singhbhum granite, is reddish brown in color and moderately to poorly sorted, with presence of subrounded to rounded pebbles of chert, vein quartz, phyllite and jasper. It is characterized by the occurrence of laterally impersistent, massive, matrix supported conglomerate which is oligomictic in nature towards south and polymictic towards north of the basin. These conglomerates are mostly immature to sub-mature, and quite similar to the overlying sandstone. This fine matrix-supported GLA facies can be the product of a more or less laminar, cohesive flow of relatively dense, sediment –fluid mixture of plastic behavior. Clasts float on the debris as a result of small density variation between the clasts and the debris, plus the cohesive strength of the clay-water slurry (Rodine and Johnson, 1976).

Granular sandstone facies (GSD)

The GSD facies is identified by reddish brown to brown color granular sandstone overlies the GLA facies (Fig.3.6B). This facies is characterized by moderately to well sorted, moderate clast: matrix ratio, textural bimodality and development of normal grading. Planar cross-stratification is more commonly found in compare to trough cross-stratification (Fig. 2B, 3a).

Sheet sandstone facies (SSD)

The SSD facies is characterized by sheets of subarkose-quartz arenite with occasional intercalations of thinly laminated siltstone. The facies shows abundant development of planar cross bedding and locally developed herringbone cross-bedding (foreset dips NNE). Paleo-current data was measured from this cross-beds (Fig.2A).This facies forms the dominant type among all the other facies. Sandstone beds in this facies tend to be sheet like with almost constant bed thickness.

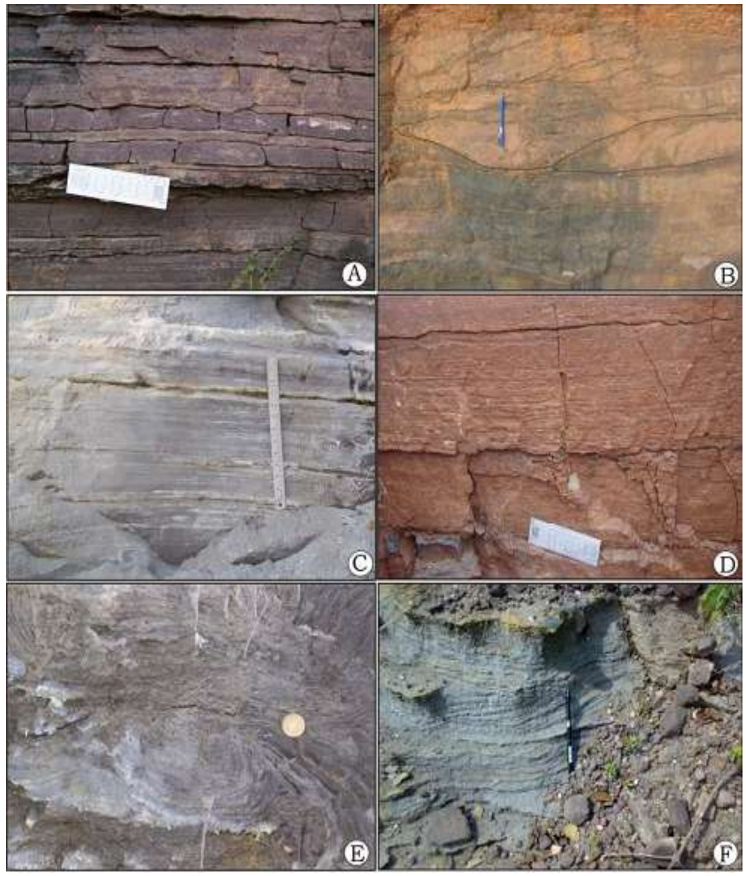

Fig. 2: (A)Sheeted sandstone facies location Bistampur, Scale: 12cm. (B) Cross bedded unit with multiple toe scour like structure locationGumua Gara river section, Scale: Pen, 12cm. (C) Rhythmic sandstone with alternate layers of sand and mud with thicker sand layer, location-Bistampur, Scale: 30cm. (D) Thinly laminated sandstone at Matgamburu, Scale: 12cm (E) Convolute lamination in rhythmic sandstone, 2.5cm diameter coin for scale, (F) planar cross bedding in rhythmic sandstone, location Bistampur, Scale: Pen,12cm.

Plane laminated sandstone facies (PLSD)

The PLSD facies is typically defined by well sorted subarkose-quartz arenite, with a moderate - high grain: matrix ratio. The sandstone is medium to fine grained. The dominant structures are planar cross bedding, wavy lamination, washed out/flat top ripples, herringbone cross-bedding (foreset dips NNE) and antidunes (Fig. 2C, D, F and 3d)

Rippled sandstone facies (RSD)

This facies is identified by profuse development of both symmetrical and asymmetrical ripples interference ripple, herringbone cross-bedding (foreset dips north westerly) (Fig.3b-c., Fig. 3 e-f), hummocky cross-stratification and multiple toe scour like structures .It is generally associated with thinly laminated sandstone facies and plane laminated sandstone facies. The wavy lamination beds occur with thin ripple laminated shale parting between two successive beds. Sandstone beds in this facies tend to be sheet like with almost constant bed thickness.

Thin laminated sandstone facies (TLSD)

This facies is characterized by the rhythmic alternation of sandstone and shale units (fig. 3.46F), in which sandy layers are thicker than shale layers.Prominent structures are convolute lamination, planar cross bedding and asymmetrical ripples (Fig.2D.).

Kolhan Shale:

The unmetamorphosed Kolhan shale sequence is more than 200 m thick, plane laminated with reddish brown colour. The Shale beds are composed of repeated alterations of very thin to thin plane bedded shale and subordinate amount of calcareous shale and siltstones. Kolhan shale is reported to be devoid of any Siliciclastic / carbonate components. The shale beds are commonly 2 cm to 8 cm thick and internally laminated.

Kolhan Limestone:

The Kolhan Limestone is impersistent and occur as patches in the shales. It is best developed towards SW of Chaibasa, near village Rajanka and Kondra and N and NW of Jagannathpur. In all these places the minimum thickness attained is nearly 20 ft. and the maximum is 65 ft. (Rajanka). The limestone can be divided into a white to pale grey, pink and pale green lower horizon consisting of thick bedded

Fig. 3 (a): Tabular cross-bedding in GSD facies characterized by parallel foreset laminae draping down between two layer parallel sets. Brunton for scale Location : Chamakpur (b-c) Exhumed Trough cross-stratifications (RSD facies).Scale Brunton Location : Surgutaria. (d) Climbing ripples with distinct migration and upbuilding of internal sediment laminae (PLSD facies). Brunton for scale. Location: Jajang (e) Mud flasers and laminated mud occurring as draped surface over ripple forms (RSD facies). Brunton for scale Location : Inganijoan. (f) Trough cross-stratifications separated by a thin erosional surface (RSD facies). Brunton for scale Location : Surgutaria rock traversed by calcite-quartz veins in which rhombohedral calcite and partly euhedral transparent quartz crystals are developed. The darker upper horizon has a foliated nature caused by parallel chloritic laminae.

Chamakpur Keonjhar Sub-Basin Depositional Environment and Facies Association

Braided fluvial plain facies association

The granular lag (GLA) and granular sandstone (GSD) facies are a part of shallow braided fluvial plain facies association. These two facies were formed in fluvial channels and bars in braided streams that gradually fanned outwards. This led to the gradual avulsion of the braided streams. The braided stream deposits gave way to the deposition of sheet-like deposits, where the process of recycling of sediments started in conjunction with the related hydrodynamic factors. The evidences in support of the braided stream are:

- Presence of lenticular or wedge shaped bed geometry (wedge thickness increases downslope) showing a transition from ortho conglomerates to granular sandstones and oriented approximately parallel to the paleo-strike of the basin.
- Elliptical pebbles oriented normal to the paleocurrent directions are rare. Presence of angular grains and abundance of rock fragments suggest a short transport from the source area. The coarsest deposits at the base of the channel are those carried in the thalweg (Allen, 1982) in between the sand bars. Local coarsening upwards sequence indicates a rapid shifting of the braided streams (channel avulsion) during deposition (Collinson, 1996).
- Where the bar is gravelly, the deposits consist of cross-stratified granules, pebbles or rarely cobbles in a single set. Where the bar is sandy, stacked sets of subaqueous dune deposits have been observed, that form a succession of cross-bedded sands whose top surface is occupied by finer sands and silts, representing the abandonment of the bar.
- Presence of local fining and coarsening upward sequence that reflect a low fluctuation in the basin tectonism and a changing scenario in the climatic condition at the time of deposition. Presence of

unidirectional (with occasional cross-paleocurrent) patterns and channel scours that suggest braided fluvial sedimentation.

- Presence of laterally intercalated, well sorted, coarse - medium - fine grained, trough cross-bedded, planar cross-bedded, and flat-bedded units suggest a rapid fluctuation in sediment supply.
- Presence of irregular boundary between the coarse and the fine grained sediment layers frequently marked by channel scours. Trough and planar cross-beddings are common structures developed as a result of the lateral and downstream advance of a mid-channel bar that finally coalesced into the adjacent branch channel.

Ephemeral Sheet Flood Facies Association: The association of sheet sandstone (SSD), plane laminated sandstone (PLSD), rippled sandstone (RSD), and thin laminated siltstone-sandstone (TLSD) facies are typical ephemeral sheet flood facies (Miall, 1996). The evidences in support of this facies association are:

- The lower part of the sheet sandstone facies is characterized by trough and large scale high angle (foreset dip 20-28 degree) planar cross-bedding almost at right angles to the elongation of sand bodies.
- The upper parts of the sheet sandstone and the plane laminated sandstone facies are characterized by both low angle frontward and high

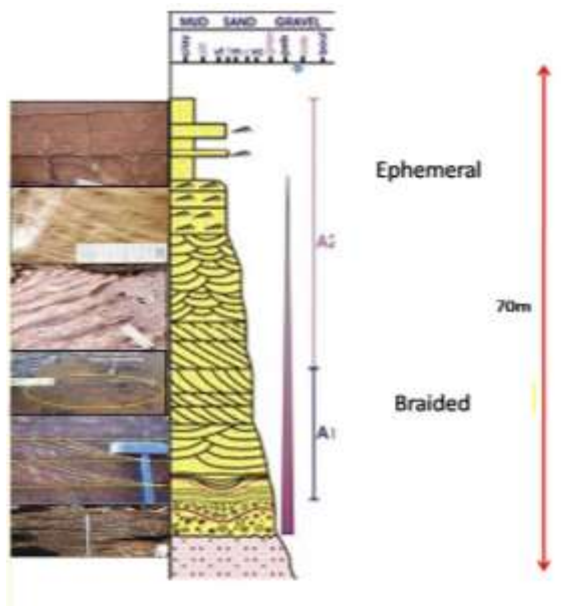

Fig.4: Composite log of the Chamakpur-Keonjharh Basin showing the sedimentary structures in each facies and the braided ephermal vertical succession

angle backward cross laminations, asymmetrical ripples, isolated lunate and linguid megaripples, and antidune cross-stratifications.

- Reactivations of erosional surfaces are often marked by thin granules and pebble layers.

- Subhorizontal parallel laminations with occasional shale chips and landward climbing-ripple laminations are also prevalent in the plane laminated sandstone facies.
- Presence of antidune cross-stratification and climbing-ripple laminations are indicative of rapid sedimentation under high suspended load (Clifton, 1969). A possibility is there of the existence of a cross-channel and transverse movement of sand bodies as transgressive sheet sands (Swift et. al., 1971; Johnson, 1975).

Chaibasa – Noamundi Sub-Basin Depositional Environment

Fan Delta Lacustrine Type: Fan-deltas are deposited immediately adjacent to highland region, usually a fault-bounded margin, and occupy a relatively a narrow space between highland and a standing body of water of shallow depth (Mc.Pherson.et.al. 1987). The geological set-up of Chaibasa-Nomundi fits the definition. The evidences in support of this are as follows (Fig 5):

- Presence of fine - medium grained, well sorted quartz rich sandstones (RSD) frequently interbedded with thin laminated siltstone-sandstone (TLSD) resemble heterolithic facies. The variability of sedimentary structures in the facies associations reflects rapid fluctuations in the supply of sediments. Records of low energy suspension fallout in the TLSD facies, presence of asymmetric ripples on the top surface of the fine-grained sandstones, and mud cracks in the TLSD facies indicate a low energy, suspension fall out during the waning phase of the sedimentation.
- Cross-laminations, antidunes, and supermature quartz arenite indicate sedimentation recycling. The sediments have been transgressed by the continuous lateral and transverse shifting of longitudinal bars that resulted in the development of sheet flats and transgressive sand sheets.
- Presence of scoured surfaces with granule layers in the GSD and PLSD facies, diffused nature of the contact between RSD and TLSD facies, and poor linkage between SSD, PLSD, and RSD facies indicate a rapid sedimentation in the upper reaches of the stream (Allen, 1982).

The Kolhan succession starts with a basal conglomerate, which is thin, laterally impersistent and becomes more and more

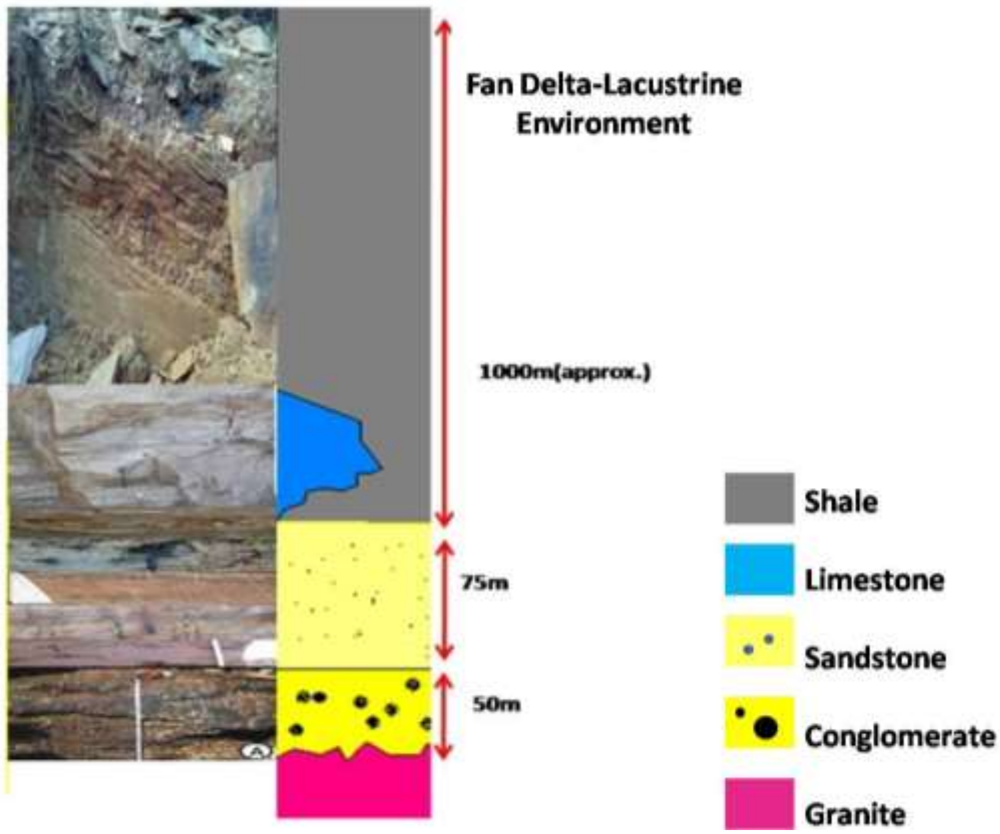

Fig. 5: Composite log of the Chaibasa-Noamundi Basin showing the sedimentary structures in each facies and the fan-delta lacustrine vertical succession.

oligomictic to the South, with the dominance of chert and jasper pebbles. Pebbles of granite and quartz are common in the somewhat polymictic types developed towards the north. The Conglomerate are mostly sub mature to immature, devoid of structure, with a matrix very similar to the overlying sandstones with which they show a highly transitional contact and wedge shaped geometry. The dominance of iron and argillaceous matter is often observed and the rapid conversion of shale from calcareous to argillaceous to ferruginous is an indicator of its non-marine nature. Presence of herringbone cross-bedding washed out ripples and occurrences of rhythmic sandstone (tidal bedding) are the evidences of tidal activity. The patches of limestone present confirms it to be of non-marine body. The sudden huge thickness of shale can be attributed to the landlocked nature of the basin.

The shallowness of the basin is indicated by the general development of thin sequences of rocks, while the stability and generally subdued morphology of the source area is suggested by the slow transport of detritus containing very little fresh feldspar grains by the sluggish streams contributing sediments in moderate amount to the Kolhan sea of the epicontinental type.

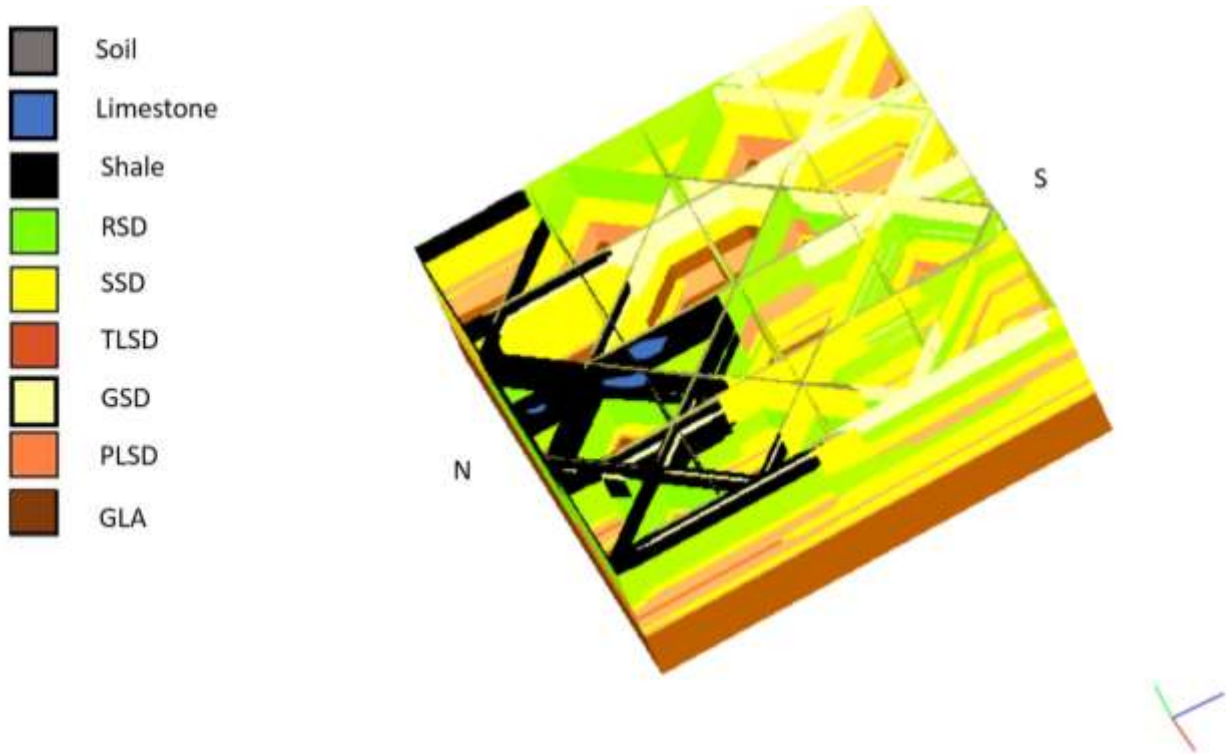

Fig.6: Fence diagram showing facies variation across the Kolhan basin

DISCUSSION

Half-Graben Basin Filling Model

In the initial stage the fault model incorporates an intrabasinal fault that soles into a sub-horizontal detachment fault; the change in the rate of increase in the volume of the basin during uniform fault displacement is zero. (Detachment type). (Fig.7a)

Both basin-bounding faults, intrabasinal faults and the intervening fault blocks rotate during extension and as a consequence, there is a change in the rate of increase of the volume of the basin.(domino type). (Fig.7 b)

During the fault growth models, the Kolhan basin grew both wider and longer through time as the faults lengthen and displacement accumulates; the change in the rate of increase in basin volume is positive. (Fig.7c). Basin fill commonly forms a fanning wedge during fluvial sedimentation, whereas lacustrine strata tend to pinch out against older synrift strata.

The transition from fluvial to lacustrine deposition and hanging wall onlap

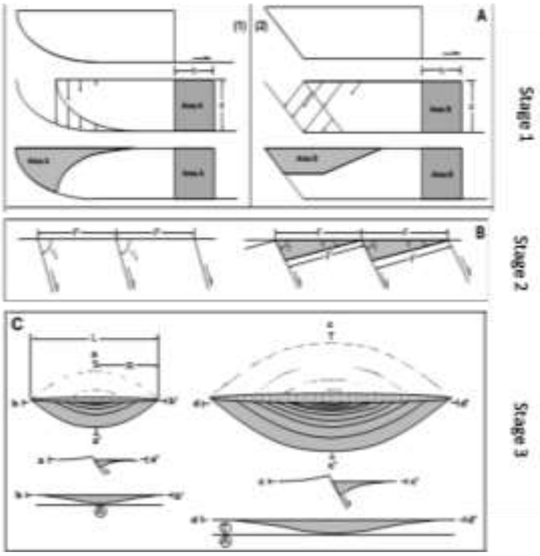

Fig.7: Illustration of half-graben basin-filling model.(A) Planar fault geometry (taken for simplicity) where there is horizontal displacement (h) on the detachment fault (B) domino fault block model in which both the faults and the intervening fault blocks rotate during extension. i is the initial dip angle of the faults; is the dip after extension; is the dip of a horizon that was horizontal before extension; F' is the initial fault spacing; F is the fault spacing after extension. (C) Essential elements of the fault growth model. All the 3 end member half-graben basin- filling models are applicable in various stages of the basin evolution. Modified from Schlische (1991).

relationships observed in the individual basins of Kolhans are best explained by these basin filling Models (Fig 8) (Schlische 1991; Schlische and Anders, 1996; Gui .et.al., 2014).

The compositional characteristics of the fluvio-deltaic deposits attest to the reworking of a sandstone- and conglomerate-bearing sequence in the source area. Therefore, the overall style of sedimentation suggest a switchover from low sinuous avulsed channels developed within an overall fluvial ephemeral streams to a delta complex under a warm humid climate system. This switchover also accounts for the carbonate platformal dominated sedimentation during the basinal closing phase. The location of half-graben development during a syn-Kolhan extensional regime is likely to have been reactivation along the Singhbhum shear zone (SSZ). Cratonic sutures such as the SSZ may have been prone to reactivation during any

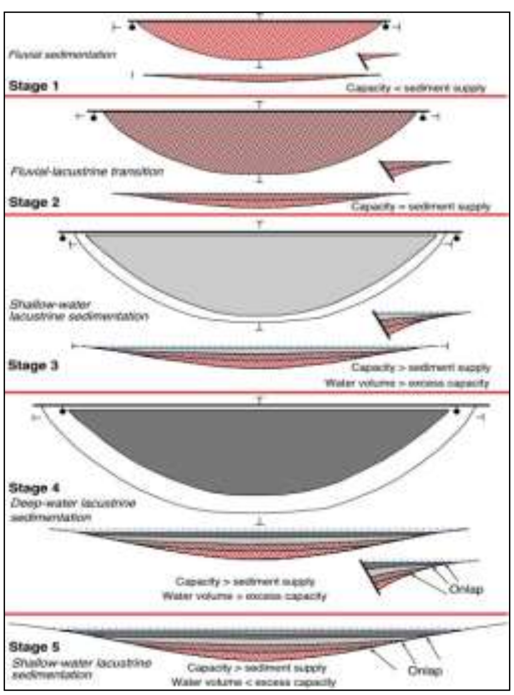

Fig.8: Filling of an evolving half-graben basin shown in map view alongwith longitudinal cross section, and transverse cross section. Dashed line represents lake level. The relationship between capacity and sediment supply determines whether sedimentation is fluvial or lacustrine. For lacustrine sedimentation, the relationship between water volume and excess capacity determines the lake depth. Modified from Schlische and Anders (1996).

subsequent tectonic episodes, leading to complex structural and sedimentological relationships as basins are created, inverted and superimposed along a long-lived shear zone throughout successive tectonic regimes (Deb and Chaudhuri, 2007). The tectonism responsible for sedimentation and deformation of the Kolhans may be related to a ca. 2.0-2.2 Ga tectonic event or by intra-cratonic reactivation of structures within a previously assembled greenstone belt. This establishes a sequence of tectonic regimes of north–south orientated compression, tectonic quiescence, denudation and north–south orientated extension, following the 2.0 Ga event in the Singhbhum region. The syn north–south orientated extension in the region may have been related to orogenic collapse of the Singhbhum shear zone (Roy and Bhattacharya, 2012). The equivalent basins of the Kolhans is the Mankarchua basin falling north of Pala Lahara (21°26': 85°11') has also been included within Kolhans by Saha(1994). It shows a faulted and sheared contact with the Pala Lahara gneiss in the south and an unconformable contact with the Malangtoli lavas in the north. Sarapalli- Kamakhyanagar (20°58': 85°35') basin has also been identified by (Saha, 1994) as another Kolhan basin. It extends for about 100 km in an east -west direction. The width of the basin is about 3km. Cross- bedded ortho-quartzite and cherty quartzite dipping steeply southward represents the dominant lithology in this basin. Near Kamakhyanagar, the quartzite is in contact with the metasediments of the Iron Ore Group.

However, it is prudent to restrict the Kolhan Group of rocks to the main Kolhan basin with its typical assemblage of Sandstone-limestone-shale /phyllite assemblage rather than sandstone/sandstone-shale or only as shale/clayey rock (Tarafdar et. al., 1974) association overlying other rocks as equivalent of Kolhans, which is present either as isolated bodies over Singhbhum granite or as outliers elsewhere in this part of eastern India.

CONCLUSION

General models for sedimentation in half-graben set-up incorporate large-scale alluvial fans as indicated by GLA-GSD-SSD-RSD-PLSD facies, entering the half-graben from the low-gradient footwall. Significantly, the model predicts a contrasting facies change between the transverse alluvial fans and the major longitudinal trunk rivers flowing along the axis. The presence of lacustrine-related facies within the Kolhans proves significant development of lake sedimentation caused

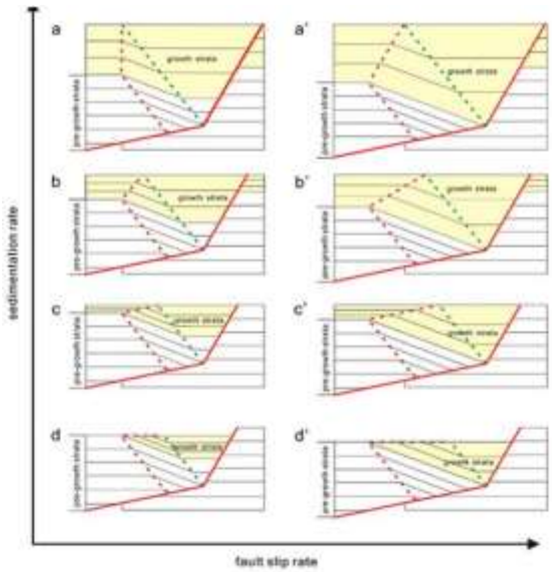

Fig. 9: Variation of sedimentation and fault rate that occurs in a half-graben set-up (After Gui *et.al*. 2014)

by interior drainage within the half-graben. The Kolhan serves as an example of sedimentary response to changing tectonic regimes associated with the SSZ (Fig. 9). Facies variation in a basin supports a hypothesis for two-stage development of the half-graben. In the initial stage, an irregular east-tilted half (Fig. 10) graben was formed by high-angle faulting on cratonic basement reactivated structures. In the later stage, movement began on the fault system, and the Iron Ore Group rose rapidly. In the process, the northern basin reversed its half-graben tilt to westward.

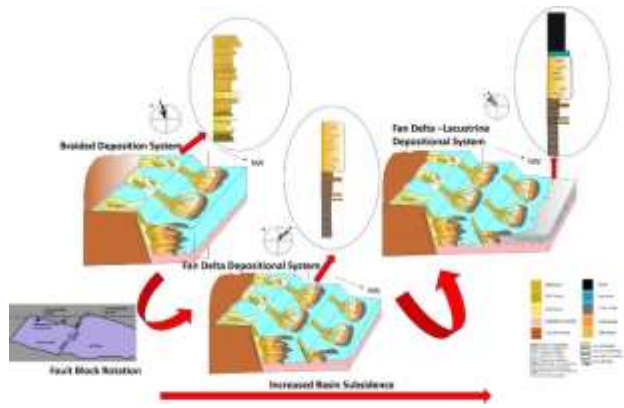

Fig. 10: Tectono-Sedimentary Model of Kolhan (The fault block rotation is denoted by schematic Diagram showing domino type fault which rotates during progressive extension. The fulcrum is the position where displacement of the hanging wall block is zero; either the limit of roll-over in isolate tilt block/half-grabens or the transition from areas of the hanging wall undergoing positive motion due to footwall uplift to areas undergoing negative).

Acknowledgement

The author is grateful to Head of the Department of Geology and Geophysics, IIT Kharagpur for providing opportunity to carry out the research and field work.

References

Acharya, S.(1984), Stratigraphy and structural evolution of the rocks of Iron Ore basin in Singhbhum, Orissa Iron Ore province: Indian Journal of Earth Science, Seminar Volume on Crustal Evolution of Indian Shield and its Bearing on Metallogeny,p.19-28.

Allen, J.R.L. (1987), *Sedimentary Structures*, Their Character and Physical Basis. Elsevier, Amsterdam, p.515- 645.

Bandhopadhaya, P.C. and Sengupta, S. (2004), Paleoproterozoic Supracrustal Kolhan Group in Singhbhum Craton, India and the Indo-African Supercontinent: Gondwana Research, v.7, p.1228-1235.

Clifton, H.E. (1969), Beach lamination: nature and origin: Marine Geology, v.13, p.607–610.

Collinson, J. D. (1996), Alluvial Sediments, in Reading, H. G. (eds.), Sedimentary Environments-Processes, Facies and Stratigraphy, Blackwell Publication, Oxford, p.37-82.

Deb,S.P. and Chaudhuri,A.K.(2007), A retreating fan-delta system in the Neoproterozoic Chattisgarh rift basin, central India- Major controls on its evolution: Bulletin of American Association of Petroleum Geology, v. 91,p.785-808.

Dunn, J.A. (1940), The stratigraphy of south Singhbhum: Memoir Geological Survey of India, v.63, p.303-369.

Gui, B., He, D., Chen, W. and Zhang, W. (2014), Migration of growth axial surfaces and its implications for multiphase tectono-sedimentary evolution of the Zhangwu fault depression, southern Songliao Basin, NE China: Journal of Geodynamics, v.75, p.53–63.

Jones, H.C. (1934), The Iron ore deposits of Bihar and Orissa: Memoir Geological Survey of India, v. 63,167-302.

Mazumder, S.K. (1996), Precambrian Geology of Peninsular Eastern India - a selective review: Indian Minerals, v. 50, p.139-174.

McPherson, J.G., Shanmugam, G., Moiola and R.J. (1987), Fan deltas and braid deltas: Varieties of coarse-grained deltas: Geological Society American Bulletin, v.99, p.331–340.

Miall, A.D. (1973), Markov chain analysis applied to an ancient alluvial plain succession: Sedimentology. 20,p. 347-364.

Miall, A.D. (1984), Principles of Sedimentary Basin Analysis. Second Edition, Springer Verlag, N.Y.; 490p.

Mukhopadhyay, D. (2001), The Archean nucleus of Singhbhum: the present state of knowledge: Gondwana Research, v.4, p.307-318.

Johnson, H.D. (1975), Tide and wave dominated inshore and shoreline sequences from the Late Precambrian, Finnmark, north Norway: Sedimentology, v. 22, p.45-73.

Roy,A.B. and Bhattacharya, H.N. (2012), Tectonostratigraphic and Geochronologic Reappraisal Constraining the Growth and Evolution of Singhbhum Archaean Craton, Eastern India: Journal of Geological Society of India, v.80, p.455-469.

Saha, A.K. (1994), Crustal Evolution of Singhbhum-North Orissa, E. India: Memoir of Geological Society of India,v. 27, 341p.

Schlische, R. W. (1991), Half-graben filling models: New constraints on continental extensional basin development: Basin Research, v.3, p.123-141.

Schlische, R.W., and Anders, M.H. (1996), Stratigraphic effects and tectonic implications of the growth of normal faults and extensional basins, in Beratan, K.K., (eds.), Reconstructing the History of Basin and Range Extension Using Sedimentology and Stratigraphy, Boulder, Colorado: Geological Society of America Special Publication, v.303, p.183-203.

Swift, D.J.P., Stanley, D.J. and Curray, J.R. (1971), Relict sediments on continental shelves:A reconsideration: Journal of Geology, v.79, p. 322-346.

Tarafdar, S.N. and Lari, T.A. (1974), Geological mapping and preliminary appraisal for iron, manganese and limestone around Gua-Chotanagra-Kumdi area, Singhbhum district, Bihar: Report GSI, 1-100p.

Jour. Indian Association of Sedimentologists, Vol. 36, No. 1 & 2 (2019), pp.19-50
ISSN Online 2582 – 2020
ISSN Print 0970 – 3268

Depositional environment and Provenance of Pilikarar Formation, Central Narmada basin, Hoshangabad District, Madhya Pradesh, India

M. G. Kale[1*] and Ashwin S. Pundalik[2]
[1] Department of Geology, Savitribai Phule Pune University, Pune - 411 007, India.
Email: mgkale@unipune.ac.in
[2] Department of Geology, St. Xavier's College, Mumbai – 400 001, India.
Email: ashwin.pundalik@xaviers.edu

Abstract: The Pilikarar Formation comprised of coarser clastics, occur as isolated as well as coalescent cones and exhibit development of bouldery conglomerate lithofacies, with both clast supported and matrix supported varieties; representing debris flow and mud flow deposits of alluvial fan respectively. Caliche nodules and rhizoliths in the middle part of Pilikarar Formation indicate semiarid climatic conditions and related subaerial exposure. Immediacy of this alluvial fan to Son-Narmada-North fault indicates that this fault provided the basin depression, geomorphic contrast together with climate favoured the debris flow process to built alluvial fan.

Granulometric studies of these sediments reveal presence of wide range of size classes, polymodal nature, moderate to very poor sorting, positive skewness and leptokurtic to platykurtic distribution; supplementing fluvial environment of deposition. Thin section studies revealed quartzose arenitic nature, indicating mineralogical maturity of these sediments. The presence of ferruginous cement is suggestive of acidic and oxidising diagenetic conditions. Presence of illite, kaolinite and montmorillonite in these sediments, further supports derivation from soils developed on these rocks. Geochemical composition of these sediments supports mixed provenance and mineralogical maturity of these sediments. Paleotemperature derived from $\delta^{18}O$ content (-1.60 ‰) of calcrete indicate moderate temperature of 21.44°C for Pilikarar Formation, thereby indicating C3-C4 mixed vegetation with dominance of C3 vegetation. The low value of pCO_2 (154.6 ppmV) derived from $\delta^{13}C$ content (-9.25 ‰), and the $\delta^{18}O$ content (-1.60 ‰) suggests evaporation and evapotranspiration as the main process in calcite precipitation, indicating meteoric diagenesis related with semi-arid climatic conditions undergone by Pilikarar sediments. The mineralogical maturity is further supported by high ZTR index together with transparent heavy mineral assemblage of augite, epidote, staurolite, garnet, sillimanite, kyanite, sphene, hornblende, zoisite, monazite, anataze and low values of provenance sensitive indices; related to derivation of these sediments dominantly from Vindhyan Supergroup, with subordinate contribution from Deccan Trap Basalts and Mahakoshal Group.

INTRODUCTION

The Central Narmada basin of Peninsular India is one of the few regions of India where Quaternary deposits are very well developed and preserved. The Narmada River is the largest westerly flowing river in to the Arabian Sea in India (Gupta et al., 2011), which flows through ENE-WSW trending Narmada-Son lineament. It is an ancient tectonic feature dated to be Precambrian (Choubey, 1971). This deep crustal structure of Narmada-Son lineament is inferred to have been initiated as a protocontinental suture during Late Archean-Early Proterozoic times and subsequently evolved as a rift generated cratonic margin during the Proterozoic times (Kale, 1986). The southern margin of central Narmada valley and northern margin of Purna-Tapti valley are defined by two almost east-west trending regional faults known as North Satpura and South Satpura faults respectively. Reactivation along these faults during Quaternary has given rise to accumulation of about 400 m thick Quaternary deposits in these valleys (Vaidyanathan and Ramakrishnan, 2008). Tiwari and Bhai (1997) recognized seven lithostratigraphic formations namely Pilikarar Formation, Dhansi Formation, Surajkund Formation, Baneta Formation, Hirdepur Formation, Bauras Formation and Ramnagar Formation in order of decreasing antiquity. On the basis of carried out field and laboratory studies, an attempt is made in this paper to reconstruct the sedimentation history of Pilikarar Formation.

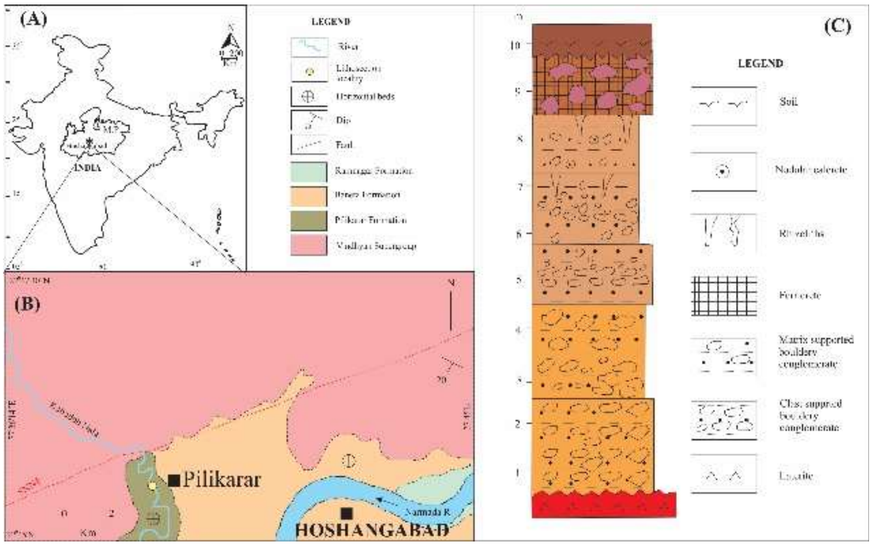

Figure 1:
A) Outline map of India showing location of study area.
B) Geological map of Pilikarar area, Central Narmada basin (modified after, Tiwari and Bhai, 1997), SNNF- Son Narmada North Fault (after, GSI, 1993; Mishra, 2015).
C) Lithosection of Pilikarar Formation, Central Narmada basin.

STUDY AREA

Pilikarar Formation (Lower Pleistocene?) is the lowermost lithostratigraphic unit of Quaternary succession of Central Narmada basin. The Pilikarar Formation has unconformable contact with Baneta Formation (Early Upper Pleistocene) which is exposed to the east Pilikarar village and rest of the area is occupied by Proterozoic Vindhyan

Supergroup rocks (Fig. 1B). The Pilikarar Formation has very restricted areal extent and is exposed in Kaliadoh Nala; which is located 1 Km west of Pilikarar village (Fig. 1B). Here about 10 meter thick section of sediments belonging to Pilikarar Formation is well exposed.

METHODOLOGY

From the Pilikarar lithosection five samples namely PK-1A, PK-1, PK-2, PK-3, PK-4 and PK-5 were systematically collected, out of which two well cemented samples (PK-1A and PK-5) were selected for thin section preparation. These were studied under the optical microscope and modal analysis was carried out by using point counter. Four samples were subjected to granulometric studies by 'Sieve and pipette' method given by Ingram (1971) and Galehouse (1971) respectively, and heavy minerals were separated from fine sand fraction (2.0 Phi to 4.0 Phi) of these samples following method given by Carver (1971). Clays separated from four samples were analysed using Phillips X-ray diffractometer at Wadia Institute of Himalayan Geology, Dehradun. The geochemical studies of four samples representing matrix of conglomerate PK-1A, PK-1, PK-2 and PK-3) was carried out on XRF (Axios, PAN analytical) and ICP-MS (Thermo X series 2) at National institute of Oceanography, Goa. Accuracy and precision of the major oxide data is better than +4%, while accuracy of trace and rare earth elements was checked using USGS standards BIR-1 and DNC-1. LOI i.e. Loss on Ignition was determined at Wadia Institute of Himalayan Geology, Dehradun. For these samples, weathering indices such as CIA i.e. Chemical index of alteration ($(Al_2O_3/Al_2O_3+Na_2O+K_2O+CaO^*) \times 100$; Nesbitt and Young, 1982), PIA i.e. Plagioclase Index of Alteration ($[(Al_2O_3 - K_2O) / ((Al_2O_3 - K_2O) + CaO^* + Na_2O)] \times 100$; Fedo et al., 1995), CIW i.e. Chemical Index of Weathering ($[Al_2O_3 / (Al_2O_3 + CaO^* + Na_2O)] \times 100$; Harnois, 1988), a modified version of CIW i.e. CIW' for carbonate-bearing siliciclastic rocks ($[Al_2O_3/(Al_2O_3+Na_2O)] \times 100$; Cullers, 2000), ICV i.e. index of compositional variability ($(Fe_2O_3+ K_2O + Na_2O + CaO + MgO + MnO + TiO_2) / Al_2O_3$; Cox et al., 1995), WIP i.e. weathering index ($100 \times (CaO^*/0.72 + 2Na_2O/0.35 + 2K_2O/0.25 + MgO/0.9)$; Parker, 1970) and W index ($\exp(0.203\ln(SiO_2) + 0.191\ln(TiO_2) + 0.296\ln(Al_2O_3) + 0.215\ln(Fe_2O_3) - 0.002\ln(MgO) - 0.448\ln(CaO^*) - 0.464\ln(Na_2O) + 0.008\ln(K_2O) - 1.374)$; Ohta and Arai, 2007) were calculated. Stable isotope composition of one rhizolith sample was determined at CSIR-National

Institute of Geophysical Research, Hyderabad, using Thermo Finnigan Delta plus XP Continuous Flow Isotope Ratio Mass Spectrometer (CF-IRMS) with attached preparation device Gas Bench II and robotic sampling arm (CG-PAL). Using the stable isotope values and following the procedure given by Friedman and O'Neil (1977), the temperature for calcite precipitation was calculated. Cerling (1999) has given method for calculating pCO_2 using $\delta^{13}C$ values following which, the value of pCO_2 for the rhizolith sample was estimated.

RESULTS

Field characteristics

The sediments of Pilkarar Formation rest unconformably over laterite with non-erosive contact, and on the top of these sediments, development of soil cover is noticed (Fig.1C). These sediments occur as small isolated (Fig.2A) as well as coalescent cones constituted of coarser clastic sediments with development of bouldery conglomerate lithofacies.

Bouldery conglomerate lithofacies is represented by thickly bedded, poorly sorted clasts ranging from granule to large boulders; floating in matrix consisting of sand, silt and clay. Their thicknesses vary from 1.5 to 2.5 m and these can be traced laterally up to 50 m. The clasts vary in size from 2 to 19.8 cm. The clasts of these conglomerates are angular to subangular with few subrounded clasts and at places slabby clast are also noticed. They are of sandstone, vein quartz, agate and laterite; floating in yellowish buff coloured matrix (Fig. 2B). Within this lithofacies two subfacies i.e. clast supported bouldery conglomerate and matrix supported bouldery conglomerate are present and are intermingling with each other (Fig. 2C). Within the clast supported bouldery conglomerate, concentration of boulders is observed in the middle as well as upper part (Fig. 2D). In the upper part of Pilikarar lithosection, clast supported bouldery conglomerate passes in to matrix supported bouldery conglomerate (Fig.1C and 2D). Decrease in the clast size is noticed in matrix supported bouldery conglomerate with dominance of pebble size clasts. Within this variety of conglomerate, development of nodular calcrete as well as rhizoliths are noticed (Fig.2D). Both normal as well as reverse grading of clasts from boulder to granule and from granule to boulder is noticed within this facies (Fig. 2B). In the uppermost part of this lithosection, the clasts are cemented by reddish brown ferruginous cement (Fig. 2E). Close up view of Fig. 2E shows angular to subrounded pebble to boulder

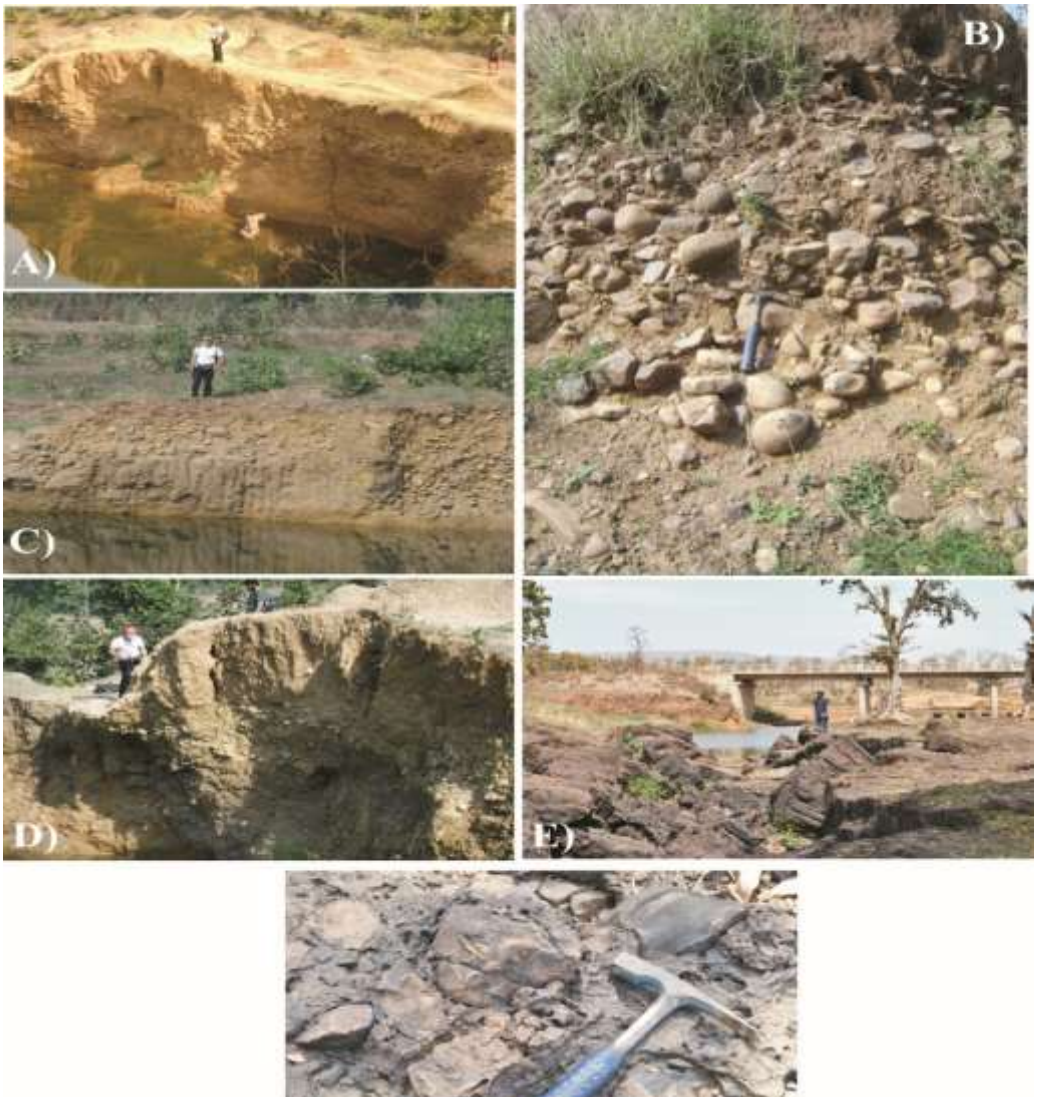

Figure 2:

A) Pilikarar Formation coarser clastics occuring as small isolated cone. Locality: Kaliadoh Nala, near Pilikarar.
B) Bouldery conglomerate consisting of subangular to rounded clasts of s andstone, basalt, vein quartz and laterite floating in yellowish buff coloured matrix consisting of sand, silt and clay. Note the normal as well as reverse grading of clasts.
C) Intermingling of clast supported bouldery conglomerate and matrix supported bouldery conglomerate.
D) Bouldery conglomerate exhibiting concentration of boulders in middle as well as upper part. Note vertical passage of clast supported bouldery conglomerate to matrix supported bouldery conglomerate. Development of nodular calcrete and rhizolith is noticed in the middle part.
E) Bouldery conglomerate in which clasts are cemented by reddish brown ferruginous cement.
F) Close-up view of 3e, exhibiting angular to subrounded pebble to boulder size clasts of sandstone bounded by reddish brown ferruginous cement.

clasts bounded by reddish brown ferruginous cement (Fig. 2F).

Thin section studies

In Pilikarar thin sections, framework grains show wide variation in grain size from silt to coarse sand, angular

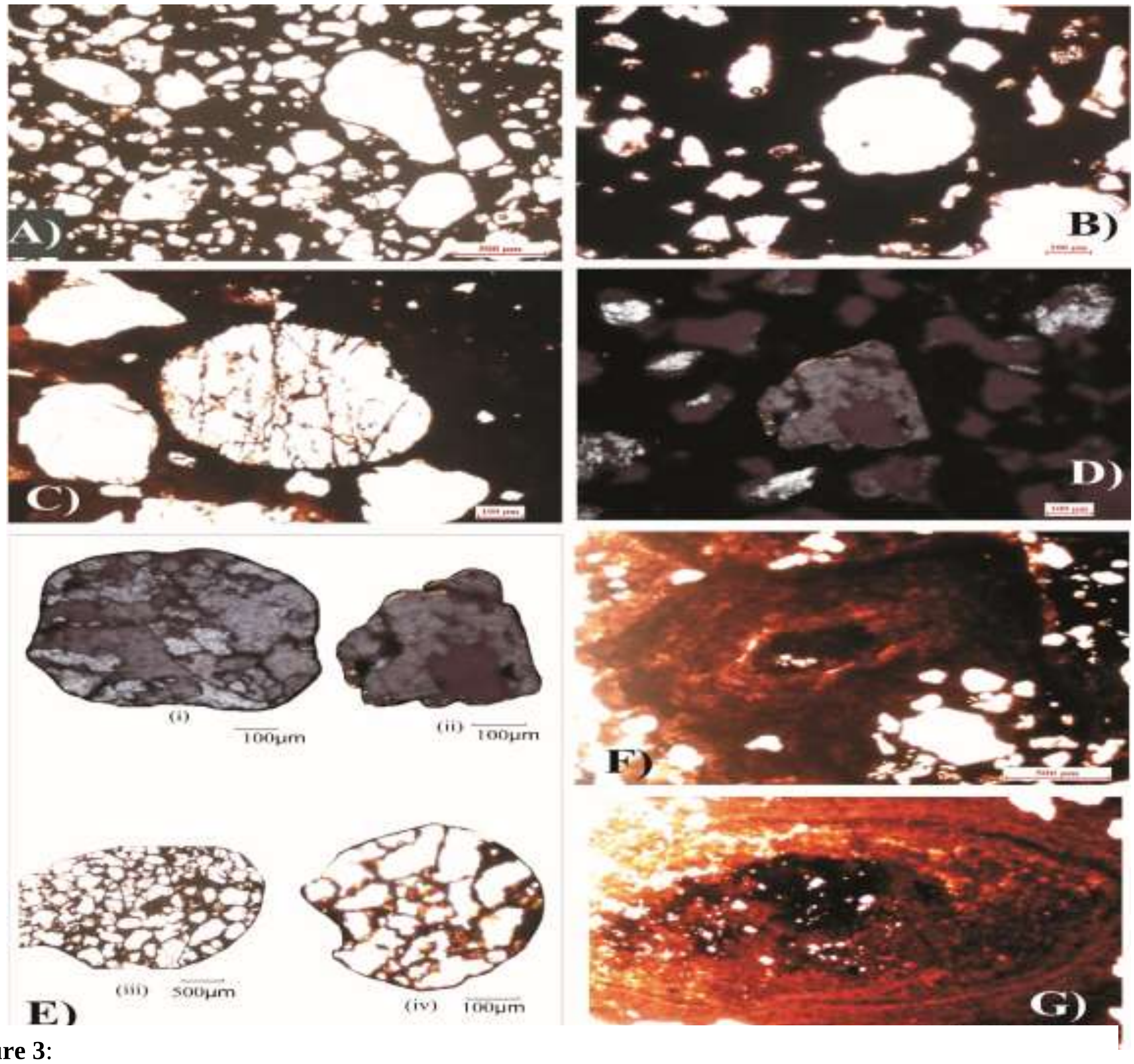

Figure 3:

A) Photomicrograph exhibiting extremely poorly sorted nature of framework grains floating in ferruginous cement (PPL).

B) Angular nature grains with occasional well rounded grain of quartz floating in ferruginous cement (PPL).

C) Embayment of dark brown ferruginous cement along the cracks of quartz grains (PPL).

D) Development of very thin isopachous rim of micritic calcite around the polycrystalline quartz grain (BCN).

E i) Polycrystalline quartz fragment consisting of large number of varying size constituent grains with sutured, irregular grain contacts (BCN).

E ii) Polycrystalline quartz fragment consisting of five varying size constituent grains with irregular grain contacts

E iii) Sandstone fragment consisting framework grains with wide variation in the size, bounded by ferruginous cement (PPL).

E iv) Subrounded medium grained sandstone fragment with fine to medium sand size framework grains floating in ferruginous cement (PPL).

F) Development of irregular concretions with in ferruginous cement (PPL).

G) Close up view of concretion with development of concentric lamination (PPL).

to subrounded nature and are observed to be floating in ferruginous cement (Fig. 3A). In these sediments, ferruginous cement is dominantly present (62.50% to 65.25%, av. 63.88%) and the framework constituents are dominated by quartz (31.23% to

33.07%, av. 34.27%) with negligible amount of K-feldspars (1.75% to 1.96%, av. 1.85%) and lithic fragments (2.03% to 3.20%, av. 2.62%); hence can be described as quartzose arenites (Okada, 1971) indicating mineralogically maturity. Within quartz, both monocrystalline and polycrystalline varieties are present. Within monocrystalline quartz, nonundulatory variety (17.09% to 18.33%, av. 17.71%) dominates undulatory variety (11.20% to 12.70%, av. 11.95%), which together dominates over polycrystalline quartz (1.44% to 3.54%, av. 2.49%). Majority of quartz grains are subangular in nature and occasionally well rounded grains of quartz are also noticed within these thin sections (Fig. 3B). Different varieties of polycrystalline quartz present include i) fragment consisting of large number of varying size constituent grains with sutured, irregular grain contacts (Fig. 3E, i and ii) consisting of five varying size constituent grains with irregular grain contacts (Fig. 3E, ii). Commonly within the quartz grains, presence of cracks is noticed, which are filled with dark brown ferruginous cement (Fig. 3C). Within K-feldspars, microcline predominates over orthoclase, and majority of feldspars are altered. Unstable lithic fragments present are dominantly of sandstones. The large sandstone fragment showing wide variation in the size of framework grains bounded by ferruginous cement is shown in Fig. 3E, iii; while Fig. 3E, iv exhibits subrounded medium grained sandstone fragment with fine to medium sand size framework grains floating in ferruginous cement. Occasionally development of very thin isopachous rim of micritic calcite around the framework grains (Fig. 3D) can also be seen in these thin sections. Within the ferruginous cement irregular concretions (Fig. 3F) and development of concentric lamination (Fig. 3G) is also noticed.

Granulometry

Granulometric studies of these sediments revealed presence of wide range of grain size classes ranging from -6.00 to 10.5 ϕ, polymodal grain size distribution, poor to very poor sorting (1.79 ϕ to 3.34 ϕ, av. 2.45 ϕ), positive skewness (0.27 ϕ to 1.26 ϕ, av. 0.66 ϕ) indicating their fine to coarse skewed nature and dominance of coarser admixture over finer and Platykurtic to very leptokurtic to (0.87 ϕ

Table 1: Heavy mineral frequency percentages along with provenance sensitive indices (Morton and Hollsworth, 1994, 1999 and Morton and Milne, 2012) and heavy mineral concentration indices (Garzanti and Ando, 2007) of sediments of Pilikarar Formation.

Sample No.	**PK-1**	**PK-2**	**PK-3**	**PK-4**	**Average**
Minerals					
Zr	63.63	51.93	46.48	46.29	**52.02**
To	5.05	22.45	8.72	9.07	**11.32**
Ru	4.04	1.45	1.36	0.98	**1.96**
Au	8.08	13.52	21.91	25.32	**17.21**
Ep	1.01	0.08	1.21	--	**0.58**
St	--	1.45	1.39	--	**0.71**
Gt	13.13	4.18	12.45	10.85	**10.15**
Sil	--	1.45	2.18	2.53	**1.54**
Ky	1.01	1.91	2.19	2.99	**2.03**
Sp	1.01	0.54	--	--	**0.39**
Zo	--	1.00	--	--	**0.25**
Mo	1.01	1.00	2.02	0.98	**1.25**
Hb	1.01	--	1.53	--	**0.64**
An	1.01	--	--	0.98	**0.50**
ZTR	72.72	75.83	56.56	56.34	**65.36**
PSI					
GZi	17.11	7.45	21.13	18.99	**16.17**
RZi	2.51	2.65	2.54	1.89	**2.40**
RuZi	5.97	2.72	2.84	2.07	**3.40**
Mzi	0.90	0.91	1.21	0.94	**0.99**
SZi	--	2.72	2.90	--	**1.41**
UTi	28.57	2.69	12.19	--	**10.86**
AmZRT	--	2.63	--	17.65	**5.07**
EpZRT	0.11	2.09	--	17.59	**4.95**
GtZRT	15.29	5.22	18.04	16.15	**13.68**
KyZRT	1.37	2.46	3.73	5.04	**2.52**

GZi	100X Garnet count/(Garnet + Zircon)
RZi	100 X TiO_2 mineral count / (TiO_2minerals+Zircon)
RuZi	100 X Rutile count / (Rutile+Zircon)
MZi	100 X Monazite count/ (Monazite + Zircon)
SZi	100 X Staurolite count / (Staurolite +Zircon)
UTi	100 X (Unstable total) / (Unstable + Tourmaline)
AmZRT	Amphibole / (Amphibole + Zircon + Tourmaline + Rutile)
EpZRT	Epidote / (Epidote + Zircon + Tourmaline + Rutile)
GtZRT	Garnet / (Garnet + Zircon + Tourmaline + Rutile)
KyZRT	Kyanite / (Kyanite + Zircon + Tourmaline + Rutile)

Zr- Zircon, To- Tourmaline, Ru-Rutile, Au- Augite, Ep- Epidote, St- Staurolite, Gt- Garnet, Sill- Sillimanite, Ky- Kyanite, Sp- Sphene, Zo- Zoisite, Spl- Spinel, Ch- Chlorite, Mo-Monazite, Hb- Hornblende, and An- Anatase, ZTR- Combined percentage of zircon, tourmaline and rutile, PSI- Provenance sensitive indices.

to 2.11 ϕ, av. 1.34 ϕ) related with mixing of two or more subequal populations. The gravel-sand-mud ratio for the clast supported conglomerate is 76:18:5, while for the matrix supported conglomerate it is 2:43:55. The log probability plots of these sediments exhibit development of better-sorted saltation population (slopes up to 78 ^{o}), poorly sorted suspension population (slopes up to 45 ^{o}) and better sorted surface creep population (slope up to 45^{o}).

Heavy mineral studies

The percentages of the transparent heavy minerals in the sediments of the Pilikarar Formation are presented in Table 1. Heavy mineral assemblage of Pilikarar Formation consists of 14 transparent heavy mineral species which include zircon, tourmaline, rutile, augite, epidote, staurolite, garnet, sillimanite, kyanite, sphene, zoisite, monazite, hornblende and anataze. Zircon (av.52.02 %) constitutes the half of the bulk transparent heavy mineral crop. The average ZTR index (Hubert, 1962) for these samples is 65.36. Most of the zircon and tourmaline grains are subrounded to rounded in nature with few euhehdral and subhedral grains (Fig.4.1 to 4.11). Many a times opaque inclusions are noticed within zircon grains (Fig. 4.4, 4.5, 4.6). Augite, epidote, staurolite, garnet, sphene and anataze grains are angular to subangular (Fig. 4.14 to 4.19). Rutile, sillimanite, kyanite, hornblende and zoisite occurs as elongated grains (Fig. 4.14, 4.15, 4.21, 4.22, 4.23, 4.25). For these sediments, various provenance sensitive indices of Morton and Hollsworth (1994, 1999) and Morton and Milne (2012) were calculated, and values of these indices are given in Table 2. The samples from Pilikarar Formation show low values of MZi (av.2.40), RZi (av.3.40), RuZi (av.0.99), SZi (av.1.41), UTi (av.10.86), AmZRT (av.1.00), EpZRT (av.0.89) and KyZRT (av.2.52) with slightly moderate values of GZi (av.16.17) and GtZRT (av.13.68) owing to high proportion of zircon in heavy mineral crop as well as high value of ZTR index.

Figure 4: Heavy mineral species from Pilikarar Formation.
1 to 6- Zircon, 7 to 11- Tourmaline, 12 and 13- Rutile, 14 and 15- Augite, 16- Epidote, 17- Staurolite, 18 and 19- Garnet, 20-Silimanite, 21- Kyanite, 22- Sphene, 23- Zoisite, 24- Monazite, 25- Hornblende and 26- Anatase.

X-ray diffraction studies

The X-ray diffraction studies of clays from Pilikarar Formation revealed illite (3.35 dA^{o} –100 %) as dominant clay mineral with subordinate kaolinite(1.78 dA^{o} – 7 % to 19 % and 1.53 dA^{o} – 9 %) and montmorillonite (4.50 dA^{o}-78 %, 2.50 dA^{o} -36 %).

Geochemical studies

The obtained values of major oxides (weight percentages), trace element composition (ppm) and chondrite normalized rare earth element composition (ppm) of Pilikarar sediment samples are given in Table 2 and 3 respectively. Pilikarar sediments show high values of SiO_2/Al_2O_3 ratio as compared to Na_2O/K_2O ratio and Fe_2O_3/K_2O ratio, due to their high quartz content compared to feldspars and ferromagnesian minerals (Pettijohn et al., 1972; Herron, 1988). On major oxide provenance discrimination diagrams of Roser and Korsch (1988), samples from

Sample No. Oxides	**PK-1A**	**PK-1**	**PK-2**	**PK-3**	**Average**
SiO_2	43.42	64.66	68.82	78.72	**63.91**
Al_2O_3	8.13	9.86	6.96	7.55	**8.13**
TiO_2	1.01	0.73	0.58	0.70	**0.76**
Fe_2O_3	38.71	14.66	3.94	4.41	**15.43**
MnO	0.19	0.17	0.03	0.10	**0.12**
MgO	0.14	0.76	0.94	0.75	**0.65**
CaO	0.16	0.40	6.87	0.87	**2.08**
Na_2O	0.10	0.17	0.22	0.64	**0.28**
K_2O	0.22	1.67	1.06	0.73	**0.92**
P_2O_5	0.15	0.06	0.03	0.02	**0.07**
LOI	7.76	6.86	10.55	5.50	**7.67**
Total	**100**	**100**	**100**	**100**	100
Weathering indices					
CIA	93.65	80.66	78.78	72.25	**81.34**
PIA	96.15	93.49	88.93	76.24	**88.70**
CIW	96.26	94.61	90.58	78.19	**89.91**
CIW '	98.09	97.23	95.06	87.76	**94.54**
ICV	3.34	1.50	1.08	1.15	**1.77**
WIP	8.17	16.16	13.63	16.49	**13.61**
W index	98.68	95.45	59.93	74.09	**82.04**

Table 2: Major element composition (Wt %) and weathering indices of sediments of Pilikarar Formation.

Pilikarar Formation show mixed provenance i.e. quartzose sedimentary and mafic igneous (Fig. 5). On A-CN-K ternary diagram of Nesbitt and Young (1984,1989) Piliarar samples plot near illite and kaolinite field (Fig.6A). The PIA values of the sediments plotted on CaO*-(Al_2O_3+K_2O)-Na_2O diagram (Fig.6B) plot near Al_2O_3 + K_2O apex, indicating intense weathering of plagioclase felspar (Fedo et al.,1995; Purevjav and Roser, 2013). The intensity and duration of weathering of these sediments are further evaluated by examining the relationships among alkali and alkaline earth elements (Nesbitt and Young, 1982) using weathering indices discussed above. CIA and CIW are used to evaluate weathering of sediment source (Nesbitt and Young, 1982; Harnois, 1988), PIA evaluates degree of plagioclase alteration (Fedo et al., 1995), CIW' is used as measure of source weathering for carbonate bearing siliciclastic rocks (Cullers, 2000), ICV is used to evaluate mineralogical maturity (Cox et al. 1995) and WIP and W index to determine the degree of recycling (Parker, 1970; Ohta and Arai, 2007). These weathering indices in combination are used to evaluate weathering of source, nature of source as well as mobility of elements during diagenesis and leaching (Jafarzadeh and Hosseini-Barzi, 2008). The values of these weathering indices for sediments of Pilikarar Formation are given in Table 2. On the plot of WIP versus CIA (Garzanti et al., 2013b), Pilikarar sediments show low WIP values associated with high CIA values and fall within the field of recycled sediments (Fig 6 C). W index of the sediments under study varies from 59.93 to 98.68% (Table 2), thereby indicating moderate to high intensity of weathering.

For discriminating tectonic setup of sediment deposition, Verma and Armstrong-Altrin (2013) have proposed a new discriminant-function-based multi-dimensional diagram, in which Pilikarar sediments plot within the continental rift field (Fig.7A). On the geochemical discrimination diagrams of siliciclastic sediments (Verma and Armstrong-Altrin, 2016), samples from Pilikarar Formation plot in passive margin field (Fig. 7B and 7C).

Pilikarar sediments show enrichment in transition trace elements and LILE's except Rb and U (Table 3, Fig. 8A). In Pilikarar Formation, concentration of transition trace elements, LILE's and HFSE's decreases from clast supported conglomerate to matrix supported conglomerate (Table 3). On the Th/Sc versus Zr/Sc binary diagram (Fig. 9) of McLennan et al.(1993), samples from Pilikarar Formation show higher value of Zr/Sc and narrow range of Th/Sc. The chondrite normalized (Lodders and Fegley, 1998) rare earth element composition of Pilikarar sediments is given Table 3 and the prepared plots are exhibited in Fig. 8B. These sediments exhibit enriched LREE and depleted HREE, and negative europium anomaly (Fig. 8B) and negative Ce anomaly (Except for PK-1A). They show fractionated REE pattern characterized by high values (av. 10.82) of La/Yb ratio (Xie et al., 2017). La/Sm value ranging from 3.04 to 4.30 for the Pilikarar sediments suggests enrichment of LREE while low value of Gd/Yb ratio is reflected in flat HREE pattern (Banerjee and Banerjee, 2010). The ratios of $(La/Lu)_n$, Co/Th, La/Sc, Cr/Th, and Th/Sc were also determined which are sensitive to the nature of the source of the sediments (Tao et al., 2014; Tawfik et al., 2017) and are given in Table 4.

Sample No.	**PK- 1A**	**PK- 1**	**PK- 2**	**PK- 3**	**Average**
Element					
Li	0.67	1.04	0.83	1.02	**0.89**
Be	7.25	6.07	3.34	3.57	**5.05**
Sc	1.54	0.94	0.59	0.68	**0.94**
V	5.03	2.57	0.72	0.94	**2.32**
Cr	1.25	1.08	0.45	0.52	**0.82**
Co	1.98	1.87	0.65	1.18	**1.42**
Ni	0.97	0.90	0.57	0.68	**0.78**
Cu	5.74	2.69	0.95	1.14	**2.63**
Zn	0.40	0.42	0.48	0.39	**0.42**
Ga	1.88	2.15	1.33	1.29	**1.66**
Rb	0.19	1.37	0.85	0.83	**0.81**
Sr	0.13	0.14	0.29	0.22	**0.20**
Y	0.80	1.44	0.75	0.73	**0.93**
Zr	0.80	0.83	0.66	0.63	**0.73**
Nb	1.30	1.59	1.10	1.31	**1.33**
Sn	0.55	0.97	0.60	0.82	**0.74**
Sb	5.30	3.21	1.33	1.49	**2.83**
Cs	0.30	1.86	1.30	1.29	**1.19**
Ba	0.80	0.99	0.68	0.55	**0.76**
Th	0.60	1.23	0.88	0.90	**0.90**
U	1.63	1.12	0.76	1.06	**1.14**
Pb	0.30	0.21	0.10	0.13	**0.19**
La	103.36	176.00	108.60	120.38	**127.09**
Ce	241.29	201.77	115.48	142.0	**175.14**
Pr	78.44	107.23	66.69	76.88	**82.31**
Nd	92.70	96.91	56.20	66.87	**78.17**
Sm	33.99	42.88	25.25	28.39	**32.62**
Eu	21.16	25.37	14.49	15.56	**19.14**
Gd	26.75	32.59	19.13	21.01	**24.87**
Tb	19.97	25.00	14.24	15.24	**18.61**
Dy	15.21	19.29	11.04	11.48	**14.25**
Ho	12.80	17.13	9.66	9.73	**12.33**
Er	12.99	17.80	10.16	9.91	**12.71**

Tm	12.68	17.44	10.16	9.72	**12.5**
Yb	12.28	16.16	9.84	9.30	**11.89**
Lu	11.48	15.92	9.64	9.04	**11.52**
Σ REE	**695.09**	**811.50**	**480.58**	**545.52**	**633.17**
La/Lu	9.00	11.06	11.27	13.32	**11.16**
Eu/Sm	0.62	0.59	0.57	0.55	**0.58**
Eu/Eu*	0.70	0.68	0.66	0.64	**0.67**
La/Yb	8.42	10.89	11.04	12.94	**10.82**
Gd/Yb	2.18	2.02	1.94	2.26	**2.10**
La/Sm	3.04	4.10	4.30	4.24	**3.92**
Y/Ho	1.31	1.77	1.63	1.57	**1.57**

1: Rudnick and Gao (2003),

2: Lodders and Fegley (1998).

Table 3: UCC normalized[1]Trace element (ppm) and chondrite[2] normalized rare earth element (ppm) composition of sediments of Pilikarar Formation.

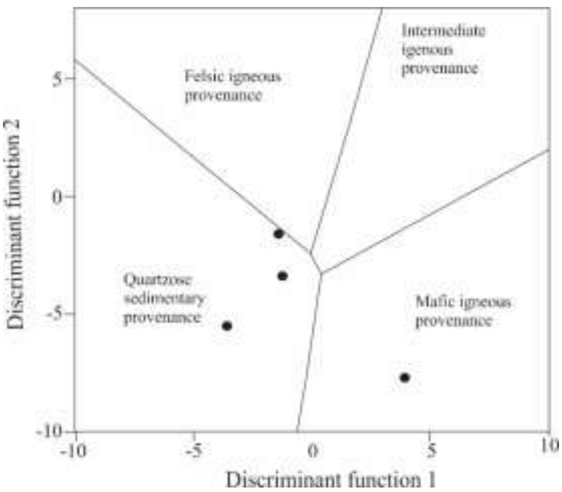

Figure 5: Discriminant function diagram for the provenance signatures of sediments from Pilikarar Formation using raw oxides (after Roser and Korsch, 1988).

Discriminant function 1= -1.773TiO2 + 0.607Al2O3 + 0.76Fe2O3 (total) - 1.5MgO + 0.616CaO + 0.509Na2O -1.224K2O - 9.09

Discriminant function 2= 0.445TiO2 + 0.07Al2O3 - 0.25Fe2O3 (total) - 1.142MgO + 0.438CaO + 1.475Na2O + 1.426K2O-6.861

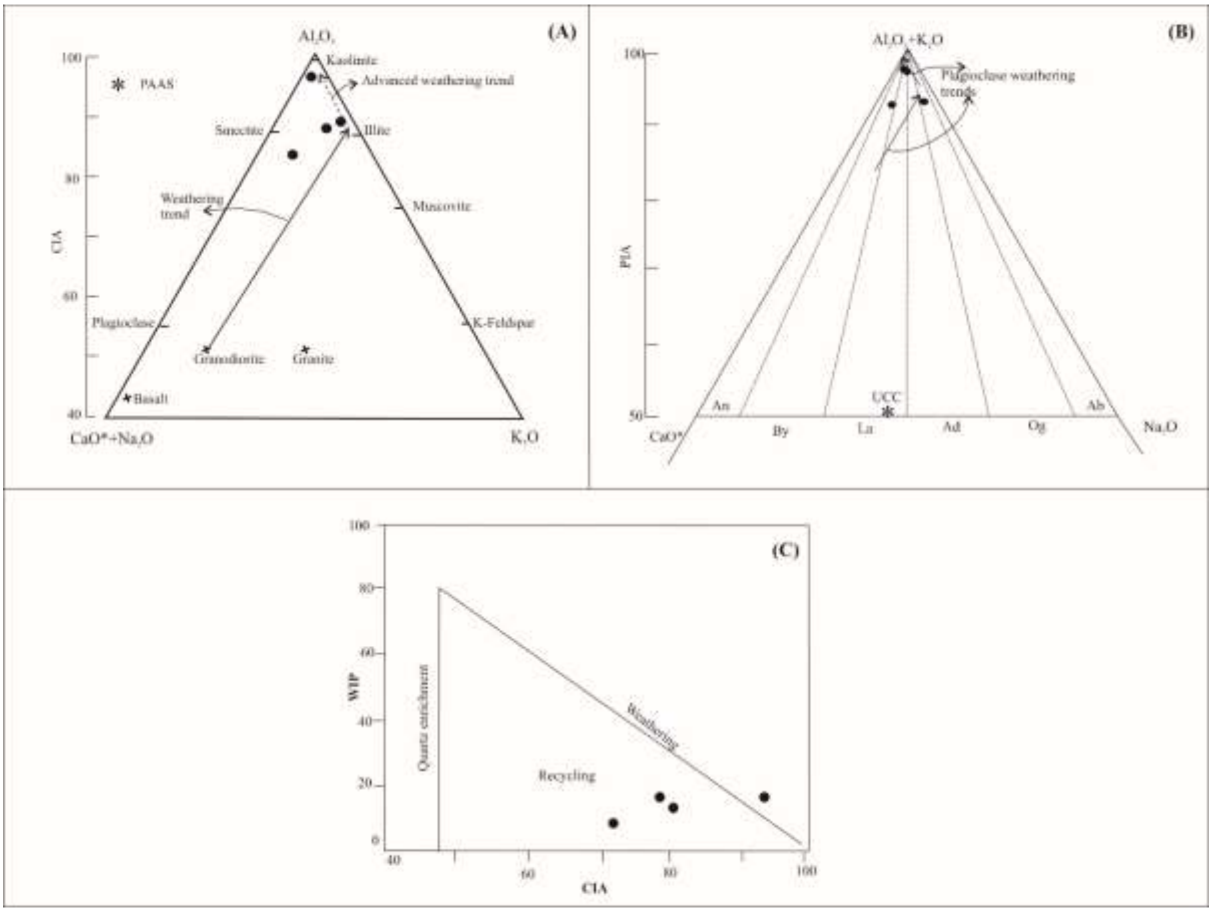

Figure 6:

A) (Na_2O+CaO)-Al_2O_3-K_2o diagram showing the weathering trends (modified after Nesbitt and Young 1984, 1989; data for granite, basalt and granodiorite after Le Maitre, 1976; Purevjav and Roser, 2013).

B) CaO^*-$(Al_2O_3+K_2O)$-Na_2O diagram showing the weathering trends (modified after Nesbitt and Young 1982, Positions of plagiclase feldspars after Purevjav and Roser, 2013). An, By, La, Ad, Og, Ab – anorthite, bytownite, labradorite, andesine, oligoclase, and albite, respectively.

C) WIP versus CIA plot for sediments of Pilikarar Formation (after Garzanti et al., 2013b).

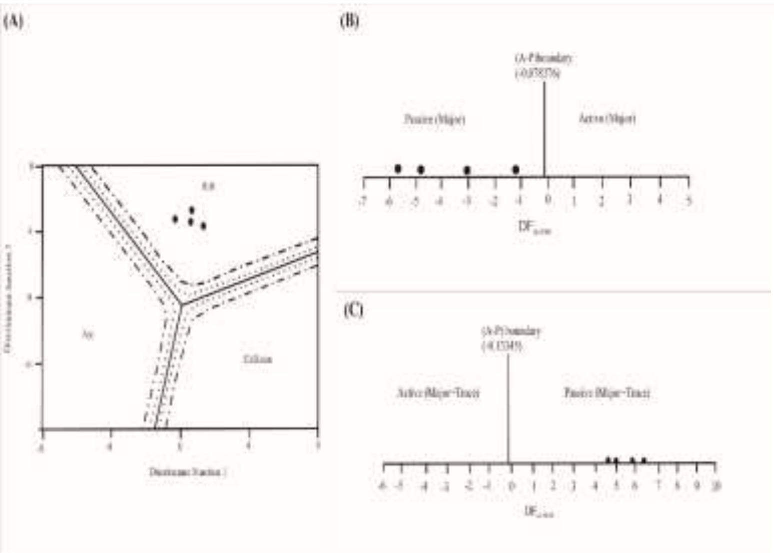

Figure 7:

A) Discriminant function multidimensional diagrams for sediments of Pilikarar Formation, the probability boundaries for 70% and 90% probabilities are also shown as dotted and dashed curves respectively.

B) Major element based multidimensional discriminant function diagram of sediments of Pilikarar Formation.

C) Major and trace element based multidimensional discriminant function diagram of sediments of Pilikarar Formation (after Verma and Armstrong-Altrin, 2016).

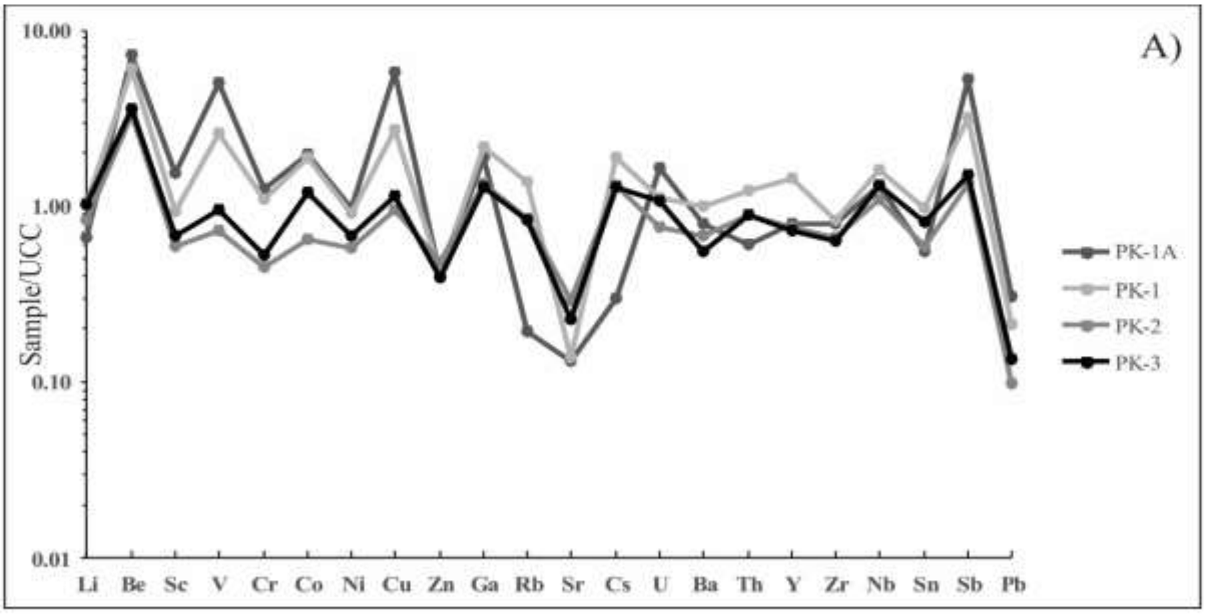

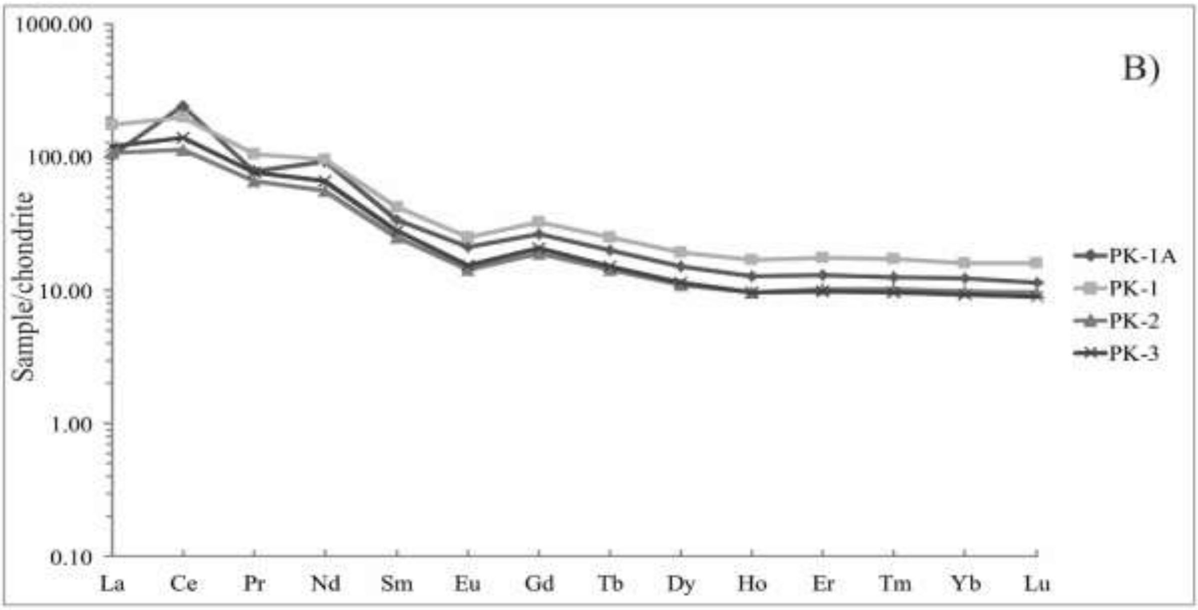

FIG. 8: A) UCC normalised trace element distribution pattern in sediments of Pilikarar Formation.
B) Chondrite normalised rare earth element pattern in sediments of Pilikarar Formation.

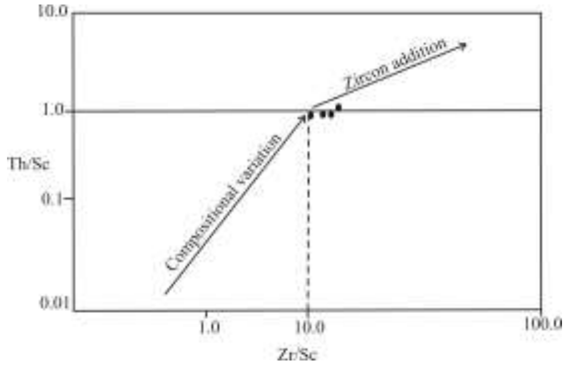

Figure 9: Th/Sc versus Zr/Sc plot for sediments of Pilikarar Formation (after McLennan etal., 1993).

	Pilikarar Sediments Range	**Average**	Sandstones[1]	Sediments from felsic source[2]	Sediments from mafic source[3]	UCC[4]	PAAS[5]
Eu/Eu*	0.64-0.70	0.67	0.71-0.95	0.40-0.94	0.71-0.95	0.66	0.71
$(La/Lu)_n$	9.0-13.32	11.16	4.37-8.27	3.0-27.0	1.10-7.0	10.39	9.86
Th/Sc	0.29-1.11	0.80	0.17-0.59	0.84-20.5	0.05-0.22	0.75	0.91
Cr/Th	4.45-18.11	8.53	21.69-67.93	4.0-15.0	25-500	8.76	7.53
Th/Co	0.19-0.82	0.46	0.17-0.43	0.67-19.4	0.04-1.40	0.61	0.63

1, 2 and 3: Cullers (1988, 1994, 2000), Cullers and Podkovyrov (2000).

4: Rudnick and Gao (2003).

5: Taylor and McLennan (1985).

Table 4: Range of elemental ratios of sediments of Pilikarar Formation compared to the ratios in similar fractions derived from felsic rocks, mafic rocks, upper continental crust and PAAS (After Tao et al., 2014).

Stable isotope studies

The obtained values of stable isotopes of oxygen and carbon for the rhizolith sample are negative i.e. the $\delta^{13}C$ content is -9.25 ‰ and $\delta^{18}O$ content is -1.60‰. According to Hays and Grossman (1991), $\delta^{18}O$ of meteoric calcite cement is an indicator of paleotemperature. The rhizolith from Pilikarar Formation is characterized by moderate paleotemperature value of 21.44°C. The $\delta^{13}C$ of soil carbonates has been used as a proxy for estimating paleoatmospheric pCO_2 (Cerling, 1999;Ekart et al. 1999; Robinson et al., 2002). The calculated value of $pCO_2$for rhizolith of Pilikarar Formation is 154.6 ppmV.

DISCUSSION

The Pilikarar Formation resting unconformably on laterite, is characterized by development of bouldery conglomerate facies representing debris flow deposits of alluvial fan (Reineck and Singh, 1980; Blair and McPherson, 1994, 2009; Chamyal et al., 1997; Sohn et al., 1999; Reading, 2006; Miall, 2006; Collinson et al., 2006; Franke et al., 2015; Chen et al., 2017). Alluvial fans are a form of fluvial depositional system characterized on the basis of geomorphic character rather than by a characteristic fluvial style (Miall, 2006). They represent the sedimentary record of upslope fluvial processes, controlled by the interaction between tectonics and climate, infused with the complex signatures of internal autogenic processes (Brooke et al., 2017). Alluvial fans are aggradational sedimentary deposits shaped overall like a segment of a cone radiating down slope from a point where a channel emerges from mountainous catchment (Bull, 1977; Blair and McPherson, 2009). The semi-conical shape of the fans is formed due to episodic avulsions of the active channel from a fixed fan apex (De Haas et al., 2018).The Pilikarar sediments under study represent debris flow dominated fan of Stainstreet and McCarthy (1993).

Debris flows are slurry-like flows of varied grain size, concentration, velocity, internal dynamics and therefore represent the most significant type of sediment gravity flow with respect to the volume of sediment delivered to the alluvial fans, which have been studied extensively (Johnson, 1970; Renwick, 1977). They are water-laden masses of sediment with volumetric sediment concentrations generally exceeding 40% (Costa, 1988; Iverson, 1997; De Haas et al., 2018). They represent extreme form of hyperconcentrated flow in which silt to boulder size grains are set in a matrix of clay grade fines and water, possess high flow density due to high concentration of suspended sediment which increases the buoyancy effect that mobilizes larger clasts (Jakob and Hungr, 2005;Ghinassi and Ielpi, 2016). In semi-arid settings like in the area under study, debris flows are generated by rare but intense rainstorm and such large energy outburst floods flush accumulated debris from the catchment valley (Reading, 2006). The resultant deposits commonly are disorganized, massive, poorly sorted, contain matrix and are clast supported, matrix supported or both, depending on position in the deposit as observed in the present case (Blair and McPherson, 1994; Chen et al., 2017). The Pilikarar alluvial fan lies at the base of Vindhyan range and is in close proximity of Son-Narmada North Fault (GSI, 1993; Mishra, 2015), therefore it is inferred that Son Narmada North Fault provided the basin depression, accommodation space and geomorphic contrast; though climate also a contributed in the debris flow process that constructed the Pilikarar alluvial fan (Chamyal et al., 1997; Chen et al., 2017). The development of isolated caliche nodules and rhizoliths is considered to be representative of secondary processes operating during inactive period between fan aggradations and semiarid climatic conditions prevailing during the deposition of these sediments related with subaerial exposure of these sediments (Allen, 1974; Reading, 1981; Blair and McPherson, 1993). The granulometric studies of these sediments reveal the presence of wide range of size classes, polymodal grain size distribution, moderately sorted to very poorly sorted nature, dominance of positive skewness and leptokurtic nature and the shape of log probability plots of these show similarity to the plots of fluvial sediments thereby supporting fluvial deposition of sediments of Pilikarar Formation (Visher, 1969; Reineck and Singh, 1980; Reading, 1981). The quartzose arenitic nature of Pilikarar sediments indicates mineralogical maturity (Okada,1971). Presence of polycrystalline quartz grains that consists of varying size constituent grains with sutured, irregular grain contactsis suggestive of gneissic derivation and their rounded nature, together with occasional presence of well-rounded quartz in these sediments indicates its polycyclic nature (Young, 1976; Blatt, 1992). The presence sandstone fragments in these sediments suggests their derivation from the sandstones of Vindhyan Supergroup exposed to the north of Pilikarar. The isopachous rim of micritic calcite around the framework grain is suggestive of meteoric vadose diagenesis initially undergone by these sediments (Longman, 1980; Tandon and Friend, 1989; Tucker and Wright, 1990; Morse and Mackenzie, 1990). The presence of ferruginous cement in large volume particularly in upper part of Pilikarar section, is the result of diagenesis of these sediments under then prevailing oxidizing and acidic conditions (Tucker, 2001; Kettanah et al., 2014). Presence of ferruginous cement along the cracks of framework grains is the product of displacive cementation (Braithwaite, 1989). Heavy mineral suite of Pilikarar Formation is characterized by dominance of zircon (av. 51.56 %) and have moderately high ZTR index of 65.36with subrounded to rounded nature of zircon, tourmaline and rutile grains support mineralogical maturity of the sediments and suggest polycyclic nature derived from Vindhyan Supergroup sediments exposed to the north and northeast of Pilikarar. The observed yellowish brown tourmaline is considered by Blatt et al. (1972), to be representative of metamorphic source. The presence of wine red rutile in these sediments is indicative of high grade metamorphic provenance (Force, 1980). The derivation of these sediments from Precambrian granites and metamorphic provenance is further supported by presence of staurolite, garnet, sillimanite, kyanite, sphene, zoisite, spinel, chlorite, hornblende, anataze. The appreciable amount of augite in this assemblage further suggests that during Pilikarar sedimentation along with Precambrian granites, metamorphics and Vindhyan Supergroup sediments, Deccan Trap basalts were also present in the source area. The samples belonging to Pilikarar Formation are characterized by very low values (<6.00) of all the provenance sensitive indices (RZi, RuZi, MZi, SZi, UTi, AmZRT, EpZRT, and KyZRT) except GZi (av. 16.17) and GtZRT (av. 13.68) which is related to low to moderate garnet, TiO_2 bearing minerals, rutile, unstable minerals and very low monazite, staurolite content. The X-ray diffraction studies of clays of these sediments support the petrographic and heavy mineral analysis of these sediments. Following Weaver (1989), the presence of illite and kaolinite are considered to be derived from Precambrian metapelites, shales, and the montmorillonite is derived from the soils developed on Deccan Trap basalts. The presence of illite in the Pilikarar sediments is considered to be derived from rocks of Vindhyan Supergroup exposed to the north of Pilikarar (Soni et al., 1987; Mohammadi et al., 2014).

Major oxide geochemistry of sedimentary rocks can be one of the determining factors for sediment maturity, provenance, weathering and tectonic setting of deposition. High values of SiO_2/Al_2O_3 ratio which is sensitive to sediment recycling and weathering process (Roser and Korsch, 1986; Roseret al., 1996; Liu et al., 2007)and the low values of Fe_2O_3/K_2O (Herron, 1988), suggest chemical maturity of Pilikarar sediments owing to their quartzose arenitic nature. Based on discriminant functions of Roser and Korsch (1988), Pilikarar Formation shows evidences of derivation from mixed provenance namely mafic igneous (Deccan basalt) and Quartzose sedimentary (Vindhyan Supergroup), thereby supporting petrography and heavy mineral studies. CIA values of sediments of Pilikarar Formation (av. 81.34%) together with CIW' (av.94.54%), ICV (av.1.77) and WIP (av.13.61) are suggestive of varied provenance, recycled nature of these sediments and indicate intense weathering of the source (Parker, 1970; Nesbitt and Young, 1982; Cox et al., 1995;Fedo et al., 1995; Bahlburg and Dobrzinski, 2009; Xie et al. 2017). With quartz enrichment, the value of WIP decreases, while CIA value remains unaffected(Xie et al., 2017). The plot of Garzanti et al. (2013b) thus distinguishes between first-cycle and recycled sediments (Garzanti et al., 2013a, 2013b; Xie et al., 2017), where recycled sediments plot in the field between the quartz enrichment trend and the UCC weathering trend closer to the X-axis (Xie et al., 2017). The position of Pilikarar sediments on this plot (Fig. 6C) supports their recycled, quartzose arenitic nature and derivation mainly from Vindhyan Supergroup rocks as observed in petrographic, heavy mineral studies. High values of PIA (av. 88.70%) indicate intense weathering of feldspars (Purevjav and Roser, 2013) supporting presence of highly altered feldspars in thin sections. The high values of W index of Ohta and Arai (2007) also justify the absence of plagioclase feldspars in the thin sections. As observed in the diagrams of Verma and Armstrong-Altrin (2013) and Verma and Armstrong-Altrin (2016), the samples from Pilikarar Formation plot within the passive margin continental rift field, which is well in agreement with intracratonic rift setting of the Narmada basin (Ghosh, 1976; Verma and Banerjee, 1992).

The trace elements such as Th, Sc, Cr and Co are extensively used to reconstruct the sediment provenance (Armstrong-Altrin et al., 2017). Thorium (9.48 ppm) and Ba (av.474.23 ppm) content of Pilikarar sediments is slightly less than that of UCC (10.5ppm and 628ppm; Rudnick and Gao, 2003). According to McLennan and Taylor (1991), concentration of Zr, Hf and Ti in sediments is greatly affected by hydraulic sorting and heavy mineral fractionation, hence the enrichment of Zr (av. 140.68 ppm) in these sediments under study seems to be directly proportional to abundance of zircon (av. 52.02 %) in these sediments. Th/Sc ratios higher than 0.8, along with the higher values of Zr/Sc (11.87) in these sediments, are indicative of an input from mature and/or recycled sources, zircon accumulation by sediment recycling and sorting (Ali et al., 2014;McLennan et al., 1993; Armstrong-Altrin et al., 2013) and can be related to the derivation of Pilikarar sediments from the matured sediments. Narrow range of Th/Sc in the samples of Pilikarar Formation indicates their derivation from mature and/or recycled source (Ali et al., 2014) i.e. mainly from Vindhyan Supergroup rocks, which substantiates clast composition as well as thin section results. Th/U and Th/Sc ratios of the sediments under study (av. 3.38 and 0.80 respectively) roughly match with UCC value of 3.8 and 0.75 (McLennan and Taylor, 1991; Liu et al., 2007; Rudnick and Gao, 2003). Elemental ratios such as Th/Sc, Th/Co and Cr/Th are extremely useful in determining provenance of the sediments (Tao et al., 2014; Tawfik et al., 2017). Comparison of these ratios with the sediments derived from felsic and mafic rocks, and UCC further supports the mixed provenance of Pilikarar sediments (Table

6). The depletion in Rb and its poor correlation with Al_2O_3 (r = -0.12) is attributed to deficiency of feldspars and/or intense chemical weathering and recycling (Tawfik et al., 2017), hence supporting the less proportion of feldspars and alteration of feldspars observed in thin section studies. Slightly depleted U in these sediments indicates weathering and recycling which results in oxidation of insoluble U^{4+} to soluble U^{6+}, and loss of U due to solution (McLennan and Taylor, 1991; Liu et al., 2007). Sr content of av. 63.09 ppm of these sediments is indicative of meteoric diagenesis of these sediments as meteoric water contains up to 150 ppm of Sr (Flugel, 1982). However, considerable depletion of Sr compared to UCC (320 ppm) can be attributed to loss of Sr during intense weathering (Kamber et al., 2005) which is in well accordance with the weathering indices.

REE patterns of the sediments are interpreted to reflect the average continental crust and thus negative Eu anomaly found in sedimentary rocks is similarly interpreted to be a feature of upper continental crust (McLennan, 1989).Thus, the obtained rare earth element composition of Pilikarar sediments showing enrichment in LREE and depletion in HREE, with negative Eu and Ce anomalies reflects the composition of upper continental crust (McLennan, 1989). Negative Ce anomaly characteristic of tholeiitic basalt(Henderson ,1984), hence its presence in Pilikarar sediments suggests derivation from Deccan Trap basalts, which is supported by presence of appreciable amount of augite in heavy mineral assemblage of these sediments. REE's are insoluble and present in very low concentrations of river and sea water; hence, the REE present in sediments are chiefly transported as particulate matter and reflect chemistry of their source (Rollinson, 1993). The Eu/Sm ratio (av. 0.58) of these sediments is close to the upper limit of the range (Eu/Sm 0.16 to 0.55) for average basalt (Henderson, 1984) and significantly lower than that of UCC (0.21). The Y/Ho ratio for these sediments (av. 1.57) is also close to that of UCC (1.47) (Piper and Bau, 2013). Thus major, trace and rare earth element compositions of Pilikarar sediments are suggestive of derivation from Vindhyan Supergroup sediments, Deccan Trap basalts and dykes from Narmada Valley (Roser and Korsch, 1988; Mahoney, 1988; Seth et al., 2009).

The obtained value -9.25 ‰ of $\delta^{13}C$, and -1.60 ‰ of $\delta^{18}O$ of the rhizolith in the Pilikarar Formation lie well within the range of world calcrete between -12 to + 4 for $\delta^{13}C$ and -9 to +3 for $\delta^{18}O$; as given by Talma and Netterberg (1983) and Salomans and Mook, (1986 a, b). The observed $\delta^{18}O$

value of -1.60 ‰ is suggestive of input of meteoric water and related meteoric diagenesis, as $\delta^{18}O$ of pedogenic carbonate is considered to be in equilibrium with that of soil water, while isotopic composition of soil water is related to that of meteoric water(Srivastava, 2001; Khadkikar et al., 2000). The obtained isotopic compositions of calcretes support pedogenic and /or shallow groundwater origin for the calcretes under study (Cerling, 1984; Beckner and Mozley, 1998; Brlek and Glumec, 2014). The negative stable isotopic composition of rhizolith ($\delta^{18}O$ = -1.60 ‰ and $\delta^{13}C$ = -9.25 ‰) are suggestive of vadose diagenetic conditions and related subaerial exposure of the Pilkarar sediments. The obtained $\delta^{13}C$ values are suggestive of paleovegetation cover mixed C3 and C4 type plants with dominance of C3 plants (Salomons and Mook, 1986a,b; Quade et al., 1989; Purvis and Wright, 1991; Wright et al., 1993; Tanner, 2010). The obtained paleotemperatures of 21.44° C of calcretes from Pilikarar Formation is an indicator of C3 dominated vegetation. According to Yamori et al., (2013), optimum temperature for photosynthesis of C3 plants is around 25°C and that for C4 plants is about 35°C, and their photosynthesis is inhibited at temperatures of about 45° C and 48° C respectively. Thus, paleotemperature estimate of rhizolith from Pilikarar Formation indicate C3-C4 mixed vegetation with dominance of C3 plants. The obtained value of $p$$CO_2$(241.5 ppmV) in general indicates semiarid climate at the time of formation of the calcrete (Li et al., 2013).

CONCLUSION

The Pilikarar Formation represent the deposits of alluvial fan on the basis of :

1. Development of bouldery conglomerate lithofacies representing debris flow deposits. The clast composition of these suggests derivation from Vindhyan Supergroup sediments, Deccan trap basalts and laterite.

2. The occurrence of Pilikarar fan at the base of Vindhyan range and its nearness to Son-Narmada North Fault suggest that both tectonics as well as climate played role in generation of debris flows to build the Pilikarar alluvial fan.

3. For the construction of Pilikarar alluvial fan, catastrophic but infrequent primary process of debris flow is responsible while the associated caliche nodules and rhizolith are the result of secondary process operative during inactive period of fan aggradations. The presence of caliche nodules and rhizoliths

particularly in middle part of Pilikarar Formation are suggestive of semi arid climatic conditions and related subaerial exposure, while presence of ferruginous cement in the uppermost part of Pilikarar Formation is suggestive of oxidizing diagenetic conditions undergone by these sediments.

4. The quartzose arenitic nature of these sediments, together with moderately high ZTR index with rounded nature of ultrastable grains along with presence of augite, staurolite, garnet, sillimanite, kyanite, sphene, zoisite, spinel, chlorite, hornblende, anataze; presence of illite, kaolinite and montmorillonite clays; major, trace and rare earth element compositions; suggests mineralogical maturity and recycled nature of Pilikarar sediments derived from mixed provenance of Precambrian granite, metapelite-shale; Vindhyan Supergroup; Deccan trap basalt and laterite.

5. The stable isotopic composition of calcrete of Pilikarar Formation and value of pCO$_2$ are suggestive meteoric vadose digenesis under moderate paleotemperature related with subaerial exposure of sediments, with dominance C3 type of paleovegetation and then prevailing semiarid conditions.

Acknowledgements:

The first author is thankful to Department of Science and Technology (DST), New Delhi; for financial assistance (SR/S4/ES-477/2009). The authors thank Head, Department of Geology, Savitribai Phule Pune University; for providing necessary facilities during this work. We thank Drs. Abhay Mudholkar, J. N Pattan, G. Parthiban, from NIO, Goa; for providing major oxide and trace, REE data respectively. Dr. D. J. Patil, NGRI, Hyderabad, is thanked for providing C and O stable isotope data.

References

Ali, S., Stattegger, K. D., Garbe-Schönberg, M., Frank, M. , Kraft, S. and Kuhnt, W. (2014). The provenance of Cretaceous to Quaternary sediments in the Tarfaya basin, SW Morocco: Evidence from trace element geochemistry and radiogenic Nd–Sr isotopes. *Journal of African Earth Science*, 90, 64–76.

Armstrong-Altrin, J. S., Lee, Y. I., Kasper-Zubillaga, J. J., and Trejo-Ramírez, E. (2017). Mineralogy and geochemistry of sands along the Manzanillo and El Carrizal beach areas, southern Mexico: implications for palaeoweathering, provenance and tectonic setting. *Geological Journal*, 52, 559-582.

Armstrong-Altrin, J. S., Nagarajan, R., Madhavaraju, J., Rosalez-Hoz, L., Lee, Y. I., Balaram, V., Cruz-Martinez, A., and Avila-Ramirez, G. (2013). Geochemistry of the Jurassic and upper Cretaceous shales from the Molango Region, Hidalgo, Eastern Mexico: implications of source area weathering, provenance, and tectonic setting. *Comptes Rendus Geosciences*, 345, 185–202.

Bahlburg, H. and Dobrzinski, A. (2009). A review of the Chemical Index of Alteration (*CIA*) and its application to the study of Neoproterozoic glacial deposits and climate transitions, In: Arnaud, E., Halverson, G.P. & Shields, G.A., (Eds.), *The Geological Record of Neoproterozoic Glaciations*. *Geological Society, London, Memoir*, 81 -93.

Banerjee, A. and Banerjee, D. M. (2010). Modal analysis and geochemistry of two sandstones of the Bhander Group (Late Neoproterozoic) in parts of the Central Indian Vindhyan basin and their bearing on the provenance and tectonics.*Journal of Earth System Sciences*, 119,825–839.

Blair, T. C. and McPherson, J. G. (1993). The Trollheim alluvial fan and facies modelrevisited; *Geological Society of America Bulletin*, 105, 564-567.

Blair, T. C. and McPherson, J. G. (1994). Alluvial fans and their natural distinction from rivers based on morphology, hydraulic processes, sedimentary processes and facies assemblages, *Journal of Sedimentary Petrology*, A64, 450-489.

Blair, T. C. and McPherson, J. G. (2009). Processes and forms of alluvial fans. In: Parsons A. J. and Abrahams A.D. (Eds.) *Geomorphology of Desert Environments*, 2nd ed., 413-467.

Blatt, H. (1992).*Sedimentary Petrology*. W. H. Freman and Co. Ltd., NewYork Oxford, IInd Edition, 514p.

Braithwaite, C. J. R. (1989). Displacive calcite and grain breakage in sandstone, *Journal Sedimentary Petrology*, 59, 258-266.

Brlek, M. and Glumec, B. (2014). Stable isotopic signatures of biogenic calcrete marking discontinuity surfaces: a case study from Upper Cretaceous carbonates of central Dalmatia and eastern Istria, Croatia. *Facies*, 60, 773-788.

Brooke, S., Whittaker, A., Watkins, S., and Armitage, J. (2017). Decoding sediment transport dynamics on alluvial fans from spatial changes in grain size, Death Valley, California. GU General Assembly Conference AbstractsVolume 19, 6677.

Buczynski, C. and Chafetz, H. S. (1987). Siliciclastic grain breakage and displacement due to carbonate crystal growth: an example from Lueders Fonnation of North Central Texas, USA. *Sedimentology*, 34, 837-843.

Bull, W. B. (1977). The alluvial fan environment. *Progress in Physical Geography*, 1, 222-270.

Carver, R. E. (Ed.) (1971). Procedures in Sedimentary Petrology. John-Wiley and Sons, New York, 653 p.

Cerling, T. E. (1984). The stable isotopic composition of modern soil carbonate and its relationship to climate.*Earth and Planetary Science Letter*, 71, 229-240.

Cerling, T. E. (1999). Stable carbon isotopes in palaeosol carbonates. In: M. Thiry and R. Simon-Coinçon (Eds.) *Palaeoweathering, Palaeosurfaces and Related Continental Deposits. Special Publication International Association of Sedimentologists* No. 27, 43–60.

Chamyal, L. S., Khadkikar A. S., Malik J. N. and Maurya D. M. (1997). Sedimentology of the Narmada alluvial fan, western India. *Sedimentary Geology*, 107, 263–279.

Chen, L., Steel, R. J., Guo, F., Olariu, C., and Gong, C. (2017). Alluvial fan facies of the

Yongchong Basin: Implications for tectonic and paleoclimatic changes during Late

Cretaceous in SE China, *Journal of Asian Earth Science,* 134, 37-54.

Choubey, V. D. (1971). Narmada Son lineament, India. *Nature Physical Science*, 55, 392-397.

Costa, J. E. (1988). Rheologic, geomorphic, and sedimentologic differentiation of water floods, hyperconcentrated flows, and debris flows. Flood Geomorphology. John Wiley & Sons New York,113-122.

Cox, R., Lowe, D. R. and Cullers, R. L. (1995). The influence of sediment recycling and basement composition on evolution of mudrock chemistry in the southwestern United States. *Geochemica et Cosmochemica Acta*, 59,2919–2940.

Cullers, R. L. (1988). Mineralogical and chemical changes of soil and stream sediment formed by intense weathering of the Danberg granite, Georgia, USA. *Lithos,* 21, 301–314.

Cullers, R. L. (1994). The controls on the major and trace element variation of shales,

siltstones, and sandstones of Pennsylvanian-Permian age from uplifted continental

blocks in Colorado to platform sediment in Kansas, USA. *Geochemica et Cosmochemica Acta*, 58, 4955–4972.

Cullers, R. L. (2000). The geochemistry of shales, siltstones and sandstones of Pennsylvanian-Permian age, Colorado, USA: implications for provenance and metamorphic studies. *Lithos*, 51, 181–203.

Cullers R. L. and Podkovyrov V. N. (2000). Geochemistry of the Mesoproterozoic Lakhanda

shales in southeastern Yakutia, Russia: implications for mineralogical and provenance control, and recycling. *Precambrian Research*, 104, 77–93.

De Haas, T., Densmore, A. L., Stoffel, M., Suwa, H., Imaizumi, F., Ballesteros-Cánovas, J. A. and Wasklewicz, T., (2018). Avulsions and the spatio-temporal evolution of debris-flow fans. *Earth Science Reviews*, 177, 53-75.

Ekart, D. D., Cerling, T. E., Montañez, I. P. and Tabor, N. J. (1999). A 400 million year carbon isotope record of pedogenic carbonate: implications for paleoatmospheric carbon dioxide. *American Journal of Science*, 299, 805–827.

Fedo, C. M., Nesbitt, H. W. and Young, G. M. (1995). Unravelling the effects of potassium metasomatism in sedimentary rocks and paleosols, with implications for weatheringconditions and provenance. *Geology*, 23, 921-924.

Franke, D., Jens, H. and Matthias, H. (2015). A combined study of radar facies, lithofacies and three-dimensional architecture of an alpine alluvial fan(Illgraben fan, Switzerland). *Sedimentology*, 62, 57–86.

Friedman, I. and O'Neil, J. R. (1977). Compilation of stable isotope fractionation factors of geochemical interest. In: Fleischer M. (Ed.) *Data of Geochemistry.U.S.Geological Survey Professional Paper* 440 KK, pp. 1-12.

Galehouse, J. S. (1971). Sedimentation analysis, In: Carver R. E. (Ed.) *Procedures in Sedimentary Petrology*, John Wiley & Sons, New York, pp. 69-94.

Garzanti, E., Padoan, M., Andò, S., Resentini, A., Vezzoli, G., and Lustrino, M., (2013a). Weathering and relative durability of detrital minerals in equatorial climate: Sand petrology and geochemistry in the East African Rift. *Journal of Geology*, 121, 547–580.

Garzanti, E., Padoan, M., Peruta, L., Setti, M., Najman, Y., and Villa, I. M., (2013b). Weathering geochemistry and Sr-Nd fingerprints of equatorial upper Nile and Congo muds. *Geochemistry Geophysics Geosystems*,14, 292–316.

Ghinassi, M. and Ielpi, A.(2016).Morphodynamics and facies architecture of stream flow-dominated, sand-rich alluvial fans, Pleistocene Upper Valdarno Basin, Italy.*Geological Society of London Special Publications*,440, https://doi.org/10.1144/SP440.1

Geological Survey of India (1993). Geological map of Son-Narmada-Tapti Lineament Zone, Central India, Special Project CRUMANSONATA, 1881-89, *Unpublished Report Geological Survey of India.*

Ghosh, D. B. (1976). The nature of Narmada Son Lineament. *Miscellaneous Publication Geological Survey of India*, 34, 119-133.

Gupta, H., Chakrapani, G. J., Selvaraj, K. and Kao, S. J. (2011). The fluvial geochemistry, contributions of silicate, carbonate and saline-alkaline components to chemical weathering flux and controlling parameters: Narmada River (Deccan Traps), India, *Geochemica et Cosmochemica Acta*, 75, 800-824.

Harnois, L. (1988). The CIW index: A new chemical index of weathering. *Sedimentary Geology*, 55**,** 319–322.

Hays, P. D. and Grossman, E. L. (1991). Oxygen isotope in meteoric calcite cements as indicators of continental paleoclimate. *Geology*, 19, 441-444.

Henderson, P. (1984).*Rare Earth Element Geochemistry*, Elsevier, Amsterdam, 510 p.

Herron, M. M. (1988). Geochemical classifications of terrigeneous sands and shales from core to log data. *Journal of Sedimentary Petrology*, 58, 820-829.

Hubert, J. F. (1962). A zircon-tourmaline-rutile maturity index and the interdependence of the composition of heavy mineral assemblage with gross composition and the texture of sandstones. *Journal of Sedimentary Petrology*, 32, 440-450.

Ingram R. L. (1971). Sieve analysis, In: Carver R. E. (Ed.) *Procedures in Sedimentary Petrology*, John Wiley and Sons, New York, pp. 49-68.

Iverson, R. M. (1997). The physics of debris flows. *Reviews of Geophysics*, 35, 245-296.

Jakob, N. and Hungr, O. (2005). *Debris flow hazards and related phenomena*. Springer Praxix Books, Chichester, UK. 739p.

Jafarzadeh, M. and Hosseini-Barzi, M. (2008). Petrography and geochemistry of Ahwaz Sandstone Member of Asmari Formation, Zagros, Iran: implications on provenance and tectonic setting. *Revista Mexicana de Ciencias Geológicas*, 25, 247-260.

Johnson, A. M. (1970). Formation of debris flow deposits.In: *Physical Processes inGeology,* San Francisco, Freeman, Cooper, 433-448.

Kale, V. S. (1986). The Narmada- Son structure A (Precambrian) reappraisal. Proceedings of Seminar 'Crustal Dynamics', Indian Geophysical Union, Hyderabad, 140-160.

Kamber, B. S., Greig, A., and Collerson, K. D. (2005). A new estimate for the composition of weathered young upper continental crust from alluvial sediments, Queensland, Australia. *Geochimica et Cosmochimica Acta* 69, 1041-1058.

Kettanah, Y. A., Kettanah, M. Y. and Wach, G. D. (2014). Provenance, diagenesis and reservoir quality of the Upper Triassic Wolfiville Formation, Bay of Fundy, Nova Scotia, Canada. *In:* Scott R. A., Smyth H. R., Morton A. C. and Richardson N. (Eds.) *Sediment Provenance studies in Hydrocarbon exploration and Production, Geological Society of London Special Publication*., 386,75-110.

Khadkikar, A. S., Chamyal, L. S. and Ramesh, R. (2000). The character and genesis of calcretes in semi-arid to sub-humid alluvial systems and its bearing on the interpretation of ancient climates. *Palaeogeography Palaeoclimatology Palaeoecology*, 142, 239–262.

Li, X., Jenkyns, H. C, Zhang, C., Wang, Y., Liu, L. and Cao, K. (2013).Carbon isotope signatures of pedogenic carbonates from SE China: rapid atmospheric pCO2 changes during middle–late EarlyCretaceous time. *Geological Magazine*,151, 1-20Cambridge university press.

Liu, S., Lin, G., Liu, Y., Zhou, Y., Gong, F. and Yan, Y. (2007).Geochemistry of Middle Oligocene–Pliocene sandstones from the Nanpu Sag, Bohai Bay Basin (Eastern China):Implications for provenance, weathering, and tectonic setting, *Geochemical Journal*, 41, 359-378.

Lodders, K., and Fegley, B. (1998). The planetary scientist's companion. Oxford University Press, New York, Oxford, 371p.

Longman, M. W. (1980). Carbonate diagenetic texture from near surface diagenetic environments, *Bulletin American Association of Petroleum Geologists*,64, 461-487.

Mahoney, J. J. (1988). Deccan Traps, In: Macdougall J. D. (Ed.), *Continental Flood Basalts*, Springer, Dordrecht, 151-194.

Mason, B. and Moore, C. B. (1982). *Principles of Geochemistry*, John Wiley and sons, New York, 344 p.

McLennan, S. M. (1989). Rare earth elements in Sedimentary rocks: Influence of Provenance and Sedimentary Processes. *Reviews in Mineralogy*,21, 169-200.

McLennan, S. M. and Taylor, S. R. (1991). Sedimentary rocks and crustal evolution revisited: tectonic setting and secular trends. *Journal of Geology*, 99, 1-21.

McLennan, S. M., Hemming, S., McDaniel, D. K. and Hanson, G. N. (1993). Geochemical approaches to sedimentation, provenance and tectonics. *Special papers Geological Society of America*, 21-21.

Miall, A. D. (2006).*The Geology of Fluvial Deposits Sedimentary Facies, Basin*

Analysis, and Petroleum Geology. Springer-Verlag Berlin Hedelberg, 582 p.

Mishra, D. C. (2015). Plume and Plate tectonics model for formation of some Proterozoic basins of India, along contemporary mobile belts: Mahakoshal-Bijawar, Vindhyan and Cuddapah basins. *Journal of The Geological Society of India*, 85, 525-536.

Mohammadi, N., Rais, S. and Habib, T. (2014).Provenance, tectonic setting and paleoclimate of Upper Bhander Sandstone in parts of Raisen district of Madhya Pradesh (India). *International Journal of Advance Earth and Environment Science*, 2, 39-45.

Morse, J. W. and Mackenzie, F. T. (1990). Geochemistry of Sedimentary Carbonates, Elsevier Amsterdam, New York, Developments in Sedimentology, 48,707 p.

Morton, A. C. and Hallsworth, C.R. (1994). Identifying provenance-specific features of detrital heavy mineral assemblages in sandstones. *Sedimentary Geology*, 90, 241-256.

Morton, A. C. and Hallsworth, C. R. (1999). Processes controlling the composition of heavy mineral assemblages in sandstones. *Sedimentary Geology*, 124, 3-29.

Morton, A.and Milne, A. (2012). Heavy mineral stratigraphic analysis on the Clair Field, UK, west of Shetlands: a unique real-time solution for red-bed correlation while drilling. *Petroleum Geoscience*, 18, 115 –128.

Nesbitt, H. W. and Young, G. M. (1982). Early Proterozoic climates and plate motions inferred from major element chemistry of lutites. *Nature*, 299, 715–717.

Nesbitt, H. W. and Young, G. M. (1984). Prediction of some weathering trends of plutonic and volcanic rocks based on thermodynamic and kinetic considerations. *Geochemica et Cosmochemica Acta*, 48, 1523-1534.

Nesbitt, H. W. and Young, G. M. (1989). Formation and diagenesis of weathering profiles. *Journal of Geology*, 97, 129–147.

Ohta, T. and Arai, H. (2007).Statistical empirical index of chemical weathering in igneous

rocks: A new tool for evaluating the degree of weathering. *Chemical Geology*, 240, 280-297.

Okada, H. (1971). Classification of sandstone: Analysis and proposal. *Journal of Geology*, 79, 509-525.

Parker, A. (1970). An index of weathering for silicate rocks. *Geological Magazine*, 107, 501-504.

Pettijohn, F. J., Potter, P. E and Siever, R. (1972). *Sand and Sandstones*, Springer Verlag New York.

Piper, D. Z. and Bau, M. (2013). Normalized Rare Earth Elements in Water, Sediments, and Wine: Identifying Sources and Environmental Redox Conditions. *American Journal of Analytical Chemistry*, 4, 69-83.

Purevjav, N. and Roser, B. (2013). Geochemistry of Silurian–Carboniferous sedimentary rocks of the Ulaanbaatarterrane, Hangay–Hentey belt, central Mongolia: Provenance, paleoweathering, tectonic setting, and relationship with the neighbouring Tsetserleg terrane. *Chemie der Erde*, 73, 481– 493.

Purvis, K. and Wright, V. P. (1991).Calcretes related to phreatophytic vegetation from

Middle Triassic Otter Sandstone of South west England. *Sedimentology*, 38, 539-551.

Quade, J., Cerling, T. E. and Bowman, J.R. (1989). Development of monsoon revealed by marked ecological shift during the latest Miocene in the Northern Pakistan, *Nature*, 342, 163-166.

Reading, H. Q.(1981).*Sedimentary Environments and Facies*, Blackwell Scientific Publications, Oxford, London, 569 p.

Reading, H. Q. (2006).*Sedimentary Environments: Processes, Facies, and Stratigraphy*, Blackwell Publishing, India, 688p.

Reineck, H. E. and Singh, I. B. (1980). *Depositional Sedimentary environments*, Springer Verlag, Berlin, Heidelburg, New York, 549 p.

Renwick, W. H. (1977).Erosion caused by intense rainfall in a small catchment in New York State, *Geology*, 5, 361-364.

Robinson, S. A., Andrews, J. E., Hesselbo, S. P., Radley, J. D., Dennis, P. F., Harding, I. C., and Allen, P. (2002). Atmospheric pCO2 and depositional environment from stable-isotope geochemistry of calcrete nodules (Barremian, Lower Cretaceous, Wealden Beds, England). *Journal of Geological Society of London*, 159, 215-224.

Rollinson, H. (1993). *Using geochemical data: evaluation, presentation, interpretation*. Pearson Education Ltd, Essex, London. 352 .

Roser, B. P. and Korsch, R. J. (1986). Determination of tectonic setting of sandstone–mudstone suites using SiO_2 content and K_2O/Na_2O ratio. *Journal of Geology*, 94, 635–650.

Roser, B. P and Korsch, R. J. (1988). Provenance signatures of sandstone-mudstone suites determined using discriminant function analysis of major of major element data. *Chemical Geology*, 67, 119-139.

Roser, B. P., Cooper, R. A., Nathan, S. and Tulloch, A. J. (1996). Reconnaissance sandstone geochemistry, provenance and tectonic setting of the lower Paleozoic terrains of the west coast and Nelson, New Zeland. *New Zeland Journal of Geology and Geophysics*, 39, 1-16.

Rudnick, R. L. and Gao, S. (2003).Composition of the continental crust In: Rudnick, R.L,

Holland, H.D and Turekian, K. K. (Eds) *Treatise on Geochemistry*, 3,1-64.

Salomons, W. and Mook, W. G. (1986 a). Isotope geochemistry of carbonate dissolution and reprecipitation in soils. *Soil Science*, 122, 15-24.

Salmons, W. and Mook, W. G. (1986b). Isotope geochemistry of carbonates in weathering zone, In: Fritz P. and Frontes J. Ch. (Eds.) *Handbook of Environmental Isotope Geochemistry*. New York,2, 239-269.

Seth, H., Ray, J. S., Ray, R., Vanderkluysen, L., Mahoney, J. J., Kumar, A., Shukla, A. D., Das, P., Adhikari, S. and Jana, B. (2009). Geology and geochemistry of Pachmarhi dykes and sills, Satpura Gondwana basin, Central India: Problems of dikes-sill-flow correlation in the Deccan Traps. *Contribution to Mineralogy and Petrology*, 158, 357-380.

Sohn, Y. K., Rhee, C. V. and Kim, B. C. (1999). Debris flow and hyperconcentrated flood-flow deposits in an Alluvial fan, Northwestern part of the Cretaceous Yongdong basin, Central Korea. Journal of Geology, 107, 111-132.

Soni, M. K., Chakraborty, S. and Jain, V. K. (1987).Vindhyan Supergroup- A review, In: *Purana Basins of Peninsular India (Middle to Late Proterozoic)*, *GeologicalSociety of India Memoir No*. 6, 87-138.

Srivastava, P. (2001). Paleoclimatic implications of pedogenic carbonates in Holocene soils of Gangatic plains, India. *Palaeogeography Palaeoclimatology Palaeoecology*, 172, 207-222.

Stainstreet, I. G. and McCarthy, T. S.(1993). The Okavango fan and the classification of subaerial fan systems, *Sedimentary Geology*, 85, 115-133.

Talma, A. S. and Netterberg, F. (1983).Stable isotope abundances in calcretes. *Geological Society of London Special Publication*, 11, 221-233.

Tandon, S. K. and Friend, P. F. (1989). Near surface shrinkage and carbonate replacement processes Arran Cornstone Formation, Scotland. *Sedimentology*, 36, 1113-1126.

Tanner, L. H. (2010). Continental carbonates as indicators of paleoclimate. In: Alonso-Zarza A.M. , Tanner L. H. (Eds.) *Carbonates in continental settings: geochemistry, diagenesis and applications. Developments in Sedimentology*, 62, 179-206.

Tao, H., Sun, S., Wang, Q., Yang, X., and Jiang, L. (2014). Petrography and geochemistry of Lower Carboniferous greywacke and mudstones in Northeast Junggar, China: Implications for provenance, source weathering, and tectonic setting. *Journal of Asian Earth Sciences*, 87, 11-25.

Tawfik, H. A., Salah, M. K., Maejima, W., Armstrong-Altrin, J. S., Abdel-Hameed, A. M. T., and El Ghandour, M. M. (2017). Petrography and geochemistry of the Lower Miocene Moghra sandstones, Qattara Depression, north Western Desert, Egypt. *Geological Journal*, pp. 1-16.DOI: 10.1002/gj.3025.

Tiwari, M. P. and Bhai, H.Y. (1997). Quaternary stratigraphy of the Narmada Valley. *Geological Survey of India Special Publication* No.46, 33-63.

Tucker, M. E. (2001). *Sedimentary Petrology*, 3rd ed., Blackwell Science, Oxford UK, 262 p.

Tucker, M. E. and Wright, V. P. (1990). *Carbonate Sedimentology*, Blackwell Scientific Publications, Oxford London, 482 p.

Vaidyanathan, R. and Ramakrishnan, M. (2008). *Geology of India*. Geological Society of India, 2, 833-906.

Verma, S. P. and Armstrong-Altrin, J. S. (2013). New multi-dimensional diagrams for

tectonic discrimination of siliciclastic sediments and their application to Precambrian basins. *Chemical Geology*, 355, 117-133.

Verma, S. P., and Armstrong-Altrin, J. S. (2016). Geochemical discrimination of siliciclastic

sediments from active and passive margin settings. *Sedimentary Geology*, 332, 1-12.

Verma, R. K. and Banarjee, P. (1992). Nature of continental crust along the Narmada–Son Lineament, inferred from gravity and deep seismic sounding data. *Tectonophysics*, 202, 375–397.

Visher, G. S. (1969). Grain size distribution and depositional processes. *Journal of Sedimentary Petrology*, 49, 41-62.

Weaver, C. E. (1989). *Clays, Muds and Shales*. Elsevier Science Publishing Company Inc., NewYork, 819 p.

Wright, V. P., Turner, M. S., Andrews, J. E. and Spiro, B. (1993). Morphology and significance of supermature calcretes from the Upper Old Red Sandstone of Scotland. *Journal of Geological Society of London*, 150, 871-883.

Xie, Y., Yuan, F., Zhan, T., Kang, C. and Chi, Y. (2017). Geochemical and isotopic characteristics of sediments for the Hulun Buir Sandy Land, northeast China: implication for weathering, recycling and dust provenance. *Catena*, 160, 170-184.

Young, W. S. (1976). Petrographic textures of detrital polycrystalline quartz as an aid to interpret crystalline source rock. *Journal of Sedimentary Petrology*, 46, 595-603.

Jour. Indian Association of Sedimentologists, Vol. 36, No. 1 & 2 (2019), pp.51-64
ISSN Online 2582 – 2020
ISSN Print 0970 – 3268

Petrographic Study of the Meso-Neo Proterozoic Kaimur Sandstone, Vindhyan Supergroup, Chittorgarh, southeastern Rajasthan, India: Implication for Provenance, Tectonic Setting and Paleoclimate

Mujeebul Hasan* and Abdullah Khan
Department of Geology, Aligarh Muslim University, Aligarh 202002, India.
*Email: mujeebkhan425@gmail.com

Abstract: Proterozoic Kaimur Sandstone succession rests unconformably on calcium carbonate-rich succession of the Khorip Group (Lower Vindhyan) in and around Chittorgarh, southeastern part of Rajasthan. The Kaimur Group consists multicoloured, medium -to fine-grained, thick beds of sandstones with thin beds of sandy shale and flagstone, display of various primary sedimentary structures such as current bedding, ripple marks and mud cracks. Kaimur quartz arenite composed of varieties of quartz with rare feldspar, mica, rock fragments, and heavy minerals. The X-ray diffraction (XRD) data has shown that quartz is more abundant with little iron oxide mineral. The provenance, tectonic setting and paleoclimatic of the Kaimur Sandstone is evaluated using integrated petrographic studies. Analysis reveals detrital derivation from granitic and metamorphic Precambrian basement source rocks of a craton interior setting with a minor quartzose recycled sedimentary rock. Intense weathering in warm and humid climate indicated lack of feldspar and rock fragments. Paleocurrent indicate flow from NW and SW.

Keywords: Kaimur Sandstone, Petrography, X-ray diffraction, Provenance, Tectonic setting, Southeastern Rajasthan.

INTRODUCTION

Mineralogical composition of siliciclastic rocks is influenced by various parameters including provenance, tectonic setting, weathering condition, sediment transport processes and depositional environment (Armstrong-Altrin, 2015, Dickinson, 1988; Johnsson and Basu, 1993; Boggs, 2006; Critelli, 2018). Siliciclastic rock provenance studies usually aim to disclose composition and geological evolution of sediment source area and to constrain the tectonic setting of the depositional basin (Verma and Armstrong-Altrin, 2013&2016; Dickinson, 1985). Quantitative mineralogical evolution of quartz, feldspar, rock fragments and undulosity in detrital quartz of sandstone are useful for investigating classification, Tectonic setting,

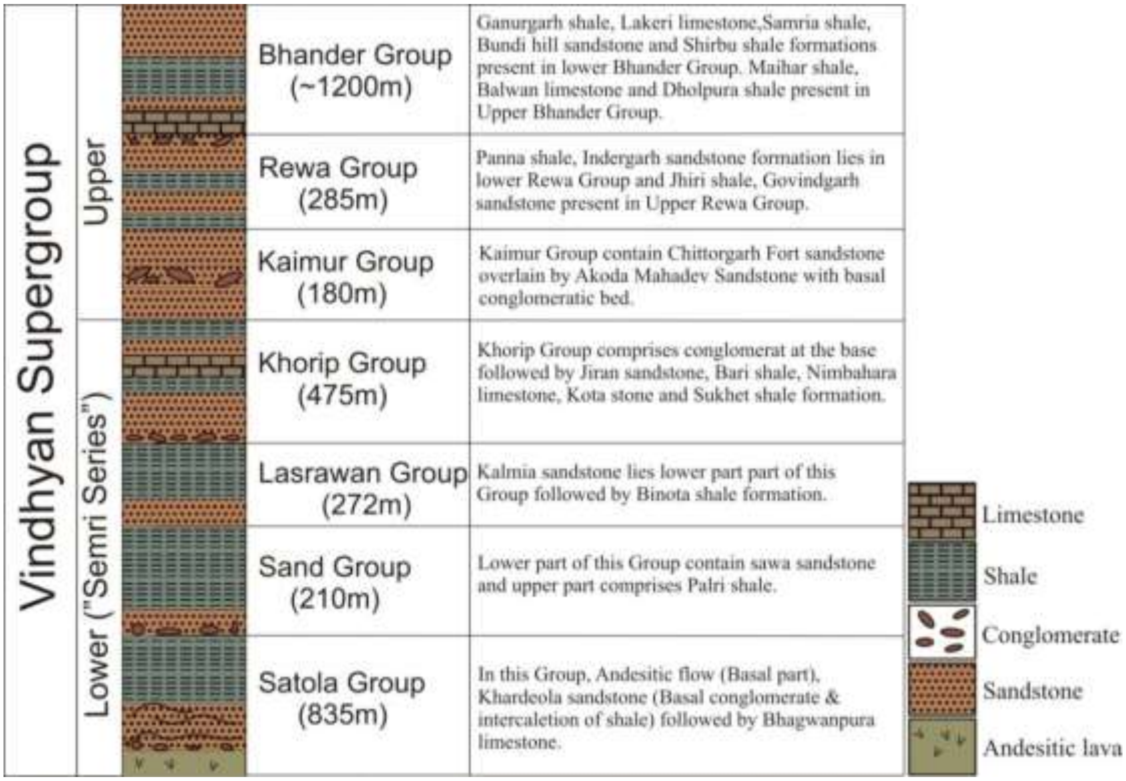

Fig. 1: Generalized lithostratigraphy and correlation of Rajasthan and Son valley columnar section, Vindhyan Supergroup, modified after Malone et al. (2008) and Khan (2013).

provenance and paleoclimatic condition of Kaimur Sandstone. Frequency of different type of quartz grain used to deduce the type of source rock (Basu et al., 1975; Tortosa et al., 1991), tectonic setting of sandstone reveal by using framework mineralogical composition (Crook, 1974; Dickinson and Suczek, 1979; Ingersoll and Suczek, 1979; Dickinson et al., 1983; Dickinson, 1985) and type of sandstone categorized by Folk (1980) classification scheme. Paleoclimatic condition during weathering of the source rock is explained by using Suttner et al. (1981) model.

From the sedimentological point of view, the Kaimur Sandstone of southeastern Rajasthan is less explored than Son Valley. In the present work, two analytical techniques used to determine the mineralogical composition of sandstone have been considered: (i) Petrography (optical analysis of thin sections); (ii) X-ray diffraction (XRD). The main objectives of this study are to evaluate source area composition, tectonic setting and to infer paleoclimatic conditions during deposition of the Kaimur Sandstones of southeastern Rajasthan.

GEOLOGICAL SETTING OF THE STUDY AREA

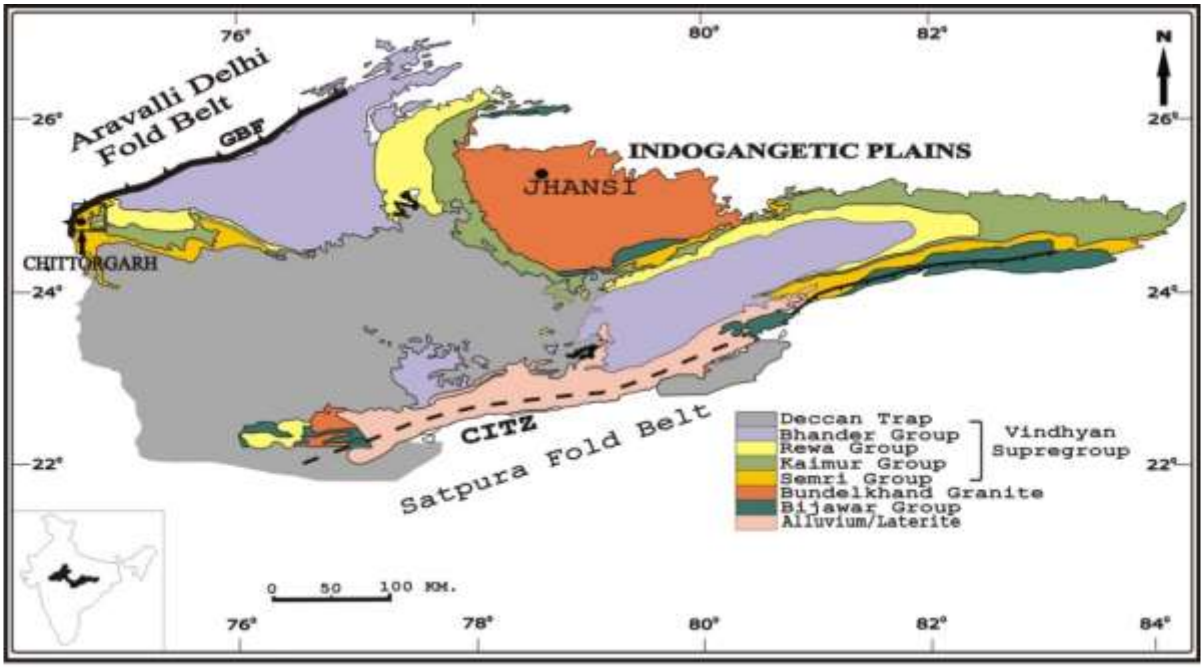

Fig. 2: Geological map of the Vindhyan Basin, Modified after Prasad and Rao (2006).

The 4500 m thick Vindhyan Supergroup is subdivided into two major successions on the basis of their distinct tectonic setting. The Lower Vindhyan developed in an intracratonic rift basin (Bose et al., 1997) and Upper Vindhyan in an intracratonic sag basin (Sarkar et al., 2002). Carbonate controlling Lower Vindhyan sedimentary succession composed by Satola, Sand, Lasrawan and Khorip Groups in ascending stratigraphic order of Rajasthan can be correlated with Semri Group of Lower Vindhyan in Son Valley (Fig. 1). The siliciclastic controlling Upper Vindhyan succession subdivided further into the Kaimur, Rewa and Bhander Groups (Chaudhari et al., 1999; Prasad, 1984; Malone et al., 2008). Unconformity was identified between the Semri and succeeding groups (Soni et al., 1987).

In Rajasthan, Vindhyan basin in NW side bounded by the Delhi-Aravali orogenic belt and to the SE by the Satpura orogenic belt. Aravali and Satpura mobile belt are tectonic in nature show inherent disturbances feature characterized by existence of major zone of displacement specified as Great Boundary Fault Zone (GBFZ) in the west and Central Indian Tectonic Zone in the south (Fig. 2). The SSW boundary is concealed below Deccan continental flood basalt and the southern continuation by Indo-Gangetic alluvial plain. Great Boundary Fault is a NE and SW trending

QFR	QtFL	QmFLt
Q= Total quartz grain (Qm+Qp), where Qm= Monocrystalline quartz Qp= Polycrystalline quartz F= Total feldspar (P+K), where P= Plagioclase K= K-feldspar R= Total rock fragments including chert	Qt= Total quartz grain (Qm+Qp), where Qm= Monocrystalline quartz Qp= Polycrystalline quartz including chert F= Total feldspar L= Total lithic fragments	Qm= Monocrystalline quartz F= Total feldspar Lt= Total lithic fragments+ Polycrystalline quartz

Table 1. Key for counted and recalculated petrographic framework grain parameters of sandstones, after Folk (1980), Dickinson and Suczek (1979), Suttner and Dutta (1986).

major lineament which separating the Aravali-Delhi orogeny from the Vindhyan basin (Khan, 2013). The Achaean Berach granite and Palaeoproterozoic Delhi-Aravali Supergroup both are the basement of Vindhyan Supergroup (Raza et al., 2012).

The Kaimur Group of Rajasthan consists predominantly of quartzitic sandstone successions and it is broadly subdivided into two formations such as Chittorgarh Fort sandstone Formation overlain by Akoda Mahadev sandstone Formation. Chittorgarh Fort sandstone is generally showing pinkish white or dirty white in colour, fine to medium grain quartzitic sandstone with variable thickness of bedding (0.2 to 1.5m) having primary sedimentary structures mainly current bedding, herringbone cross-bedding, ripple marks and mud cracks. Akoda Mahadev sandstone formation contain Badanpur conglomerate in the basal portion and intercalation of silty shale present in the upper portion (Prasad, 1984). Kaimur formation occurs as small isolated ridges and hillocks in the vicinity of Chittorgarh but extensively, forming parallel ridges trending North-south, farther east. It is underlain by laminated to splintery Sukhet shale with variable sharp to intercalated contact and sandstone which crop out farther away in northeastern part of study area

SAMPLING AND ANALYTICAL TECHNIQUE

Petrographic analysis

Thirty four unweathered sandstone samples were taken from relatively less disturbed part of the Kaimur Sandstone outcrop with variation of lithofacies. The thin sections were prepared and examined under optical microscope. K-feldspar was identified mainly by staining of thin section by sodium cobaltinitrite solution (Carver, 1971). Modal analysis was performed using point-counting technique for evaluating quantitative mineralogical aspect of sandstone. About 300-350 framework grains were counted per thin section using Gazzi Dickinson point-counting technique (Ingersoll et al., 1984).

The parameters used in this study are provided in Table 1 and the relative proportion of quartz, feldspar and rock fragment are summarized in Table 2. Data are plotted on the diagrams proposed by Folk (1980), Basu et al. (1975), Tortosa (1991), Dickinson et al. (1985) and Suttner et al. (1981), to determine type of sandstone, source rock composition, tectonic setting and paleoclimatic condition.

Sample	**QFR**			**QtFL**			**QmFLt**		
	Q	F	R	Qt	F	L	Qm	F	Lt
KFST-1	99.44	0.00	0.56	100.00	0.00	0.00	93.60	0.00	6.40
KFST-2	100.00	0.00	0.00	100.00	0.00	0.00	94.06	0.00	5.94
KFST-3	98.87	0.00	1.13	98.87	0.00	1.13	93.68	0.00	6.32
KFST-4	99.52	0.28	0.20	99.72	0.28	0.00	93.05	0.28	6.67
KFST-5	98.59	0.00	1.41	98.59	0.00	1.41	95.04	0.00	4.96
KFST-6	98.62	0.00	1.38	99.74	0.00	0.26	92.90	0.00	7.10
KFST-7	100.00	0.00	0.00	100.00	0.00	0.00	92.67	0.00	7.33
KFST-8	96.49	0.46	3.05	96.98	0.46	2.56	86.00	0.47	13.53
KFST-9	100.00	0.00	0.00	100.00	0.00	0.00	93.22	0.00	6.78
KFST-10	97.51	0.00	2.49	98.06	0.00	1.94	89.18	0.00	10.82
KFST-11	98.79	0.00	1.21	98.79	0.00	1.21	94.42	0.00	5.58
KFST-12	98.44	0.00	1.56	99.20	0.00	0.80	94.17	0.00	5.83
KFST-13	100.00	0.00	0.00	100.00	0.00	0.00	93.12	0.00	6.88
KFST-14	98.25	0.48	1.27	98.88	0.48	0.64	88.51	0.48	11.01
KFST-15	98.65	0.00	1.35	98.65	0.00	1.35	89.55	0.00	10.45
KFST-16	98.51	0.00	1.49	98.51	0.00	1.49	95.17	0.00	4.83
KFST-17	100.00	0.00	0.00	100.00	0.00	0.00	90.12	0.00	9.88
KFST-18	99.52	0.00	0.48	100.00	0.00	0.00	94.54	0.00	5.46
KFST-19	98.81	0.30	0.89	99.70	0.30	0.00	91.03	0.30	8.66
KFST-20	97.26	0.00	2.74	98.06	0.00	1.94	93.58	0.00	6.42
KFST-21	100.00	0.00	0.00	100.00	0.00	0.00	93.00	0.00	7.00
KFST-22	99.79	0.00	0.21	100.00	0.00	0.00	94.57	0.00	5.43
KFST-23	98.38	0.00	1.62	98.38	0.00	1.62	91.00	0.00	9.00
KFST-24	100.00	0.00	0.00	100.00	0.00	0.00	94.04	0.00	5.96
KFST-25	100.00	0.00	0.00	100.00	0.00	0.00	94.88	0.00	5.12
KFST-26	99.04	0.00	0.96	99.40	0.00	0.60	92.80	0.00	7.20
KFST-27	99.20	0.00	0.80	100.00	0.00	0.00	95.22	0.00	4.78

KFST-28	100.00	0.00	0.00	100.00	0.00	0.00	91.89	0.00	8.11
KFST-29	99.30	0.00	0.70	100.00	0.00	0.00	91.85	0.00	8.15
KFST-30	99.62	0.38	0.00	99.62	0.38	0.00	93.46	0.38	6.16
KFST-31	98.79	0.00	1.21	99.42	0.00	0.58	90.37	0.00	9.63
KFST-32	98.82	0.00	1.18	100.00	0.00	0.00	89.34	0.00	10.66
KFST-33	99.28	0.00	0.72	100.00	0.00	0.00	89.94	0.00	10.06
KFST-34	99.54	0.00	0.46	99.54	0.00	0.46	91.80	0.00	8.20

Table 2: Recalculated percentage of detrital grain modes of Kaimur Sandstone of Chittorgarh, Rajasthan

X-ray diffraction analysis

Bulk powder samples of Kaimur Sandstones have been quantitatively analyzed by X-ray diffractometer (Rigaku Ultima IV, CIF Jamia Millia Islamia, New Delhi) for their mineral composition. The samples have scanned in 2θ

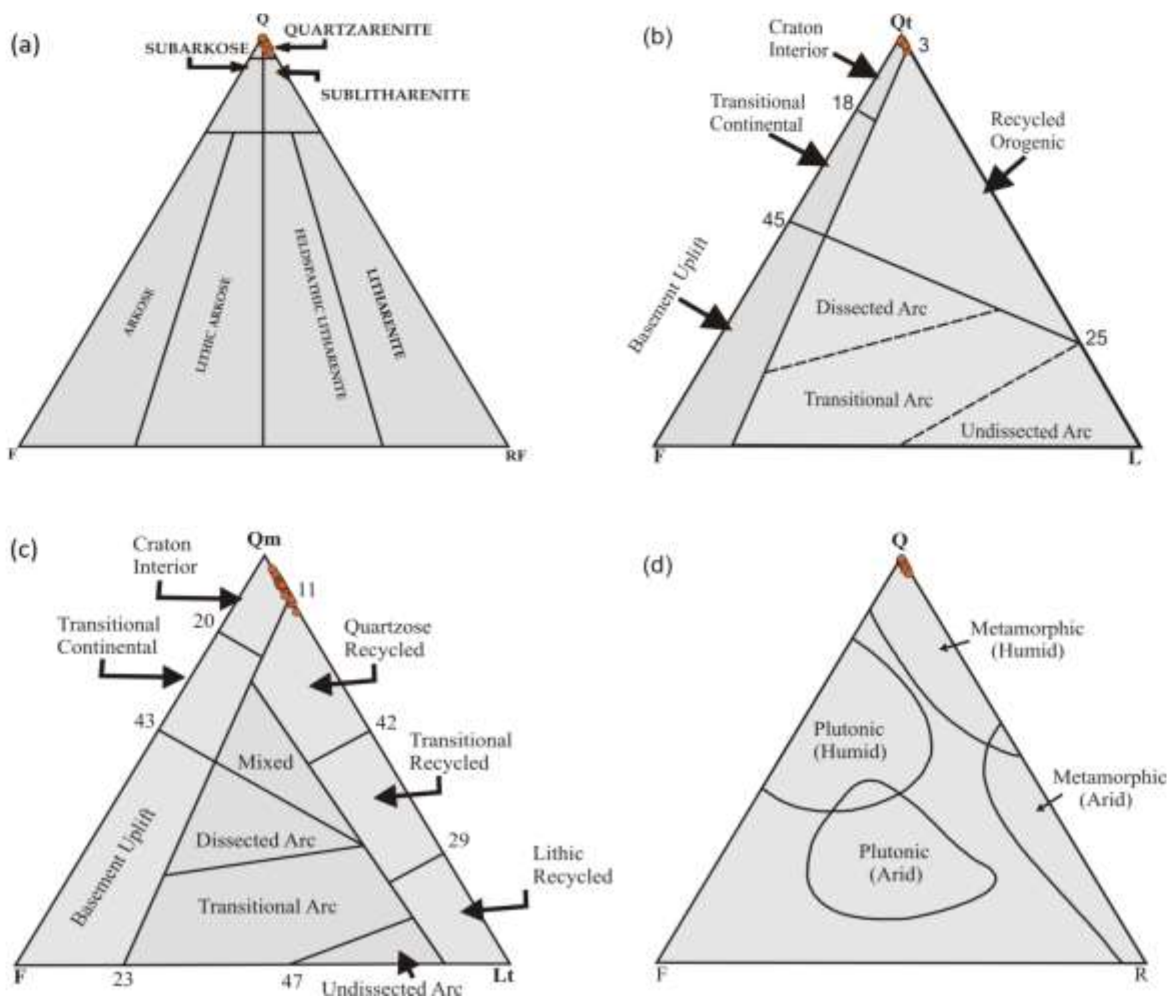

Fig. 3: Ternary plots of Kaimur Sandstone. QFRF diagram, after Folk (1980), QtFL & QmFLt diagram, after Dickinson (1985) and QFR diagrams, after Suttner et al. (1981).

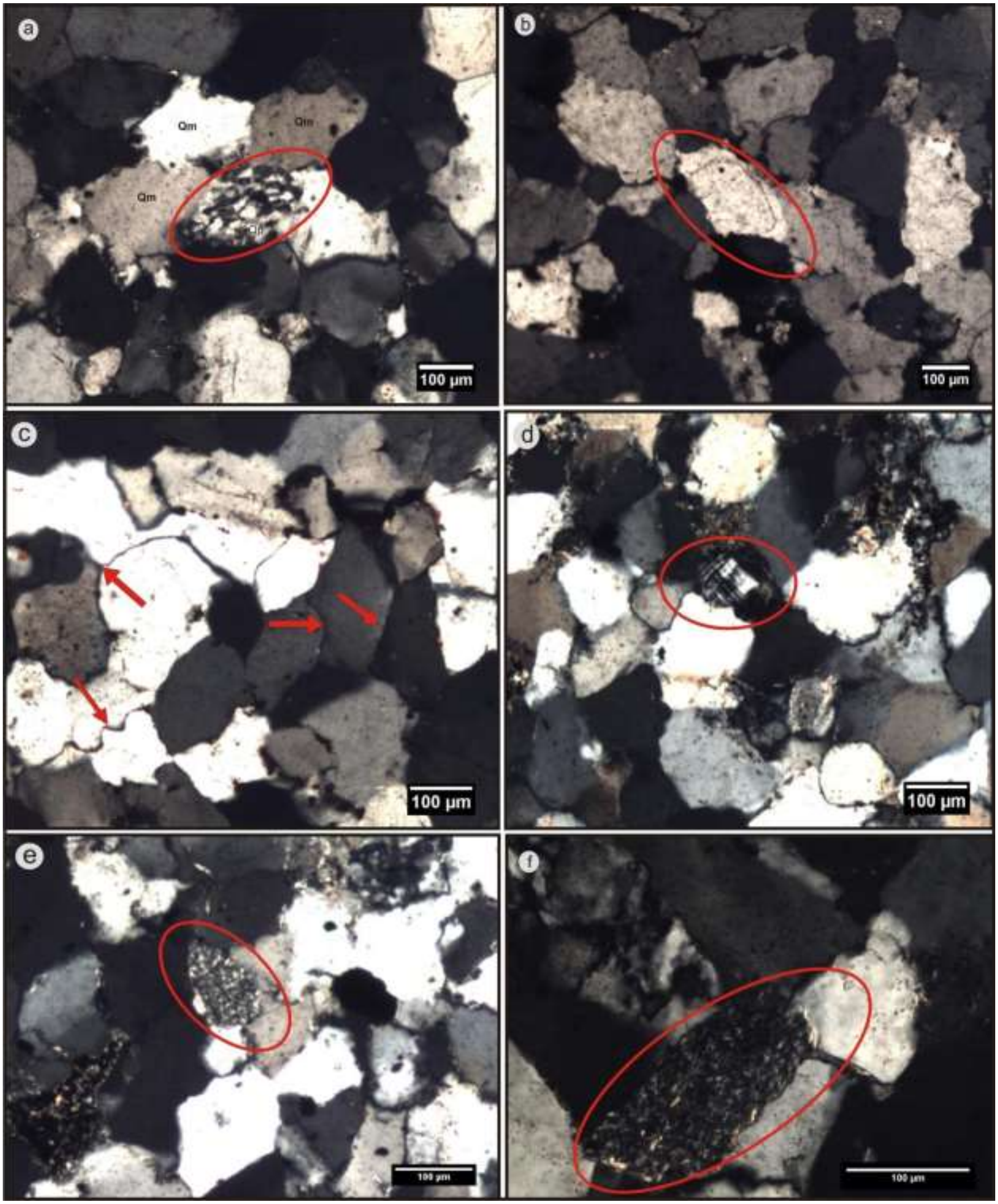

Fig. 4: Photomicrographs of Kaimur Sandstones (a) Medium size polycrystalline quartz grain, (b) Grain of quartz with silica overgrowth, (c) An arrow shows grain contacts and quartz triple junction, (d) Microcline grain, (e) Detrital subrounded chert, (f) Shale fragment.

range of 10°-80° with X-rays using Cu (λ=1.540598) target source for crystalline phase identification. Obtained "Intensity vs. 2 theta" data plotted by origin pro 9 software and minerals peaks identified by using PANalytical HighScore Plus software.

RESULTS

Sandstone petrography and x-ray diffraction

Kaimur Sandstone is showing medium- to fine-grained with subangular to subrounded that are moderately to moderately well sorted. Mineralogically, the detrital grain of the sandstone sample is mainly dominated by quartz (98.75%) with scarcity of feldspar (0.03%), lithic fragments (0.5%), mica (0.5%) and heavy minerals (0.2%) are also present in minor amount. In QFRF triangular diagram, all the sandstone samples data are showing tight clustering in quartzarenite field (Fig. 3a) indicating Sandstone is mainly quartzarenite with small variation in its mineralogy.

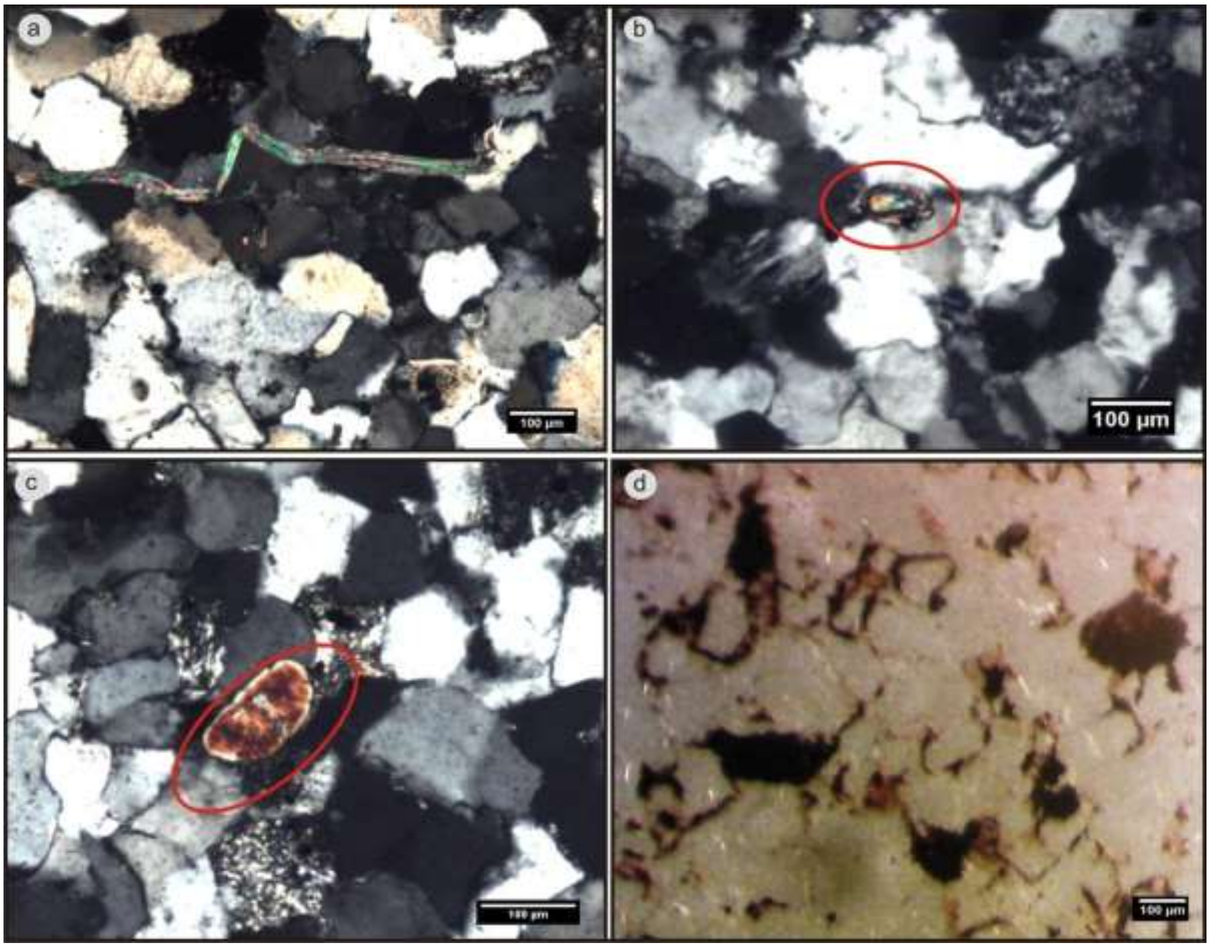

Fig. 5: (a) Sparkling colour of bended muscovite flake between quartz grains, (b) Rounded zoned zircon grain, (c) Rounded brown tourmaline, (d) black colour iron cement present between quartz grains.

Both undulose and non undulose quartz occur in Kaimur Sandstone, dominant quartz

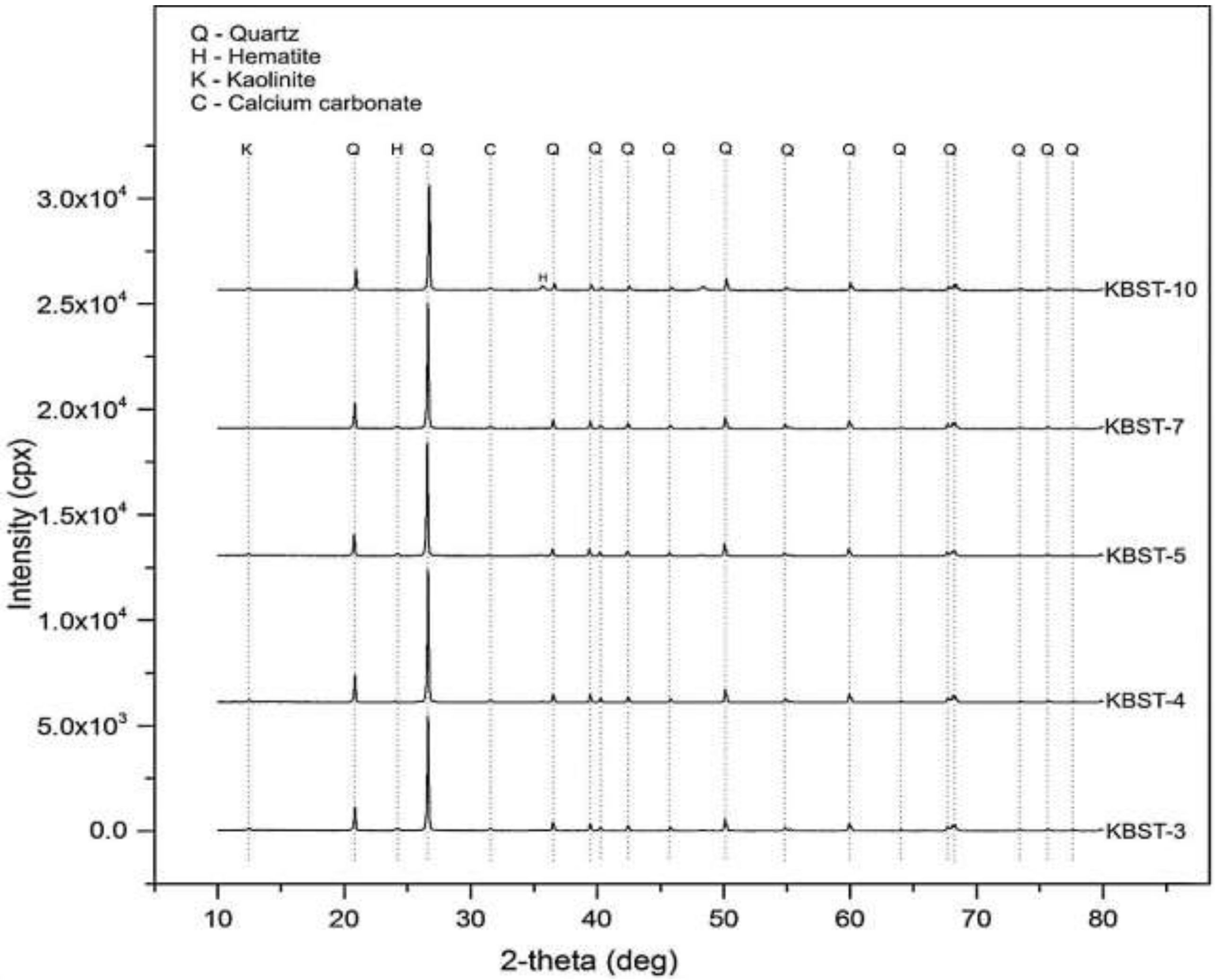

Fig. 6: X-ray diffraction pattern of Kaimur Sandstone shows peaks of Quartz, Hematite, Kaolinite, Calcium carbonate.

grains is monocrystalline quartz (Qm) with low polycrystalline quartz (Qp) grains (Fig. 4a). Silica overgrowth (Fig. 4b), quartz triple junction and dominant long and concavo-convex contact are common (Fig. 4c). Detrital feldspar grains present as microcline and plagioclase varieties, microcline (Fig. 4d) is dominant over plagioclase feldspar. Rock fragments are very rare in thin section and identified rock fragments are mainly chert (Fig. 4e), shale (Fig. 4f) and phyllite. Subrounded chert is more dominant than other rock fragments. Bended sparkling colour of muscovite (Fig. 5a) and heavy minerals mainly zircon (Fig. 5b), tourmaline (Fig. 5c) and rutile present in sandstone. The framework grains are bunded together by both cement and matrix. The matrix is mainly clay minerals with some of fine detrital constituents formed as results of framework grain alteration and precipitation, as well as the other matrix minerals being recrystallized. Silica and iron oxide (Fig. 5d) is the main cementing material of framework grains of Kaimur Sandstone.

Mineralogical studies of Kaimur Sandstone using bulk X-ray diffraction spectrum analysis (Fig. 6) revealed that high intensity and dominant quartz (Q) with minor iron oxide (H) peaks and very rare calcite (C) peak. Clay minerals, mainly Kaolinite (K) shows minor peak, so Kaolinite probably exist as pore-filling aggregates. The XRD study indicates that the Kaimur Sandstone mainly consist of quartz, with little iron oxide and very rare calcium carbonate, so silica and hematite are the main binding material of framework quartz grains.

DISCUSSIONS

Source rock and paleoclimate evaluation

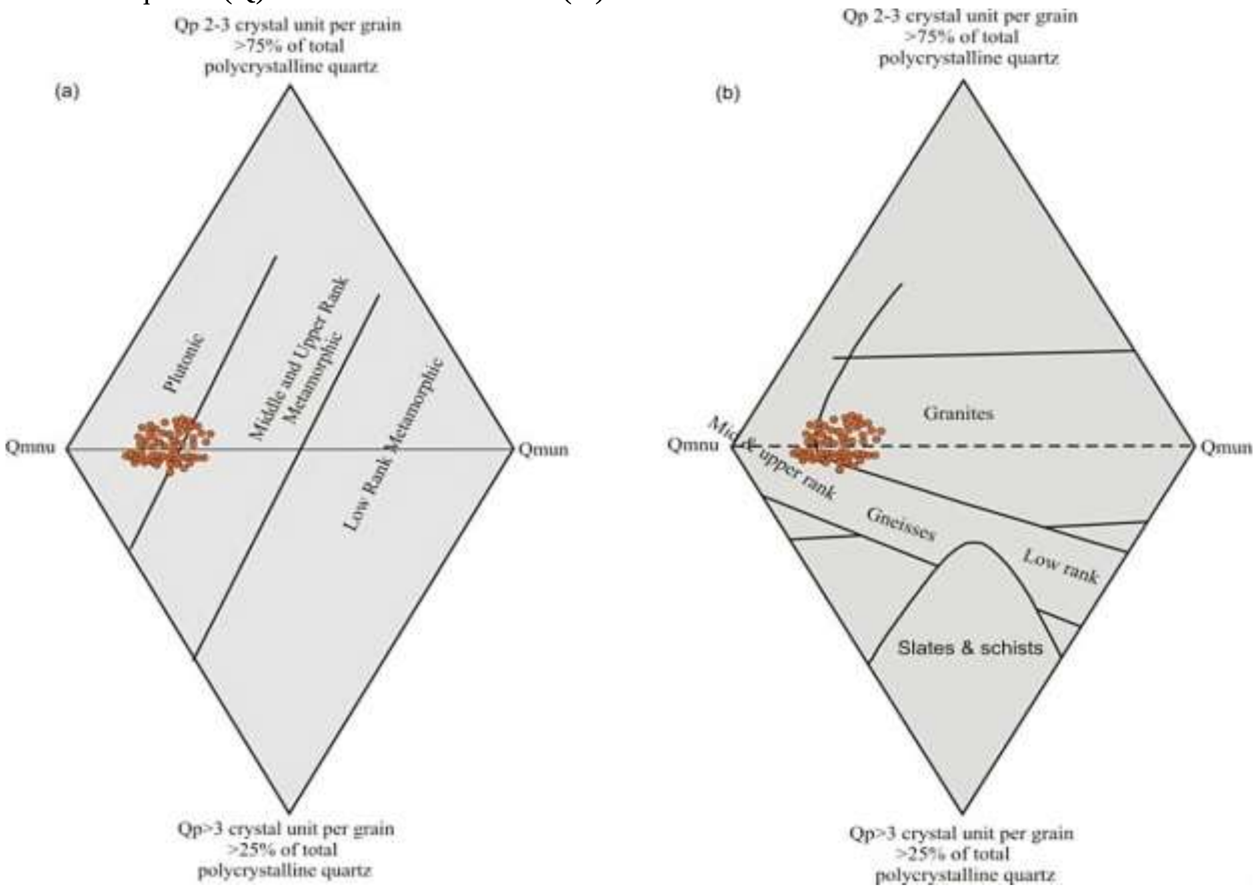

Fig. 7: Diamond diagram plot of Kaimur Sandstone, plot between polycrystalline quartz vs. non-undulatory and undulatory monocrystalline quartz. Qmnu: Low undulosity monocrystalline quartz grains; Qmun; High undulosity polycrystalline quartz grains; Qp 2-3: Coarse-grained polycrystalline quartz grains; Qp>3: Fine-grained polycrystalline quartz grain. Kaimur Sandstone is compared with provenance field, after Basu et al. (1975) and Tortosa et al. (1991).

Provenance of Kaimur Sandstone can be determined by various petrographic methods such as undulosity and polycrystallinity of the quartz grains (Basu et al., 1975), feldspar type (Pittman, 1970) and assemblage of heavy minerals (Morton, 1985). Source rock of this sandstone is mainly established by type of quartz and investigation of heavy minerals because feldspar and rock fragments is very rare in the sandstone samples. In sandstone sample dominant medium to strong undulose monocrystalline quartz grain suggest metamorphic origin with slightly undulose to non undulose quartz grain suggest plutonic source (Basu, 1975; Potter, 1978a). According to Basu et al. (1975) and Tortosa et al. (1991), polycrystalline quartz vs. non-undulatory and undulatory monocrystalline quartz plotted in diamond diagrams suggesting a gneissic-plutonic provenance (Fig. 7a & b).

The heavy minerals identified are mainly zircon, tourmaline and rutile suggest alkaline plutonic rock source (Wanas and Abdel-Maguid, 2006) with minor amount of garnet indicate metamorphic source rock (Morton, 1985; Morton et al., 1992) and moderately rounded to rounded zircon grain suggest reworked sedimentary sources (Sharma and Chutia, 2013). Mineral inclusions of zircon and opaques seen in some monocrystalline quartz grain indicate plutonic origin quartz (Krynine, 1940). Therefore, the presence of heavy mineral varieties suggested that the Kaimur Sandstone is derived from igneous, metamorphic and sedimentary rock sources.

The scarcity of feldspar and rock fragments suggest source rocks experienced long period of intensive weathering in a warm humid climate (Pettijohn et al., 1987; Amireh, 1991) and also suggesting that sandstones were derived from low relief cratonic interior (Burnett and Quirk, 2001). In QFR ternary diagram (Suttner et al., 1981), Kaimur Sandstone of the Chittorgarh area plot in metamorphic source with humid climate field (Fig. 3d). Igneous and metamorphic source rock was weathered under relatively warm and humid climatic condition which destroyed feldspar and other unstable component. Presence of shale and chert fragments suggests derivation from sedimentary source rock and phyllite rock fragments indicate low to medium metamorphic rocks in the source area. Shale and phyllite are unstable rock fragments which mostly destroyed in humid climate, so rare preservation of this lithics indicates very slow transportation rate of source material and/or low subsidence rate of passive tectonic setting.

NE-SE paleocurrent data analyzed from cross-bedded sandstones suggested provenance lies in NW to SW direction (Prasad, 1984), so Palaeoproterozoic Delhi-Aravali Supergroup including Berach granite rocks are the most probable source of this sandstone.

Tectonic Setting

Tectonic setting of sandstone is first determined by using the framework mineralogy (Crook, 1974), defined sandstone composition with major provenance type such as craton interior, basement uplifts, recycled orogens, magmatic arcs (Dickinson and Suczek, 1979; Dickinson et al., 1983).

Tectonic setting of Kaimur Sandstone determine by using detrital components plotted on QFL ternary diagram that having major provenance type such as craton interior, basement uplift, recycled orogeny and magmatic arc (Dickinson and Suczek, 1979; Dickinson et al., 1983; Dickinson, 1985). Modal analysis data of sandstone were plotted on QtFL and QmFLt ternary diagrams of Dickinson (1985), shows that sandstone fall mainly in craton interior field and partially in recycled orogenic field (Fig. 3b & 3c). In QtFL ternary diagram, all samples are clustered near quartz pole indicating that sandstone is commonly mature, which originate from stable cratonic source. Mature sandstone derived from relatively low-lying granitoid and gneissic rocks, supplemented by recycled sand from associated platform or passive margin basin.

Conclusions

Based on petrographic data of Precambrian Kaimur Sandstone of Chittorgarh area in Southeastern Rajasthan is chiefly medium- to fine-grained and moderately to moderately well sorted quartzarenite, having quartz predominantly with scarcity of feldspar and rock fragments. The cementing materials are mainly silica, iron oxide and clay.

Quartz overgrowth, bended mica laths and grain contacts (concavo-convex, suture and long) suggested rock has undergone mechanical compaction due to overburden pressure.

Detrital components of sandstone were derived from craton interior and quartzose recycled orogen rocks that were deposited along former passive continental margins. Metamorphic and igneous rocks of stable craton were the most important source rocks for the Kaimur Sandstone. This interpretation is supported by the northwesterly and southwesterly provenance from Paleocurrent data, so rocks the Delhi-Aravali Supergroup including Berach granite are the most probable source of this sandstone.

The XRD study shows that the sandstone samples have nearly same minerals, Kaimur Sandstone is composed of quartz with minor amount of iron oxide and rare calcite.

Acknowledgments:

We thank the Chairman, Department of Geology, Aligarh Muslim University, Aligarh for providing necessary facilities to carry out the research work. The authors are also thankful to the University Grants Commission, New Delhi for financial support.

References

Amireh, B. S. (1991), Mineral composition of the Cambrian-Cretaceous Nubian Series of Jordan: provenance, tectonic setting and climatological implication. Sedimentary Geology, v. 71, p. 99-119.

Armstrong-Altrin, J. S. (2015), Evaluation of two multi-dimensional discrimination diagrams from beach and deep sea sediments from the Gulf of Mexico and their application to Precambrian clastic sedimentary rocks. International Geology Review, v. 57(11-12), p. 1446-1461.

Basu, A., Young, S. W., Suttner, L. J., James, W. C., Mack, G. H. (1975), Re-evaluation of the use of undulatory extinction and polycrystallinity in detrital quartz for provenance interpretation. Journal of Sedimentary Research, v. 45(4), p. 873-882.

Boggs, S. (2006), Principles of sedimentology and stratigraphy: Pearson Prentice Hall. Upper Saddle River, New Jersey, p. 581.

Bose, P. K., Banerjee, S., Sarkar, S. (1997), Slope-controlled seismic deformation and tectonic framework of deposition of Koldaha Shale, India. Tectonophysics, v. 269, p. 151-169.

Burnett, D. J., Quirk, D. G. (2001), Turbidite provenance in the Lower Paleozoic Manx Group, Isle of man; implications for the tectonic setting of Eastern Avalonia. Journal of Geological Society of London, v. 158, p. 913-924.

Carver, R. E. (1971) Procedures in Sedimentary Petrology. Wiley-interscience (New York), p 653.

Chaudhari, A. K., Mukhopadhyay, J., Patranabis-Deb, S., Chanda, S. K. (1999), The Neoproterozoic cratonic successions of peninsular India. Gondwana Research, v. 2, p. 213-225.

Critelli, S. (2018), Provenance of Mesozoic to Cenozoic circum-Mediterranean sandstones in relation to tectonic setting. Earth-science reviews, v. 185, p. 624-648.

Crook, K. A. W. (1974), Lithogenesis and geotectonics: The significance of compositional variation in flysch arenites (greywackes). Society of Economic Paleontology and Mineralogist, v. 19, p. 304-310.

Dickinson, W. R. (1985), Interpreting provenance relations from detrital modes of sandstones. In: Zuffa, G.G. (ed.), Provenance of Arenites. Reidel Publishing Company, Reidel, p. 231-247.

Dickinson, W. R. (1988), Provenance and Sediment Dispersal in Relation to

Paleotectonics and Paleogeography of Sedimentary Basins. In: Kleinspehn K.L., Paola C. (eds) New Perspectives in Basin Analysis. Frontiers in Sedimentary Geology, p. 3-25.

Dickinson, W. R., Beard, L. S., Brakenridge, G. R., Erjavec, J. L., Ferguson, R. C., Inmam, K. F., Knepp, R. A., Lindberg, F. A., Ryberg, P. T. (1983), Provenance of North American Phanerozoic sandstones in relation to tectonic setting. Geological Society of American Bulletin, v. 94, p. 222-235.

Dickinson, W. R., Suczek, C. A. (1979), Plate-tectonics and sandstones composition. American Association of Petroleum Geologist Bulletin, v. 63, p. 2164-2182.

Folk, R. L. (1980), Petrology of sedimentary rocks. Austin (Texas, U.S.A.) Hemphill Publishing Company, p. 182.

Ingersoll, R. V., Bullard, T., Ford, R., Grimm, J., Pickle, J., Sares, S. (1984), The effect of grain size on detrital modes: a test of the Gazzi Dickinson point-counting method. Journal of Sedimentary Petrology, v. 54, p. 103-116.

Ingersoll, R. V., Suczek, C. A. (1979), Petrology and provenance of Neogene sand from Nicobar and Bengal fans, DSDP sites 211 and 218. Journal of Sedimentary Research, v. 49(4), p. 1217-1228.

Johnsson, M. J., Basu, A. (1993), Processes controlling the composition of clastic sediments. Geological Society of America, p. 284:342.

Khan, A. A. (2013), Paleogeography of the Indian Peninsula vis-à-vis Geodynamic and Petrotectonic Significance of the Vindhyan Basin With Special Reference to Neo-Meso Proterozoic, Jour. Ind. Geol. Cong., v. 5(1), p. 65-76.

Krynine, P. D. (1940), Petrology and genesis of the Third Bradford Sand (No. 29). School of Mineral Industries, Pennsylvania State College, p. 533.

Malone, S. J., Meert, J. G., Banerjee, D. M., Pandit, M. K., Tamrat, E., Kamenov, G. D., Pradhan, V. R., Sohl, L. E. (2008), Paleomagnatism and detrital zircon geochronology of the upper Vindhyan sequence, Son Valley and Rajasthan, India: A ca.1000 Ma closure age for the Purana basins?. Precambrian Research, v. 164, p. 137-159.

Morton, A. C. (1985), Heavy Minerals in Provenance Studies. In: Zuffa G.G. (eds) Provenance of Arenites. NATO ASI Series (Series C: Mathematical and Physical Sciences), Springer Dordrecht, v. 148, p. 249-250.

Morton, A. C., Davies, J. R., Waters, R. A. (1992), Heavy minerals as a guide to turbidite provenance in the Lower Paleozoic Southern Welsh Basin: a pilot study. Geological Magazine, v. 129, p. 573-580.

Pettijohn, F. J., Potter, P. E., Seiver, R. (1987), Sand and Sandstone. Springer-Verlag New York, p. 533.

Pittman, E. D. (1970), Plagioclase as an indicator of provenance in sedimentary rocks. Journal of Sedimentary Petrology, v. 40, p. 591-598.

Potter, P. E. (1978a), Petrology and chemistry of modern big river sands. Journal of Geology, v. 86, p. 423-449.

Prasad, B. (1984), Geology, sedimentation and palaeogeography of the Vindhyan Supergroup, southeastern Rajasthan. Memoirs of the Geological Survey of India, v. 116(1-2), p. 1-107.

Prasad, B. R., Rao, V. V. (2006), Deep seismic reflection study over the Vindhyans of Rajasthan: implications for geophysical setting of the basin. Journal of earth system science, v. 115(1), p. 135-147.

Raza, M., Khan, A., Bhardwaj, V. R., Rais, S. (2012), Geochemistry of Mesoproterozoic sedimentary rocks of upper Vindhyan Group, southeastern Rajasthan and implications for weathering history, composition and tectonic setting of continental crust in the northern part of Indian shield. Journal of Asian earth sciences, v. 48, p. 160-172.

Sarkar, S., Banerjee, S., Chakra borty, S., Bose, P. K. (2002), Shelf storm flow dynamics: insight from the Mesoproterozoic Rampur Shale, central India. Sedimentary Geology, v. 147(1-2), p. 89-104.

Sharma, J. N., Chutia, A. (2013), Petrography and heavy mineral analysis of Tipam sandstones exposed on the Tipam hill of Sita Kunda area, upper Assam, India. South East Asian Journal of Sedimentary Basin Research, v. 1, p. 28-34.

Soni, M. K., Chakarborty, S., Jain, V. K. (1987), Vindhyan Supergroup - a review. In: Purana Basin of India (Middle to Late Proterozoic). Geological Society of India Memoir, v. 6, p. 87-138.

Suttner, L. J., Basu, A., Mack, G. H. (1981), Climate and the origin of quartz arenites. Journal of Sedimentary Research, v. 51(4), p. 1235-1246.

Suttner, L. J., Dutta, P. K. (1986), Alluvial sandstones and paleoclimate-framework mineralogy. Journal of Sedimentary Petrology, v. 56, p. 329-345.

Tortosa, A., Palomares, M., Arribas, J. (1991), Quartz grain types in Holocene deposits from the Spanish Central System: some problems in provenance analysis. Geological Society London (Special Publications), v. 57(1), p. 47-54.

Verma, S. P., Armstrong-Altrin, J. S. (2013), New multi-dimensional diagrams for tectonic discrimination of siliciclastic sediments and their application to Precambrian basins. Chemical Geology, v. 355, p. 117-133.

Verma, S. P., Armstrong-Altrin, J. S. (2016), Geochemical discrimination of siliciclastic sediments from active and passive margin settings. Sedimentary Geology, v. 332, p. 1-12.

Wanas, H. A., Abdel-Maguid, N.M. (2006), Petrography and geochemistry of the

Cambro-Ordovician Wajid Sandstone, southwest Saudi Arabia: Implications for provenance and tectonic setting. Journal of Asian Earth Sciences, v. 27, p. 416-429.

Jour. Indian Association of Sedimentologists, Vol. 36, No. 1 (2019), pp.65-83
ISSN Online 2582 – 2020
ISSN Print 0970 – 3268

Source and processes from core sediment samples off Mahanadi and Krishna rivers, western Bay of Bengal

Janhavi Kangane, Ganapati N. Nayak* and Shabnam Choudhary

Department of Marine Sciences, Goa University, Goa- 403206, India.
*Corresponding author- gnnayak@unigoa.ac.in

Abstract: A total of sixteen samples representing surface,10 cm and 20 cm of sediment core depth between water depth of 25 m and 2600 m from the continental shelf region off Mahanadi and off Krishna were analyzed for grain size, clay minerals, total organic carbon and selected elements to understand the source and processes. The study revealed an overall decrease in sediment size from shallow to deeper water depth as well as from Mahanadi (north) to Krishna (south), indicating transportation direction. Total organic carbon content is low (<1%) and higher content was associated with finer sediment fraction. High sand content in shallow water stations off Mahanadi indicates high hydrodynamic conditions as compared to that off Krishna. High smectite content off Krishna suggests Deccan Basalt and their associated black cotton soil as their source whereas high illite content off Mahanadi suggests source belongs to Archean Proterozic Gneissic complex (APGC) along with its major supply from the Himalayan region through Ganges and Brahmaputra. Ba values obtained off Mahanadi indicate the source of felsic rocks. High concentration of Fe, Mn and Ti off Krishna supports the source of basic igneous rocks. Relatively high coarse sediment (sand) as well as high illite content off Mahanadi river mouth, suggests a change in land use pattern and climate in the catchment area of rivers.

Key words: Mahanadi, Krishna, Clay Minerals, Metals, TOC

Introduction

Rivers are the major linkage between terrestrial and ocean environment. They are one of the important pathways by which products of weathering on the continents are carried to the adjacent continental shelf. Sediment accumulation and distribution on the continental shelf reflect the influence of the processes that operated in the area. Thus, understanding the characteristics of the sediment in the regions of the continental shelf off different river mouths is essential for understanding source along with the processes involved during and after sediment deposition. Bay of Bengal like the Arabian Sea is landlocked in the north and are influenced by a seasonal reversal of the monsoon winds. Despite, all these similarities, both are largely distinct in their geochemical processes.

The sediment characteristics namely grain size, organic carbon, metal concentrations have been used earlier as proxies to understand nutrient cycling and productivity changes in the Bay of Bengal. Shelf sediments of the Ganges delta with emphasis on the western part of Bengal was studied by Mallik (1976), and reported that the sediments at the Hooghly River mouth, part of the great Ganges-Brahmaputra delta sediment, consist of sands, silts, clays and their various admixtures and there has been addition of coarser sediments from the rivers like Hooghly and Dhamra. Rao (1960) investigated organic matter content in the continental shelf sediments off the east coast and reported low organic carbon due to low plankton production and intense oxidation conditions. Krishna et al. (2013) stated that the strong influence of river discharge on the relative composition of sediment organic matter (OM) through transportation of terrestrial OM from the peninsular India. Rao et al. (1988) studied the clay mineral suites in the Bengal shelf and explained that the clay minerals in sediments closely reflect their sources but their relative abundance depends largely on the energy conditions of the shelf environment and the properties of the individual clay minerals. According to Pragatheeswaran et al. (1986), the sediments off Chennai are more contaminated in heavy metals and organic carbon than Visakhapatnam shelf sediments. Muthuraj and Jayaprakash (2008) studied the distribution of trace metals in the sediments of the Bay of Bengal and revealed higher concentration of trace metals owing to finer grain size and higher organic carbon. Tripathy et al. (2014) and Mazumdar et al. (2015) studied major and trace elements in the Bay of Bengal slope and plain region and inferred the factors controlling the distribution and preservation of the elements as well as changes in provenances. Mazumdar et al. (2015) further, stated that the sediment geochemistry enables distinction of specific contributing sources, which could potentially be related to modern climatic and geomorphological conditions. Das and Krishnaswami (2007) mentioned that significant association of Fe and Ti from Krishna Basin sediments indicates their source as Deccan Basalt. However, from the point of view of geochemical aspects, studies on provenance and sedimentary processes are few in the Bay of Bengal. Therefore, the objective of the present study is to understand the source and depositional processes occurring in the continental shelf region off Mahanadi and Krishna river mouth. In this study, an attempt is made to fill the gap of knowledge on sedimentary processes and identification of provenance through geochemical proxies.

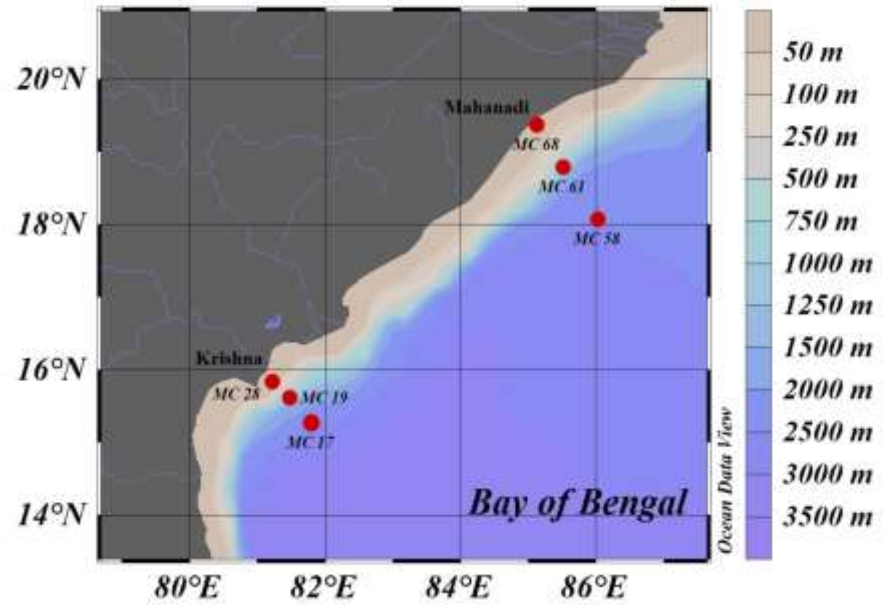

Fig1. Location of the sediment core sample

Study area

The study area lies off Mahanadi and Krishna river mouth regions (Fig.1). The Krishna and Mahanadi rivers drain the Indian subcontinent and deposit the sediment load into the Krishna and Mahanadi offshore basins along the western margin of the Bay of Bengal. The Krishna River originates in the Western Ghats at an elevation of 1337 m above mean sea level and estimated sediment flux of the river is 67.72 $*10^6$ ton yr^{-1} (Ramesh and Subramanian, 1988). While Mahanadi River originated in the Eastern Ghats at an elevation of 80 m above mean sea level. The geology of Mahanadi river catchment area is characterised by the Precambrians of Eastern Ghats. The rock types include khondalites, charnockites, leptynites, granites, gneisses, along with limestones, sandstones and shales of the Gondwanas. The coastal tracts constituted by the recent deltaic alluvium of the river with littoral deposits (Chakrapani and Subramanian, 1990; Meert et al., 2010; Mazumdar et al., 2015). While the Krishna river catchment area consisting of late Archaean and early Proterozoic crystalline rocks, Tertiary Deccan traps (basalt) and recent sediments outcrop locally (Ramesh and Subramanian, 1988). The coastal region of Mahanadi experiences subtropical climate with a temperature of about 21°C and 29º C in winter and summer respectively (Hart, 1999), whereas in the coastal Krishna the climate is humid with the highest temperature of around 35°C (Das and Panchal, 2018). The area receives bulk precipitation from south-west monsoon during June to September while northeast monsoon provides precipitation from October to January. In the northern Bay of Bengal, the fresh-water discharge stratifies and changes the surface water circulation and salinity (Levitus and Boyer, 1994; Benshila et al., 2014; Saalim et al., 2018). Because of its narrow shelf, nutrient concentrations are almost negligible in deeper regions, despite the huge amount of nutrients brought by river system (Qasim, 1977; Sen Gupta et al., 1977; Sarma, 2002). As compared to the Arabian Sea productivity in Bay of Bengal is very low due to strong stratification, cloud cover and turbidity (Madhupratap et al., 1996, 2003).

Materials and Methods

Sampling and Collection

A total of six sediment cores, three each from transect off Mahanadi and off Krishna collected from water depth, ranging from 29 to 2500 m are used in the present study. The samples were collected using multi-corer onboard RV Sagar Kanya (Cruise no. 308) in the month of January 2014 (Table 1) and investigated to understand the source and processes in the recent past of Western Bay of Bengal. The samples were subsampled at 1 cm interval, labeled and brought back to the laboratory in a frozen condition for analysis. In the laboratory, samples were dried at 60° C in the oven and used for further analysis. For the present study, samples from 0-1, 10-11 and 20-21 cm core depth were analyzed.

Transect	Core no.	Water depth (m)	Latitude (˚N)	Longitude (˚S)
Off Mahanadi	MC 68	29.2	19˚36.48	85˚13.09
	MC 61	1537.9	18˚78.29	85˚52.30
	MC 58	2386.4	18˚06.61	86˚03.25
Off Krishna	MC 28	31.6	15˚82.96	81˚22.37
	MC 19	1463	15˚61.18	81˚48.39
	MC 17	2574	15˚26.69	81˚79.88

Table 1: Location and water depth (m) of sediment cores

Laboratory analysis

The samples for grain size analysis were washed with distilled water to remove salinity and then treated with 10 % sodium hexametaphosphate to dissociate clay particles and hydrogen peroxide was added to oxidize the organic matter. Grain size was then determined using pipette method (Folk, 1968) which is based on Stoke's settling velocity principle. A portion of each subsample was powdered and homogenized in an agate pestle and mortar, and used for the determination of TOC using the Walkley (1947) Black method, modified by Jackson (1958). The glycolated clay slides were scanned from 3º to 30º 2Ɵ at 1.2º 2Ɵ/min on Rigaku Altima IV using nickel-filtered CuKα radiation. Clay minerals were identified and quantified following the procedure given by Biscaye (1965).

Smectite crystallinity was measured from the ratio of the height of the smectite peak above the background (p) and the depth of valley (V) on the low angle side of the peak. Illite crystallinity was calculated measuring the width (Δ2θ) from the peak height of diffraction peak of illite (Biscaye, 1965). Illite chemistry was calculated from the ratio of 5 and 10 Aº peak areas of illite. Further, sediment samples were digested using HF, HNO_3 and $HClO_4$ acid mixture with a ratio of 7:3:1 for total metal analyses. The concentration of Fe and Mn were determined using Atomic Absorption Spectrometer (Thermo Scientific-SOLAAR M6 AAS model) and Ti and Ba using Induced coupled plasma–mass spectrometry (ICP-MS). Together with the samples, certified reference standards from the National Institute of Standards and Technology, USA were digested and run, to test the analytical accuracy of the method. The average recoveries were 90–97%. Internal chemical standards obtained from Merck were used to calibrate the instrument and recalibration checks were performed at regular intervals.

Results and Discussion

Distribution of sediment components off Mahanadi and Krishna River

In transect M1 (0-1 cm) off Mahanadi river mouth sand (34.9%) and silt (26.09%) was found to be high at MC 68 and low at MC-61 with values of 0.75% and 24.04% respectively. Clay concentration was highest at MC 61 (75.2%) and lowest at MC 68 (39%). TOC increased with water depth and found to be high at MC 58 (0.75%) and lowest at MC 68 (0.42 %). Along the transect K1 (0-1 cm) off Krishna river mouth sand (8.19%) and silt (57.97%) was found to be high at MC 28 and low at MC 17 with values of 0.22% and 30.34% respectively. Clay was found to be high at MC 17 (69.44%) and low at MC 28 (33.84%) while TOC was found to be higher at MC 19 (0.97%) and lowest at MC 28 (0.48%).

In transect M2 (10-11 cm), sand was found to be high (79.98%) at MC 68 and low (0.24%) at MC 61 while, silt was found to be high at MC 58 (30.44%) and low at MC 68 (1.61%). Clay concentration was highest at MC 61 (72.88 %) and lowest at MC 68 (18.4%). TOC exhibited an increasing trend from MC 68 (0.09%) to MC 58 (0.93%). Along the transect K2 (10-11 cm) off Krishna river mouth sand (7.68%) and silt (50.63%) was found to be high at MC 28 whereas lower concentration of sand (0.25%) was found at MC 17 and silt at MC 19 (26.42%). Further, clay concentration was found to be high (73.28%) at MC 19 and low (41.68%) concentration at MC 28. TOC in this transect was found to be high at MC 19 (0.94%) and lowest at MC 28 (0.68%).

Along the transect M3, (20-21 cm) relatively high concentration of sand (4.85%), silt (53.44%) and TOC (0.96%) was found at MC 58 and low at MC 61 while high (74.88%) content of clay was found at MC 61 and low (41.71%) at MC 58. In the transect K3 (20-21 cm) sand (0.38%) and silt (21.45%) was found to be high at MC 19 and low at MC 17 while clay concentration was found to be high (79.44%) at MC 17 and low (78.16%) at MC 19. TOC was found to be high (0.97%) at MC 19 and low (0.82%) at MC 17.

Further, the data on sediment components of all the studied cores are presented in figure 2 for easy understanding the variations.

Source and transport mechanism of sediment components

Among the sediment components in transects off Mahanadi and Krishna river mouth sand and silt, concentration decreased with increasing water depth away from the coast. Clay concentration was predominant along all transects and found to be higher at a depth of 1537 m along the Mahanadi river transect. When the concentration of sediment components was compared from Mahanadi (north) to the Krishna (south) river mouth regions, the grain size decreased indicating a direction of transport from north to south. The topography, lithology and catchment area of Mahanadi facilitates the erosion processes due to the change in land use pattern and climate (Beura, 2015). The increased process of erosion supplied a huge amount of sediment load to the Mahanadi River resulting in the decreased carrying capacity of the river and deposition of coarser sediments off Mahanadi river mouth. The occurrence of coarser grain size sediments off river mouth due to tidal effect and accumulation of sediments from terrestrial input was reported by Raj and Jayaprakash (2008). The distribution of sediment components along transects indicated the possible direction of transportation from shore to offshore and material supply from rivers to the bay. Further, decrease in grain size from off Mahanadi to Krishna river mouth regions indicated relatively higher energy environment prevailing off Mahanadi facilitating deposition of coarse grain sediment and preventing accumulation of finer sediments. TOC showed an increasing trend on moving away from the coast in transect of Mahanadi while along transect off Krishna TOC was found to be higher at 1463 m depth. Overall, TOC concentration was found to be low (<1%) in the study area despite relatively high sediment influx draining through the rivers. Organic matter must have been transported through suspended mode along with finer sediments and carried away from the coast.

Distribution of clay minerals off Mahanadi and Krishna River

Along the transect M1 (Table 2), illite showed high (65.57%) concentration at MC 68 and low (57.73%) concentration at MC 61. Kaolinite showed high (26.18) concentration at MC 61 and lowest (14.67%) concentration at MC 58. Smectite (21.11%) and chlorite (2.63 %) showed high concentration at MC 58 while lowest concentration of chlorite (1.3%) and smectite (14.75%) was found at MC 61 and MC 68 respectively. In the transect K1 (Table 3), a higher concentration of illite (34.78%) was found at MC 28 and lower concentration (7.37%) at MC 17. Kaolinite showed high concentration (15.09%) at MC 19 and lowest concentration (11.52%) at MC 17. Smectite was found to be high (78.8%) at MC17 and low (50.72%) at MC 28 while, chlorite was found to be high (2.51%) at MC19 and low at MC 28 (1.31%).

Along the transect M2 (Table 2), illite was found to be highest (75.36%) at MC 68 and lowest (57.14%) at MC 58. Kaolinite (19.04%) and chlorite (3.17%) were found to be higher at MC 61 and lower at MC 68 with values of 11.41% and 1.63% respectively. Smectite was found to be higher at MC 58 (25.92%) and lower at (11.59%) MC 68. In the transect K2 (Table 3), illite was found to be high (26%) at MC 19 and low (15.38%) at MC 28. Kaolinite (18.53%) and chlorite (3.08%) were found to be higher at MC 17 and showed lower values at MC 19 (8.55%) and MC 28 (1.92%). Smectite showed highest concentration (69.23%) at MC 28 and low value at MC 17 (61.08%).

Along the transect M3 (Table 2), illite (69.23%) and chlorite (2.79%) showed higher concentration at MC 58 and lower concentration with values of 60.46% and 1.32% respectively at MC 61 while kaolinite (22.51%) and smectite (15.69%) showed higher concentration at MC 61 and lower concentration at MC 58. In the transect K3 (Table 3), illite was found to be high (34.78%) at MC19 and low (17.88%) at MC 17 while kaolinite, chlorite and smectite were found to be higher at MC17 and lower at MC 19.

Further, the data on clay minerals of all the studied cores are presented in figure 2 for easy understanding the variations.

Provenance and environmental significance indicated by clay minerals

Illite is the dominant clay mineral followed by kaolinite, smectite and chlorite in all the samples studied off Mahanadi river mouth (Table 2) while off Krishna river mouth (Table 3) region smectite was the dominant clay mineral followed by illite, kaolinite and chlorite. Illite showed a -decreasing trend on moving away from the coast off Mahanadi river mouth similar to that of sand indicating that it has been derived from the weathering of rocks present in the catchment area. Higher abundance of illite in the off Mahanadi sediments compared to Krishna sediments indicated its supply from felsic source rock which belongs to Archean Proterozoic Gneissic Complex (APGC) (Mazumdar et al., 2015). Illites are widely formed due to glacial weathering under arid conditions in cold regions from muscovite (Weaver, 1989). The presence of muscovite mica, associated with metamorphic rocks such as phyllites must be the major source of illite which must have been dispersed by turbidity currents from Ganges and Brahmaputra (Kolla and Biscaye, 1973; Rao and Rao, 1977; Kolla and Rao, 1990). The decrease in illite concentration from Mahanadi (north) to Krishna (south) is possibly due to loss of energy towards Krishna which prohibits illite-rich sediment to reach southwards. Smectite forms due to chemical weathering in the low latitude region (Biscaye, 1965). High concentration of smectite off Krishna river mouth indicated that it has been derived from the Deccan trap basalts (Raman et al., 1995; Kulkarni et al., 2015; Mazumdar et al., 2015) and from late Archaean and early Proterozoic crystalline rocks drained through peninsular rivers. Higher values of smectite off Krishna river mouth suggested that low energy conditions prevailed in the region as under low energy conditions smectite gets deposited with finer grain size while a high concentration of illite off Mahanadi River indicated high energy condition which is also evident by grain size distribution. Kaolinite is also present which must have formed from rocks such as

Archean granites, gneisses, charnockites and khondalites by alteration of minerals like K-feldspar and other typical aluminosilicate like sillimanite. Sillimanite alters into gibbsite during chemical weathering which in turn changes into kaolinite (Nakagawa et al., 2006; Rao and Raman, 1979; Soman and Machado, 1986). Chauhan and Vogelsang (2006) suggested a low concentration of kaolinite in this region possibly due to its equatorward dispersal. Chlorite is available in lower concentration as compared to other clay minerals may be due to the unstable nature of chlorite under humid conditions (Diju and Thamban, 2006). The results obtained are in good agreement with those obtained earlier by Raman et al. (1995) and Phillips et al. (2014). Smectite and illite crystallinity and illite chemistry were calculated for identification of degree of weathering and confirmation of the source of clay minerals. Smectite crystallinity in most of the samples varied from 1.5 to 2.0 $\Delta°2\theta$ suggesting the occurrence of moderately crystalline smectite in the study area. Illite crystallinity was 0.2 $\Delta°2\theta$ indicating the dominance of very well crystalline illite derived from the physical weathering which is also supported by illite chemistry. It was found below 0.5 in samples off Mahanadi River indicating the presence of Fe-Mg rich illite derived from physical weathering of rocks from the Himalayan region while the samples off Krishna River suggested Al-rich illite formed through hydrolysis (Bejugam and Nayak, 2017) probably from leaching of felsic rocks of Eastern Ghats.

Distribution of metals off Mahanadi and Krishna River

In the transect M1(Table 2), metals like Fe, Mn and Ba (8.66%, 2.7% and 777 ppm respectively) were found to be higher at MC 58 and lower (3.59%, 0.16% and 314 ppm respectively) at MC 68 while Ti was found to be higher (2.26%) at MC 68 and lower (0.49%) at MC 61. Along the transect K1(Table 3), all the metals like Fe, Mn, Ti and Ba (8.37%. 0.14%, 2.27% and 224 ppm respectively) showed higher concentration at MC 28 while Fe (5.93%) and Ti (0.71%) showed lower concentration at MC 19 and Mn (0.07%) and Ba (200 ppm) at MC17.

Along the transect M2 (Table 2), Fe was found to be higher (5.03%) at MC 61 and lower (1.33%) at MC 68. Mn (0.11%) and Ti (0.83%) was found to be higher at MC 68 and lower at MC 58 with values of 0.04% and 0.4% respectively while Ba was found to be higher (401 ppm) at MC 58 and lower (351 ppm) at MC 68. In transect K2 (Table 3), metals like Fe, Mn and Ti (6.66%, 0.09% and 1.62% respectively) were found to be higher at MC 28 while Fe (5.96%) and Mn (0.02%) were found lower at MC 19 and Ti showed lower values at MC 17. Ba was found to be higher (272 ppm) at MC17 and lower (144 ppm) at MC 28.

Along transect M3 (Table 2), Fe (4.4%) and Mn (0.1%) showed high concentration at MC 61 and low concentration at MC 58 while Ti and Ba were found high (0.47% and 497 ppm respectively) at MC 58 and low (0.4% and 361 ppm respectively) at MC 61. In transect K3 (Table 3), Fe, Mn and Ti were found high at MC 19 and low at MC 17 while Ba showed almost similar concentration at MC 17 (219 ppm) and at MC 19 (217 ppm).

Further, the data on metals of all the studied cores are presented in figure 2 for easy understanding the variations.

Source and processes governing the distribution of metals

Metals in the study area are present in the order of Fe>Ti>Mn> Ba (Table 3). Fe content was lower in transects off Mahanadi river mouth region as compared to transect off Krishna River and its concentration in the study area was higher than Post Archean Australian Shale (PAAS) values of 5%. The average Fe concentration in continental crust is 5.63 % (Taylor, 1964) and Fe content in Deccan basalts varies from ~9-11 % (Pattanayak and Shrivastava, 1999). These iron-rich source rocks upon weathering produce iron-rich clay minerals, Fe-rich oxyhydroxides and unaltered ferromagnesium minerals (Das and Krishnaswami, 2007). Ti concentration in the samples was higher than PAAS value of 0.6 %. High Ti values off Krishna indicate mafic source rocks while along transect off Mahanadi Ti was slightly lower indicating a dominance of felsic source rocks. High Ti concentration off Krishna River may be derived from Deccan Trap basalts which are rich in titanium (Das and Krishnaswami, 2007; Bejugam and Nayak, 2017). Mazumdar et al. (2015) stated that the Mahanadi River basin comprises Late Archaean and early Proterozoic granite batholiths, tonalite-trondjhemite gneisses (TTGs), and chanockites and khondalites of the Eastern Ghats constitute 56% of the catchment area. Further, they mentioned that relatively higher illite contents in the Mahanadi basin sediments compared to the K-G basin samples suggest the dominance of felsic source rocks, which characterize the Archaean-Proterozoic Gneissic Complex. This supports the results of the present study of higher illite in the northern transects off Mahanadi River mouths and higher smectite in samples off Krishna river mouths. Along the Mahanadi river transects Mn concentration was slightly higher as compared to transect off Krishna. Mn concentrations were higher than crustal PAAS values of 0.09% (Taylor and McLennan, 1985) in majority of the samples indicating the presence of structurally unsupported hydroxides. Along Mahanadi river transect Ba showed an increasing trend on moving away from the coast similar to that of organic carbon indicating its biogenic origin from marine productivity. While along the Krishna River Ba is found enriched in the surface samples suggesting that it has been derived from the terrigenous influx. Deccan basalts show restricted mobility of Ba after weathering (Das and Krishnaswami, 2007) which is attributed to the low Ba concentration off Krishna river mouth. Further, Ba is noted to be higher at deeper water depths in most of the transects as the formation of barytes in the water column takes place well below the photic zone (Babu et al., 2002) as it requires sufficient water depth for their preservation. The increase of Ba with water depth was reported earlier by Von Breymann et al. (1990) and Calvert and Price (1983) in the surface sediments off NW Arabian Sea and Namibian continental slope respectively.

It is noted that relatively the concentration of Fe and Ti was found to be higher in the off Krishna sediments whereas Mn and Ba were higher off Mahanadi indicating Ba may also be supplied from weathering of acid igneous rocks from the catchment of Mahanadi in addition to its biogenic nature.

Conclusion

The investigation of sediment samples representing the surface, 10 cm and 20 cm of sediment core from off Mahanadi and off Krishna, western Bay of Bengal indicated sediment transportation from near shore to offshore and from Mahanadi (north) to Krishna (south). Higher hydrodynamic conditions off Mahanadi river mouth was responsible for retaining coarser sediments comparative to off Krishna river mouth regions. Clay mineral study and metal analysis revealed that mafic igneous rocks present in the catchment area of Krishna River and felsic igneous rocks present in the catchment of the Mahanadi River are the major source for smectite and illite abundance in the study area respectively. Variation in sediment size, abundance and distribution of clay minerals and metals in the study area indicated change in provenance, land use - land cover pattern and climate in the catchment area of rivers, and also depositional processes.

Acknowledgement

The authors place on record thanks to Dr. Rajeev Saraswat, Scientist and Mr.

Girish Prabhu, NIO, Goa for kindly extending the instrumental facility of X-ray diffractometer. The authors are also grateful to Dr. Anoop Kumar Tiwari, Scientist; Dr. Waliur Rehman, Scientist and Lathika N Padmanabhan, Scientist, ESSO-NCAOR, Goa for their assistance in the metal analysis.

Mahanadi	Water depth (m)	Sub sample	Sand (%)	Silt (%)	Clay (%)	TOC (%)	Illite (%)	Kaolinite (%)	Chlorite (%)	Smectite (%)	Fe (%)	Mn (%)	Ti (%)	Ba (ppm)
Transect M1 (0-1cm; n=3)														
MC 68	29.2	0-1 cm	**34.9**	**26.09**	39	0.42	**65.57**	17.88	1.78	14.75	3.59	0.16	**2.26**	314
MC 61	1537.9	0-1cm	0.75	24.04	**75.2**	0.6	57.73	**26.18**	1.3	14.77	5.25	0.24	0.49	369
MC 58	2386.4	0-1 cm	11.9	24.58	63.52	**0.75**	57.77	14.67	**2.63**	**21.11**	**8.66**	**2.7**	0.82	**777**
Transect M2(10-11cm; n=3)														
MC 68	29.2	10-11 cm	**79.98**	1.61	18.4	0.09	**75.36**	11.41	1.63	11.59	1.33	**0.11**	**0.83**	351
MC 61	1537.9	10 -11cm	0.24	26.87	**72.88**	0.48	63.88	**19.04**	**3.17**	13.88	**5.03**	0.08	0.47	397
MC 58	2386.4	10 -11 cm	0.52	**30.44**	69.04	**0.93**	57.14	14.67	2.25	**25.92**	4.52	0.04	0.4	**401**
Transect M3(20-21cm; n=2)														
MC 61	1537.9	20-21 cm	0.23	24.88	**74.88**	0.57	60.46	**22.51**	1.32	**15.69**	**4.4**	**0.1**	0.4	361
MC 58	2386.4	20- 21cm	**4.85**	**53.44**	41.71	**0.96**	**69.23**	12.58	**2.79**	15.38	4.27	0.06	**0.47**	**497**

Table 2: Sediment component, TOC, clay minerals and metals off Mahanadi

Krishna	Water depth (m)	Sub Sample	Sand (%)	Silt (%)	Clay (%)	TOC (%)	Illite (%)	Kaolinite (%)	Chlorite (%)	Smectite (%)	Fe (%)	Mn (%)	Ti (%)	Ba (ppm)
	Transect K1(0-1cm; n=3)													
MC 28	31.6	0-1 cm	**8.19**	**57.97**	33.84	0.48	**34.78**	13.17	1.31	50.72	**8.37**	**0.14**	**2.27**	**224**
MC 19	1463	0-1cm	0.35	37.25	62.40	**0.97**	24.87	**15.09**	**2.51**	57.51	5.93	0.08	0.71	218
MC 17	2574	0-1 cm	0.22	30.34	**69.44**	0.88	7.37	11.52	2.30	**78.80**	7.47	0.07	0.92	200
	Transect K2(10-11cm; n=3)													
MC 28	31.6	10-11 cm	**7.68**	**50.63**	41.68	0.68	15.38	18.47	1.92	**69.23**	**6.66**	**0.09**	**1.62**	144
MC 19	1463	10 - 11cm	0.29	26.42	**73.28**	**0.94**	**26.00**	8.55	2.44	63.00	5.96	0.02	0.98	212
MC 17	2574	10 – 11 cm	0.25	27.34	72.20	NA	17.3	**18.53**	**3.08**	61.08	6.58	0.05	0.79	**272**
	Transect K3(20-21cm; n=2)													
MC 19	1463	20-21 cm	**0.38**	**21.45**	78.16	**0.97**	**34.78**	13.17	1.31	50.72	**7.46**	**0.08**	**0.95**	217
MC 17	2574	20 – 21cm	0.22	20.34	**79.44**	0.82	17.88	**14.07**	**1.56**	**66.48**	6.16	0.02	0.73	**219**

Table 3: Sediment component, TOC, clay minerals and metals off Krishna, NA Not Analyzed

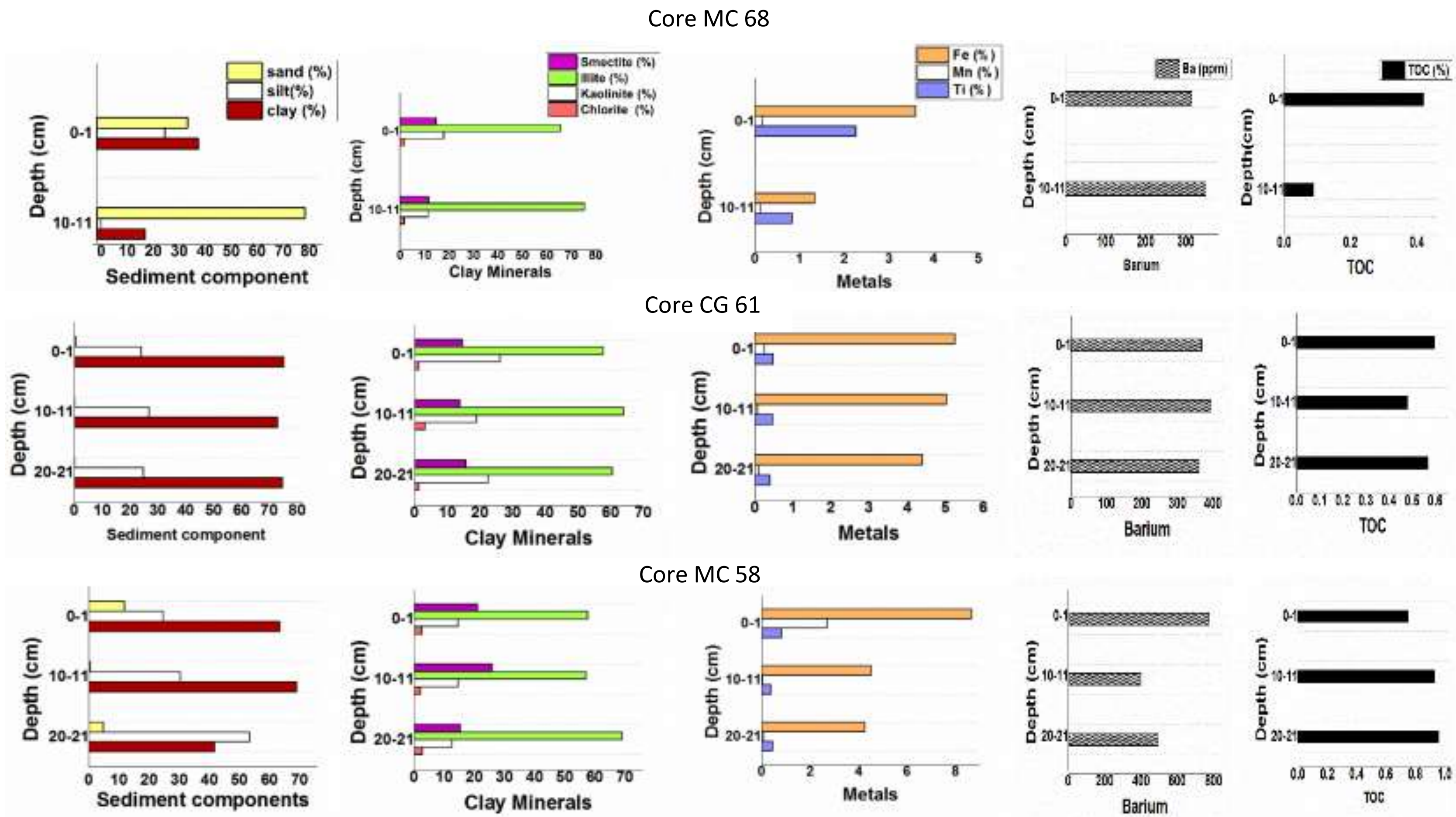
Core MC 68
sand (%)
silt(%)
clay (%)
Depth (cm)
Sediment component
Smectite (%)
Illite (%)
Kaolinite (%)
Chlorite (%)
Clay Minerals
Fe (%)
Mn (%)
Ti (%)
Metals
Ba (ppm)
Barium
TOC (%)
TOC
Core CG 61
Sediment component
Clay Minerals
Metals
Barium
TOC
Core MC 58
Sediment components
Clay Minerals
Metals
Barium
TOC

A

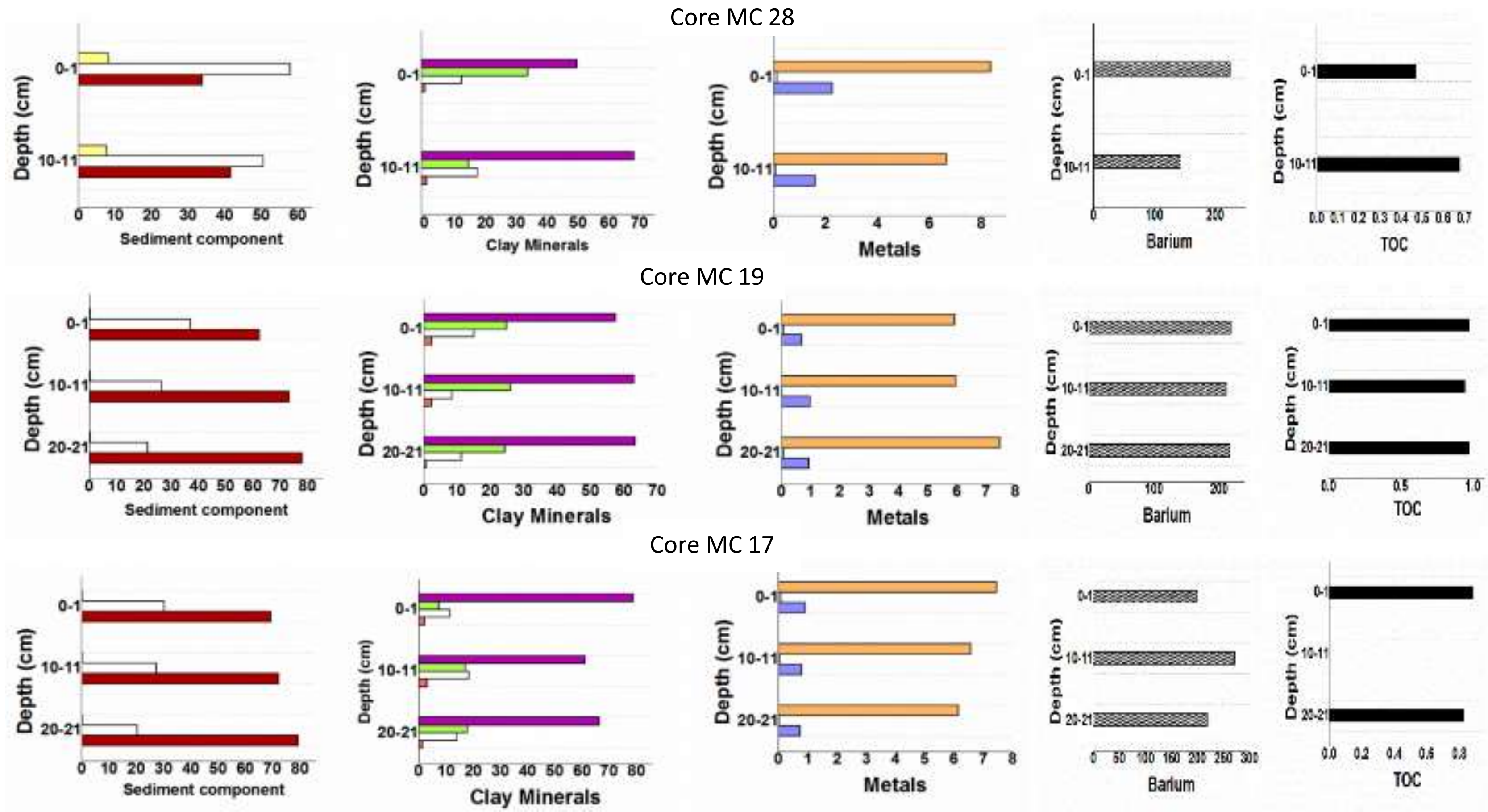

B

Fig. 2. Down core variation of sediment components, clay minerals and selected metals off Mahanadi (A) and Krishna (B) river mouths.

References

Babu, C.P., Brumsack, H.J., Schnetger, B. and Böttcher, M.E. (2002). Barium as a productivity proxy in continental margin sediments: a study from the eastern Arabian Sea. *Marine Geology*, *184* (3*)*,189-206.

Bejugam, P. and Nayak, G.N. (2017). Source and depositional processes of the surface sediments and their implications on productivity in recent past off Mahanadi to Pennar River mouths, western Bay of Bengal. *Palaeogeography, Palaeoclimatology, Palaeoecology*, *483*, 58-69.

Benshila, R., Durand, F., Masson, S., Bourdallé-Badie, R., de Boyer Montégut, C., Papa, F. and Madec, G. (2014). The upper Bay of Bengal salinity structure in a high-resolution model. *Ocean Modelling*, *74,* 36–52.

Beura, D. (2015). Floods in Mahanadi river, Odisha, India: its causes and management. *International Journal of Engineering and Applied Science*, *2* (2), 51-55.

Biscaye, P.E. (1965). Mineralogy and sedimentation of recent deep-sea clay in the Atlantic Ocean and adjacent seas and oceans. *Geological Society of America Bulletin*, *76* (7), 803-832.

Calvert, S.E. and Price, N.B. (1983). Geochemistry of Namibian shelf sediments. In: *Coastal Upwelling Its Sediment Record*, 337-375. Springer US.

Chakrapani, G.J. and Subramanian, V. (1990). Preliminary studies on the geochemistry of the Mahanadi river basin, India. *Chemical Geology,* 81, 241-253.

Chauhan, O.S. and Vogelsang, E. (2006). Climate induced changes in the circulation and dispersal patterns of the fluvial sources during late Quaternary in the middle Bengal Fan. *Journal of Earth system science*, *115* (3), 379-386.

Das, A. and Krishnaswami, S. (2007). Elemental geochemistry of river sediments from the Deccan Traps, India: implications to sources of elements and their mobility during basalt–water interaction. *Chemical Geology*, *242* (1), 232-254.

Das, A. and Panchal, M. (2018). Krishna River Basin. In: Singh D. (eds) *The Indian Rivers*, 339-351. Springer, Singapore, 339-351.

Diju, S. and Thamban, M. (2006). Clay mineral and textural variations in the sediments of Chandragiri River, estuary and shallow marine realms off Kasaragod, Kerala. *Journal of Geological Society of India*, *67*, 189-196.

Folk R.L. (1968). Petrology of Sedimentary rocks. Austin, Texas: Hemphill,177.

Hart, G. F. (1999). The deltas of peninsular India. *Journal of Asian Earth Sciences,* 39, 483-515.

Jackson, M.L. (1958). Soil chemical analysis. *Prentice-Hall, Inc. Englewood*

Cliffs, NJ, 45 -46. http://www.geol.lsu.edu/WDD/PUBLICATIONS/HartIndrpt00/india.html

Kolla, V. and Biscaye, P.E. (1973). Clay mineralogy and sedimentation in the eastern Indian Ocean. *Deep Sea Research, 20 (*8*)*, 727-738.

Kolla, V. and Rao, N.M. (1990). Sedimentary sources in the surface and near-surface sediments of the Bay of Bengal. *Geo-Marine Letters, 10* (3), 129-135.

Krishna, M. S., Naidu, S. A., Subbaiah, Ch. V., Sarma, V. V. S. S. and Reddy, N. P. C. (2013). Distribution and sources of organic matter in surface sediments of the eastern continental margin of India. *Journal of Geophysical Research: Biogeosciences*, 118, 1484–1494 doi:10.1002/2013JG002424, 2013.

Kulkarni, Y.R., Sangode, S.J., Bloemendal, J., Meshram, D.C. and Suresh, N. (2015). Mineral magnetic characterization of the Godavari River and western Bay of Bengal sediments: Implications to source to sink relations. *Journal of the Geological Society of India*, *85* (1), 71-78.

Levitus, S. and Boyer, T.P. (1994). World Ocean Atlas, volume 4, temperature (No. PB–95-270112/ XAB; NESDIS–4). National Environmental Satellite, Data, and Information Service, Washington, DC, United States.

Madhupratap, M., Prasanna Kumar, S., Bhattathiri, P.M.A., Kumar, M.D., Raghukumar, S., Nair, K.K.C. and Ramaiah, N. (1996). Mechanism of the biological response to winter cooling in the northeastern Arabian Sea. *Nature*, *384*, 549–552.

Madhupratap, M.M., Gauns, M., Ramaiah, N., Kumar, S.P., Muraleedharan, P.M., De, Sousa, S.N., Sardessai, S. and Muraleedharan, M. (2003). Biogeochemistry of the Bay of Bengal: physical, chemical and primary productivity characteristics of the central and western Bay of Bengal during summer monsoon 2001. *Deep-Sea Research*-II, *50*, 881–896.

Mallik, T.K. (1976). Shelf sediments of the Ganges delta with special emphasis on the mineralogy of the western part, Bay of Bengal, Indian Ocean. *Marine Geology*, *22* (1),1-32.

Mazumdar, A., Kocherla, M., Carvalho, M.A., Peketi, A., Joshi, R.K., Mahalaxmi, P., Joao, H.M. and Jisha, R. (2015). Geochemical characterization of the Krishna–Godavari and Mahanadi offshore basin (Bay of Bengal) sediments: a comparative study of provenance. *Marine and Petroleum Geology*, *60*, 18-33.

Meert, J.G., Pandit, M.K., Pradhan, V.R., Banks, J., Sirianni, R., Stroud, M. and Gifford, J. (2010). Precambrian crustal evolution of Peninsular India: A3.0

billion year odyssey. *Journal of Asian Earth Sciences, 39(6), 483-515*.

Muthuraj, S. and Jayaprakash, M. (2008). Distribution and enrichment of trace metals in marine sediments of Bay of Bengal, off Ennore, south-east coast of India. *Environmental Geology*, *56* (1), 207-217.

Nakagawa, M., Santosh, M., Yoshikura, S., Miura, M., Fukuda, T. and Harada, A. (2006). Kaolin deposits at Melthonnakkal and Pallipuram within Trivandrum block, southern India. *Gondwana Research*, *9*(4), 530-538.

Pattanayak, S.K. and Shrivastava, J.P. (1999). Petrography and major-oxide geochemistry of basalts from the Eastern Deccan Volcanic Province, India. *MEMOIRS-Geological Society of India*, *2*, 233-270.

Phillips, S.C., Johnson, J.E., Underwood, M.B., Guo, J., Giosan, L. and Rose, K. (2014). Long-timescale variation in bulk and clay mineral composition of Indian continental margin sediments in the Bay of Bengal, Arabian Sea, and Andaman Sea. *Marine and Petroleum Geology*, *58* (A), 117-138.

Pragatheeswaran, V., Loganathan, B., Ramesh, A. and Venugopalan, V.K. (1986). Distribution of heavy metals and organic carbon in sediments off Madras and Visakhapatnam. *Mahasagar*, *19* (1), 39-44.

Qasim, S.Z. (1977). Biological productivity of the Indian Ocean. *Indian Journal of Marine Sciences*, *6*, 122–137.

Raman, C.V., Rao, G.K., Reddy, K.S.N. and Ramesh, M.V. (1995). Clay mineral distributions in the continental shelf sediments between the Ganges mouths and Madras, east coast of India. *Continental Shelf Research*, *15* (14), 1773-1793.

Ramesh, R. and Subramanian, V. (1988). Temporal, spatial and size variation in the sediment transport in the Krishna River basin, India. *Journal of Hydrology*, *98 (*1-2*)*, 53-65.

Rao, A.T. and Raman, C.V. (1979). Clay input from the red sediments of Visakhapatnam Coast. *Indian Journal of Marine Sciences, 8,* 38 – 41.

Rao, M.S. (1960). Organic matter in marine sediments off east coast of India. *AAPG Bulletin*, *44 (*10*)*, 1705-1713.

Rao, N.V.N.D. and Rao, M.P. (1977). Clay mineral distribution in sediments of the eastern part of the Bay of Bengal. *Indian Journal of Marine Sciences*, *6 (*2*)*, 166-168.

Rao, V.P., Reddy, N.P. and Rao, C.M. (1988). Clay mineral distribution in the shelf sediments off the northern part of the east coast of India. *Continental Shelf Research*, *8* (2*)*, 145-151.

Saalim, S.M., Saraswat, R., Sukhorie, T. and Nigam, R. (2018). Assessing the ecological preferences of agglutinated benthic foraminiferal morphogroups from the western Bay of Bengal. *Deep Sea Research Part II: Topical Studies in Oceanography*, *161*, 38-51. https: DOI: 10.1016/j.dsr2.2018.02.002

Sarma, V.V.S.S. (2002). An evaluation of physical and bio-geochemical processes regulating perennial suboxic conditions in the water column of the Arabian Sea. *Global Biogeochemical Cycles, 16*, 1082.

Sen Gupta, R., De Sousa, S.N. and Joseph, T. (1977). On nitrogen and phosphorous in the western Bay of Bengal. *Indian Journal of Marine Science, 6,* 107–110.

Soman, K. and Machado, T. (1986). Origin and depositional environment of the china clay deposits of south Kerala. *Proceedings of the Indian Academy of Sciences-Earth and Planetary Sciences*, *95*(2), 285-292.

Taylor, S.R. (1964). Abundance of chemical elements in the continental crust: a new table. *Geochimica et Cosmochimica Acta, 28 (*8*),* 1273-1285.

Taylor, S.R. and McLennan, S.M. (1985). The continental crust: its composition and evolution. Blackwell Scientific Publications, Oxford.

Tripathy, G.R., Singh, S.K. and Ramaswamy, V. (2014). Major and trace element geochemistry of Bay of Bengal sediments: implications to provenances and their controlling factors. *Palaeogeography, Palaeoclimatology, Palaeoecology,* 397, 20–30.

Von Breymann, M.T., Emeis, K.C. and Camerlenghi, A. (1990). Geochemistry of sediments from the Peru upwelling area: Results from ODP Sites, 680, 682, 685 and 688. *Proceeding of ODP Science Results, 112*, 491-503.

Walkley, A. (1947). A critical examination of a rapid method for determining organic carbon in soils-Effect of variations in digestion conditions and of inorganic soil constituents. *Soil Science, 63* (4), 251-264

Weaver, C.E. (1989). Clays, muds, and shales. In: *Developments in sedimentology* Elsevier, 44.

Jour. Indian Association of Sedimentologists, Vol. 36, No. 1(2019), pp.84-100
ISSN Online 2582 – 2020
ISSN Print 0970 – 3268

Significance of Parting lineation in paleoslope studies: An example from fluvial Siwalik sandstones of Ramnagar-Kaladungi area, Nainital, Uttrakhand

Sarvesh Misra[1], Meenal Mishra[1] and Ram Chandra Tewari[2]
[1]School of Sciences, Indira Gandhi National Open University, Maidan Garhi, New Delhi-110068, sarveshmisra@geologist.com/meenalmishra@ignou.ac.in
[2]Geology Department, Sri. J. N. P. G. College Lucknow-22600 (Retired), ram.tewari9@gmail.com

Abstract: Parting lineation, a characteristic feature of many fine grained sandstone and siltstone, is widely used as additional parameter to deduce sediment transport direction especially where cross bedding and ripples marks are poorly developed. The Lower and Middle Siwalik Subgroups of Ramnagar-Kaladungi area exhibit paucity of cross-bedding, though parting lineation are well developed. A sum of 680 measurements of parting lineation from Lower (531) and Middle (149) Siwalik Sub group are statistically analyzed. Results suggest north-northeast – south-southwest line of sediment transport in the Lower and Middle Siwalik Subgroups of study area. The deduced line of sediment movement is in conformity with the southerly sediment transport obtained using cross-bedding data in this area and elsewhere in other parts of Siwalik foreland basin. These two-dimensional sedimentary structures may, therefore, provide additional support in deducing palaeoslope.

Keywords: Siwalik Group, Parting lineation, Palaeoslope, Ramnagar-Kaladungi.

Introduction

Primary sedimentary structures, characteristics of depositional sedimentary environments have long been used to interpret sediment dispersal pattern and hydrodynamics of fluvial system. Among these, the cross bedding and ripple marks are primarily used as directional structures (Potter and Pettijohn, 1977). Apart from hydrodynamic implications, the other sedimentary features as orientation of plant fossils (Tewari, 1998a), channel sandstone bodies (Tewari, 1998b), elongate imbricated clasts, and parting lineation are also useful in deciphering the line of sediment transport especially in areas where more reliable parameters are not so well recorded. Thus, these primary features of sedimentary rocks have been considered as additional tools in interpreting depositional conditions and sediment dispersal. Moreover, individual sedimentary structures depict flow direction at that geographic point and at that instant of time but for regional problems statistical treatment of populations of sedimentary structures is desired (Boggs, 1995).

The Middle Miocene-Pleistocene Siwalik sandstones of Ramnagar-Kaladungi area of Uttrakhand and elsewhere in neighboring parts of basin show less cross bedding structures and ripple marks (Tandon, 1991; Khan and Tewari, 2015), though these sandstones are characterized by abundant parting lineation. The purpose of present study is to analyze statistically

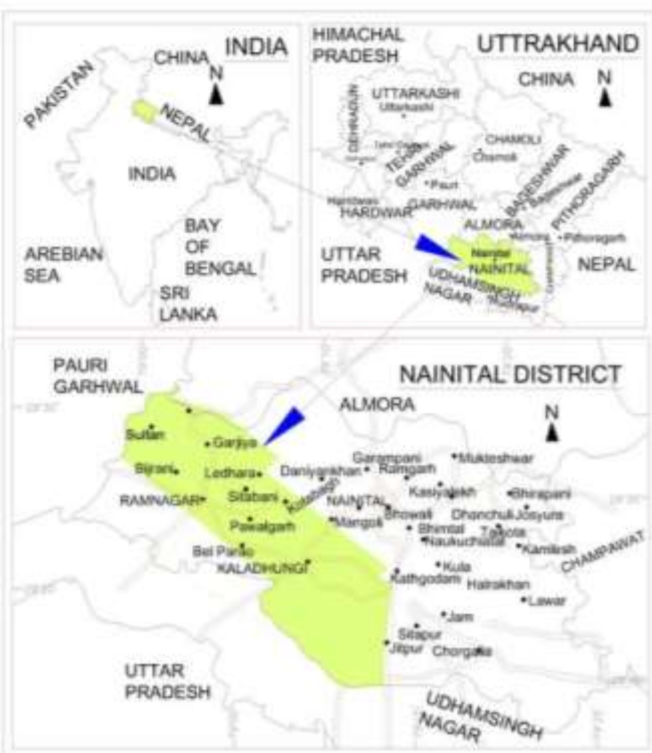

Fig.1: Location Map of the Ramnagar-Kaladungi . Area, Nainital, Uttrakhand

parting lineation with a view to decipher the line of sediment transport through space and time during Lower-Middle Siwalik sedimentation. The deduced mean is compared with the sediment transport direction obtained from less developed cross bedding data. Results are interpreted in terms of sediment transport and hydrodynamic conditions during Lower-Middle Siwalik sedimentation.

Geological and Tectonic setting

Siwalik basin extends for about 2500km along the tectonic strike from the Brahmputra River in the east to the Potwar plateau and Bannu plain in the west. On the basis of faunal assemblage Pilgrim (1910) subdivided Siwalik Group into three broad divisions in the Potwar region and parts of western Himalaya as Lower, Middle and Upper Siwalik Subgroups. This threefold classification has been extensively accepted, although irregular distribution of fossiliferous sections, rapid lateral lithofacies variation and discontinuity of strata are major constrains in this classification on regional scale. The basic and fundamental framework of Siwalik stratigraphy was laid down by pioneer efforts of Meddlicot (1864), Wynne (1878), Oldham (1893), Holland and Tipper (1913), Pilgrim (1913), Cotter (1933) and Lewis (1937). Early workers, considering three Subgroups, further classified the Siwalik Group into seven Formations as Kamlial, Chingi, Nagri, Dhok Pathan, Tatrot, Pinjore, and Boulder Conglomerate in ascending order largely on palaeontological basis (Pilgrim, 1913) with a very little lithological control. It is now well known for Siwalik Group that time boundaries often cut obliquely through litho-boundaries. The available vertebrate fossils are of very local extent and do not permit to establish a biostratigraphic subdivision of regional significance. The abandonment of chronostratigraphic terms is necessitated to eliminate the further confusions and complications of Siwalik Group of rocks as the fossiliferous horizons are separated by large intervals of un-fossiliferous strata and the different divisions of the Siwalik Group are distinguished purely on the basis of lithological characters. The Siwalik stratigraphy traditionally bears a tripartite classification in India, Lower, Middle and Upper in the rank of formations/subgroups (Auden, 1935; Pascoe, 1950; Itihara et. al., 1972; Kayastha, 1979; Yoshida and Arita, 1982; Tokuoka and Yoshida, 1984; Acharyya, 1976, 1994; Bashyal et. al., 1989; Mandal *et al.*, 2014), although their structural sequence, in general, evinces position-reshuffling between the formations because of post-depositional thrusts (Mitra *et al.*, 2010; Mandal *et al.* 2014 and references therein). Present workers have divided and discussed the Siwalik Group into three subgroups, viz., Lower, Middle and Upper Siwalik subgroups and their formations (Valdiya, 2010).

The study area is located between Ramnagar and Kathgodam, the two major townships of Nainital District, Uttrakhand and falls between the north latitude 29◦14’:19◦31’ and east longitude 79◦58’:79◦31’ in Survey of India toposheet No. 53 O/3 and O/7 covering about 800 square meter (Fig.1). The Ramnagar-Kaladungi area of Uttrakhand, northern India represents the eastern part of the Siwalik foreland basin. In general agreement to the regional stratigraphic setting, the Siwalik Group of the Ramanagar-Kaladungi area is, likewise, represented by Lower, Middle and Upper Siwalik subgroups with distinct lithological characters. These three subdivisions are well demarcated in the geological map of Ramnagar-Kaladungi area (Fig. 2). Local gradational contacts observed in upward transitions from the Lower to Middle and Middle to Upper Siwalik. Further subdivisions into Formations are not shown in the available geological map, perhaps due to structural complexity and lateral lithofacies variations. Therefore, the Siwalik Group of the study area is analyzed and discussed under the three broad divisions of Lower, Middle and Upper. The regional strike of Siwalik rocks is east-west and the dips are steep and highly variable from 30º to 82º direct towards NE.

Sedimentary Characters

Lower, Middle and Upper Subgroups represent about 1600m, 750m and 600m respectively. It is interesting to note that Siwalik sediments of the given area broadly represent coarsening upward succession from Lower through Middle up to Upper Siwalik Subgroup. The Lower and Middle Siwalik Subgroups are the subject matter of this study. The sedimentary characters of these subgroups as observed in the field are

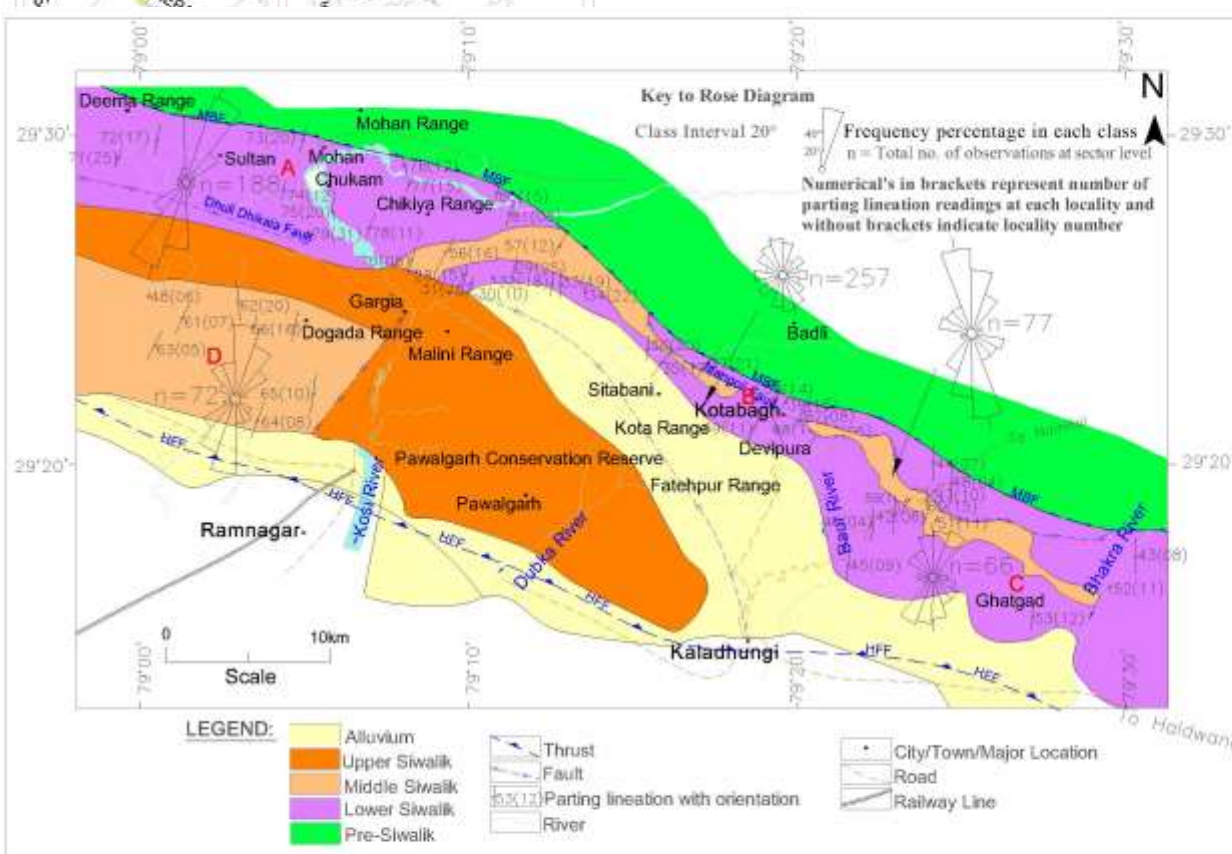

Fig. - 2 Geological map of Ramnager-Kaladungi area, District Nainital, Uttrakhand. Also shown the orientation of parting lineation at outcrop and sector level.

discussed here.

The Lower Siwalik Subgroup occurs all along southern boundary in the study area up to Kotabagh and is also exposed in the northwestern part of the area west of Kosi River (Fig. 2). The total thickness of Lower Siwalik in the east of Kathgodam is estimated up to 2000m (Karunakaran and Ranga Rao, 1979), though in the area under investigation only1800m thick Lower Siwalik sediments are recorded. In conformity with the other areas, the Lower Siwalik succession exposed here shows interbedded mudstone, siltstone, and fine grained sandstone. The lower most part of the Lower Siwalik is dominated by mudstone over sandstone where mudstone shares about 75%. The sandstones are tabular sheet like and multistory showing thin horizontal beds and occasional low angle planar cross beds. The ripple marks and parting lineations are well developed on bedding surfaces. On the average individual sandstone bodies are 0.5 to 3m thick and traceable along the strike for tens of meters. The multistoried sandstone bodies are up to 10m thick, where each body is separated by thin mudstone layer. Sandstones are highly indurated and often include concretions. The associated mudstones are on the average 0.5 to 2m, and rarely up to 3.5m. The mudstones are laminated as well as bioturbated. The upper part of the Lower Siwalik subgroup is marked by alternating beds of medium to coarse grained sandstone and variegated to dark grey mudstone. Sandstones are thicker than the mudstone beds and exhibit salt and pepper like appearance at places. The trough cross bedded to ripple cross-laminated, fine grained greenish grey sandstone interbedded with greenish grey to red purple mudstone with thin isolated lignite bands are rarely seen in the middle succession. Planer cross bedded fine to very fine grained greenish grey sandstone are also observed at the top of Lower Siwalik section close to the Main Boundary Thrust. Spheroidal weathering and bioturbation in greenish grey variegated to purple mudstone is not uncommon at places.

The Middle Siwalik Subgroup is exposed along the right bank of Kosi River towards north where it bends southwards, and to the north of Kotabagh as well as along the Kaladungi-Nainital road (Fig. 2), measuring about 120m and 760m in two stratigraphic sections. In general, there is an increase in the thickness of sandstone in the Middle Siwalik. These sandstones are medium to coarse grained and less indurated showing peculiar salt and pepper texture. The Middle Siwalik sandstones are more channel shaped and multistoried than sheet like, interbedded with thin grey to black mudstone. The lower unit of about 300m is thickly bedded**,** multistoried grey sandstone containing lenses of intervening mudstones. Thickness of sandstone bodies varies from 4 to 15m. Grey sandstone bodies are as thick as 35m and contain multiple, vertically stacked channel deposits separated by internal erosion surfaces. The lower contacts of sandstone bodies are generally erosive and nearly planar, and the upper contact grades into overlying mudstones. Calcrete, mud balls, mud pellets, and extrabasinal quartzite clasts overlie basal erosional surfaces of many sandstone bodies. Scour-and-fill, horizontal beds, large scale trough cross-bedding and low angle planar cross beds are commonly developed in medium to coarse grained sandstone beds, whereas ripple marks are seen in medium to fine grained sandstone. Among these, the scour and fill structure commonly occurs in the basal parts of sandstone overlain by pebble beds. Close examination of individual sandstone bodies reveal fining upward sequence with respect to grain size and thickness of cross bedding. Similar feature of Middle Siwalik sandstones is recorded elsewhere in other areas (Khan and Tewari, 2011, 2015). However, the overall succession of Middle Siwalik exhibits coarsening upward cycle as sandstone beds of the upper bodies are coarser than the lower throughout this area and in other parts of Siwalik basin (Bhardwaj, 1981; Misra, 1981). The sandstone bodies exhibit lateral facies variation at places and grades to mudstone. The interbedded grey to brown mudstones with spheroidal weathering and bioturbation at places are well exposed. The calcrete nodules, immature palaeosols are also observed in the massive brown to grey mudstone at places.

Fig.-3: Photograph of sandstone surface showing parting lineation in Lower Siwalik, near Kotabagh.

As stated above, the Siwalik sandstones do not show much cross bedding and ripple mark structures. In addition, parting lineation is well developed on many exposed surfaces of fine grained sandstone and siltstone of the Lower and Middle Siwalik (Fig. 3). They exhibit long narrow parallel to sub-parallel linear structures occurring generally in clusters. Individual lineation is 2-3 mm wide and extends to a few meters on a given outcrop. Due to fine to very fine grain size and low relief, it is sometimes difficult to measure accurate orientation. In view of their occurrences in fine grained rocks (Potter and Pettijohn, 1977), they are not recorded in the Upper Siwalik subgroup.

Analytical Methodology

In the present paper parting lineation (two dimensional linear structures) observed on the exposed bedding surfaces of fine grained Lower and Middle Siwalik sandstones are analyzed statistically. Sampling procedure for collecting two-dimensional orientation data is not guided by any pre-designed conventional plan apparently because of paucity of suitable structures and inaccessibility due to dense forest cover. Moreover, the data is collected largely along the road sides and the banks of rivers and their tributaries. Hence, all the accessible outcrops are taken into account and at least 4 to 6 measurements are recorded at each outcrop. The area under study is arbitrarily divided into sectors in such a manner that each sector contained a minimum of 40 measurements and includes at least 4 localities. The parting lineation orientation so collected in different parts of Ramnagar-Kaladungi area is 528 readings from the Lower and 149 from the Middle Siwalik, respectively. The Upper Siwalik subgroup is not included in the present study because of the paucity of parting lineation.

Parting lineation data was collected from 50 localities of fine grained sandstone and siltstone units as and where it is well preserved. In view of the steep dips of Siwalik rocks (35^o -75^o), the data so collected is corrected for tectonic tilt using Schmidt Stereographic net following the method outlined in Potter and Pettijhon (1977). The tilt corrected data is analyzed to deduce mean orientation, consistency ratio, variance and standard deviation following Currey (1956) and Potter and Pettijohn (1977). The orientation data is grouped at 20^o class intervals and analyzed at each outcrop, and also grouped into arbitrary sectors, and further separately for the Lower, and Middle Siwalik subgroups. Such hierarchical analysis at outcrop, sector and formation (sub-group) levels is the conventional method and provides detailed overview of dispersal patterns of sediments through space and time.

A popular practice for presenting directional data is the current rose or rose diagram, which is a histogram converted to a circular distribution. The parting lineation orientation data is therefore plotted as rose diagrams using 20° class interval as recommended to represent two-dimensional structures (Potter and Pettijohn, 1977). Each class shows relative percent frequency distribution of the data, where the modal class records maximum frequency of occurrences. When measurements of structures which show direction of movement are plotted, the rose diagram indicated the line of direction towards which the current flowed. Most distribution produces a single dominant mode (unimodal), although some have two or more sub equal modes (bimodal, polymodal).

Geological Interpretation

Lower Siwalik Subgroup:

The orientation of parting lineation in the Lower Siwalik varies from unimodal to polymodal distribution at locality level, however, the unimodal distribution is more common than bimodal or polymodal distribution. The orientation of parting lineation exhibit unimodal at sector level as well as Subgroup level with modal class confined to 0-20° class in A and C sectors and 40°-60° class in B sector. The modal class is 0-20° for pooled data at subgroup level. Computed mean orientation of parting lineation at 3 sectors of Lower Siwalik varies from 02º-19º to 182º-199º (Table-1). The corresponding consistency (L %) varies from 18% to 78% and variance from 470 to 2071, suggesting moderate consistency of depositing streams (Potter and Pettijohn, 1967; Selley, 1968)

Table-1: VECTOR (ϕv), VECTOR MAGNITUDE (l%), STANDARD DEVIATION (S) AND VARIANCE (S^2) OF PARTING LINEATION

SECTOR Locality	locality number	OUTCROP LEVEL n	ϕv	L%	SECTION LEVEL N	ϕv	L%	S0	S^2
MIDDLE SIWALIK									
D	48	6	10º	13					
	61	7	25º	84					
	62	20	175º	97	72	177º	51	53	1085
	63	5	28º	76					
	64	8	20º	93					

	65	10	8º	96					
	66	16	16º	77					
E	70	8	196º	68					
	56	16	30º	80					
	57	12	29º	72					
	58	5	35º	85	77	29º	48	36	1320
	59	10	32º	78					
	60	15	176º	68					
	51	11	15º	18					
<u>LOWER SIWALIK</u>									
A	71	25	18º	45					
	72	17	12º	80					
	73	20	15º	66					
	74	14	10º	48					
	75	20	170º	40					
	76	12	176º	60					
	77	15	23º	40	188	2º	18	46	2071
	78	11	19º	72					
	79	31	130º	22					
	80	15	15º	48					
	81	8	21º	63					
B	28	15	10º	48					
	29	25	15º	63					
	30	10	158º	16					
	31	28	10º	32					
	32	18	7º	57					
	33	19	178º	66					
	34	22	12º	39					
	35	17	14º	60					
	36	20	37º	90					
	37	21	37º	94					
	38	14	16º	35	257	19º	48	33	1099
	39	15	32º	65					
	67	8	28º	78					
	68	14	150º	18					
	69	11	27º	80					
C	44	7	12º	88					
	48	4	3º	94					
	47	13	45º	67					
	42	6	4º	97					

46	4	1°	83					
41	4	1°	46	66	2°	78	22	470
45	9	5°	76					
43	8	1°	88					
52	11	15°	18					
53	17	2°	65					

The above parameters of parting lineation evidently suggest north-northeast –

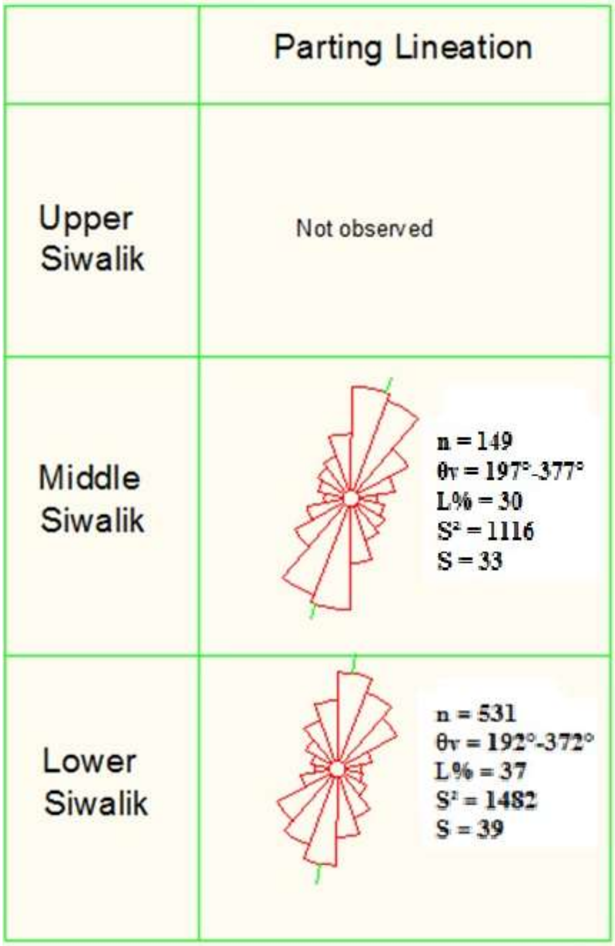

Fig. 4: Summary of sediment transport deduced from parting lineations in Lower and Middle Siwalik Subgroup, Ramnagar-Kaladungi area

south-southwest line of sediment transport during Lower Siwalik sedimentation in this area (Fig. 4).

Middle Siwalik Subgroup:

In contrast to the Lower Siwalik, the parting lineation is comparatively less abundant and confined to the lower part of the Middle Siwalik Subgroup. In the upper part of the succession the frequency of parting lineation is markedly decreased. The orientation of parting lineation exhibits unimodal distribution at locality as well as Subgroup level. The mean line of flow ranges between 10° -176° to 190°-356° (Table-1). The consistency ratio (L%) ranges from 13% to 97% at locality level showing scattering of parting lineation from between localities. At sector level it varies from 48% to 51% and at Subgroup level it is 30%, indicating the scattering decreases when data are lumped together. The variance ranges from 1010 to 1320 at sector level and at subgroup level it is 1116. Corresponding overall rose diagram of the Middle Siwalik Subgroup also showed that its line of transport is north-northeast-south-southwest (Fig. 4).

Palaeocurrent and Palaeoslope:

The Middle Miocene to Pleistocene Siwalik Group is largely fluvial deposited in front of rising Himalaya by a network of streams of variable sinuosity and discharge which flowed from north-northeast to south-southwest (Tandon, 1976, 1991, Singh, 1996, Khan and Tewari, 2015). A detailed statistical analysis of parting lineation in study area suggests that Siwalik sediments were largely transported along north-northeast-south-southwest in this area through space and time. The outcrop level analysis suggests variation in mean orientation of parting lineation from 01^o-178^o to 181^o-358^o with moderate consistency ratio. It implies north-northeast/north-northwest—south-southwest / south-southeast line of transport throughout the Lower Siwalik sedimentation of Ramnagar-Kaladungi area. The grouped data in the three sectors, likewise, indicate similar trend. The pooled data for the entire exposed Lower Siwalik Subgroup of Ramnagar-Kaladungi area further show similar north-northwest to south-southeast line of sediment transport (Fig. 4). The statistical parameters of parting lineation so computed are suggestive of moderately sinuous to meandering stream pattern of Lower Siwalik Rivers corroborating the regional depositional models of Lower Siwalik by early workers (Tandon, 1991; Khan and Tewari, 2011, 2015). Thus, the present analysis evidently shows that the Lower Siwalik Subgroup of given area was deposited by meandering streams which flowed consistently from north-northwest to south-southeast through space and time.

The succeeding Middle Siwalik, exhibit an increase in proportion of sandstone bodies over mudstone. The analysis of parting lineation indicates north-northeast-south-southwest line of transport in space and time at individual outcrops, sectors and subgroup levels; corresponding vector strength and variance are 48% to 51% and 1085 to 1320. These parameters together with increased amount of sandstone bodies characterize braided (bed load) stream pattern for the deposition of Middle Siwalik subgroup. Elsewhere in other areas, the Middle Siwalik succession has been interpreted as low sinuous stream deposits (Tandon, 1991).

Thus the analysis of parting lineation suggests that the Lower, and Middle Subgroups of Ramnagar Kaladungi area of Uttrakhand, were deposited along north-northeast-south-southwest flowing network of streams through space and time. Moreover, the computed statistical attributes together with the increase of sandstone over mudstone are features corroborate a progressive increase in paleoslope and corresponding decrease in the sinuosity of depositing streams from meandering to braided through time from Lower to Middle Siwalik. The north-northest-south-southwest line of transport of Siwalik sediments here deduced is in general agreement with the southerly directed palaeocurrents in different sectors of Siwalik sediments of India (Parkash et al., 1974; Agrawal and Singh, 1983; Kumar and Nanda, 1989; Kumar et al. 2004; Deopa and Goswami, 2014; Khan and Tewari, 2015) Pakistan (Visser and Johnsson, 1978; Tauxe and Opdyke, 1982; Ullah et al., 2009; Abbasi and Friend, 2000) and Nepal (Ulak, 2009, Nakayama and Ulak, 1999; Syangbo and Tamrakar, 2013; Tamrakar and Syangbo, 2014). The similarity and consistency of southerly palaeocurrent direction, transverse to Himalayan orogen, through Siwalik sedimentation through space (east-west) and time (Lower to Upper) is significant and suggestive of corresponding Himalayan uplifts from the Lower to Middle Siwalik sedimentation in this area.

Conclusions

The Lower and Middle Siwalik Subgroups of Ramnagar-Kaladungi of Uttrakhand are characterized by interbedded mudstones and sandstones. The sandstone interbeds increase in number and thickness through time from Lower to Middle Siwalik. These Siwalik sandstones do not show a fair amount of cross-bedding and ripple marks throughout the area, though parting lineation is widely developed on the exposed bedding surfaces of sandstones. These linear structures are therefore used to deduce the line of sediment transport through space and time in the given Siwalik sandstones, which is compared with the palaeocurrents deduced from locally developed cross-bedding data.

Computed mean orientation of parting lineation from pooled data from 36 outcrops of Lower Siwalik shows north-northeast-south-southwest line of sediment transport with moderate consistency of depositing streams. Likewise the mean orientation from 14 outcrops of Middle Siwalik, through time, exhibits more or less similar line of sediment transport (north-northeast-south-southwest) with greater consistency. The palaeocurrents based on locally developed cross bedding data in the given area suggests north-northeast to south-southwest palaeoflow in space and time. The closely comparable results of cross bedding orientation and parting lineation suggest that this linear structure should be used as an additional parameter in palaeoslope studies. It is further suggested that the plain bed transport producing parting lineation was the dominant mechanism of sediment dispersal during Lower and Middle Siwalik sedimentation.

Acknowledgements

One of the authors (SM) is grateful to faculty members of Geological Discipline, School of Sciences, Indira Gandhi National Open University for their constant encouragement. He is thankful to Shri Rangeet Kumar Srivastawa, Senior Manager (Civil), NHPC Limited who always remained helping in preparation of drawings. Thanks are also due to the anonymous reviewers of the JIAS for many useful suggestions.

References

Abbasi and Friend, 2000, Exotic conglomerates of the Neogene Siwalik succession and their implications for the tectonic and topographic evolution of the Western Himalaya. *Geological Society Special Publication*, *170*: 455-466.

Acharyya, S.K., 1976, On the nature of the Main Boundary Fault in Darjeeling sub-Himalaya, Geol. Surv. India, Misc. Publ. 24: 395-408.

Acharyya, S. K., 1994; The Cenozoic Foreland Basin and tectonics of the eastern sub-Himalaya: Problems and prospects; In: Siwalik Foreland Basin of Himalaya (eds) Kumar R, Ghosh, S. K. and Phadtare, N. R., Him. Geology 15, 3-51.

Agrawal S.C. and Singh, I. B., 1983, Palaeoenvironment and trace fossils of the Middle Siwalik sediments, Hardwar, Uttar Pradesh, Journ. palaeontological Society of India, Vol. 28, 50-55.

Auden, J. B., 1935, Traverses in the Himalayan, Records of Geological Survey of India, 62 (2): 123-167.

Bashyal, R. P., DelCaillau, B., Herail, G., 1989, Thrusting and orogenesis: The Himalayan Front in Central Nepal, Journal of Nepal Geological Society, 6: 11-20.

Bhardwaj, B. D., 1981, A coarsening upward cycle in the Siwalik sequence of Tista valley, eastern Himalaya: An example of fluvio-deltaic sedimentation, Journ. Indian Assocc. Sedimentologist, V-2: 68-77.

Boggs Sam jr., 1995, Principles of Sedimentology and Stratigraphy, Fourth Edition, Pearson Prentice Hall Pearson Education, Inc. Upper Saddle River:662p

Cotter, G DE. P., 1933, The geology of the part of Attok district. Rec. Geol. Surv. India V-55 (I): 63-161.

Currey, J. R., 1956 The analysis of two-dimensional orientation data, Journ. Geology; V. 64: 117-131

Deopa, T and Goswami, P. K., 2015; Channel morphology, hydrology and geomorphic positioning of a Middle Miocene river system of the Siwalik foreland basin, India, Geological Magazine, Volume 152(1): 12-27.

Holland, T. H. and Tipper, G. H., 1913, Indian Geological terminology Mem. Geol. Surv. India, V-43, pp. 1-12227Pilgrim, G. E. (1913): Correlation of the Siwalik with Mammal horizons of Europe. Rec. Geological Survey of India, 43: 264-326.

Idhara, M., Shibasaki, T., and Miyamoto, N., 1972, Photogeological survey of the Siwalik ranges and the Terai Plain, Sothern Nepal, Journal of Geosciences of Osaka University, 15: 77-98.

Karunakaran, C. and Ranga Rao, A.,1979, Status of exploration for hydrocarbons in the Himalayan region- contributions to stratigraphy and structure. Miscellaneous Publications of Geo; Survey of India 41,: 1-66.

Kayastha, N. B. 1979, Report on Geology of Kailali-Kanchanpur area, Far Western Nepal, Unpublished Report of Department of Mines and Geology, Kathmandu: 27p

Khan, Z. A. and Tewari, R. C., 2011, Paleochannel and paleohydrology of Middle Siwalik (Pliocene) fluvial system, Northern India. Journal of Earth Science, 120: 531-543

Khan, Z. A. and Tewari, R. C., 2015, Paleocurrents, paleohydraulics, and Paleogeography of Miocene-Pliocene Siwalik Foreland Basin of India. Advances in Geology, 2015: 1-14.

Kumar, R. and Ghosh, S. K., 1991, Sedimentological studies of the Upper Siwalik Boulder Conglomerate of Mohand area, District Saharanpur, U.P. Journal Himalayan Geology, 2: 169-176

Kumar, R. and Nanda, A. C., 1989, Sedimentology of Middle Siwalik subgroup of Mohand Area, Dehradun Valley, India, Journal Geological Society of India, 34: 597-616.

Kumar R., Sangode S. J., and Ghosh S. K. 2004, A multistory sandstone complex in the Himalayan foreland basin, NW Himalaya, India, Journal of Asian Earth Sciences, 23 (3): 407-426.

Lewis, G.E., 1937, New Siwalik correlation, American Journal Science, 34: 191-204.

Mandal S, Sarkar, S., Chakraborty N., Bose P.K., Liu M and Wang Y, 2014, Palaeogeography, palaeohydraulics and palaeoclimate of the Mio–Pliocene Siwalik Group, eastern India, Journal of Palaeogeography, 3 (3): 270-296**.**

Medllicot, H. B., 1864, On the Geological Structure and Relations of the Southern Portion of the Himalayan Ranges, between the Rivers Ganges and Ravee, Memoirs of the Geological Survey of India, III (2) .

Mitra, G., Bhattacharyya, K., Mukul, M., 2010. The Lesser Himalayan Duplex in Sikkim: Implications for variations in Himalayan shortening. Special Issue of Journal of Geological Society of India, 75: 289-301.

Misra, Sarvesh, 1981, Petrography and palaeocurrent trends in Jamrani area, District Nainital. U. P., Unpublished M. Phil Thesis, Aligarh Muslim University, Aligarh, 56p

Nakayama, K. and Ulak, P. D., 1999. Evolution of the fluvial style in the Siwalik Group in the foothills of Nepal Himalaya. Sedimentary. Geology, 125: 205–222.

Oldham, R. D., 1893, A manual of the geology of India- Strtigraphical and structural geology, Government of India publication.

Parkash, B.; Bajpai, I. P. and Saxena, H. P., 1974, Sedimentary structures and palaeocurrents of the Siwalik exposed between Yamuna and Gola rivers, U. P., Geological Magazine 111: 1-14.

Pascoe, E. D. 1950, A Manual of the Geology of India and Burma. Third edition, vol.i revised and largely re-written by the late Sir Edwin H. Pascoe, Government of India Publication. 438p

Pilgrim, G. E., 1910, Preliminary note on the revised classification of Tertiary freshwater deposits of India. Rec. of Geol. Serv. India 40, pp 185-205.

Pilgrim, G. E., 1913, The correlation of the Siwaliks with mammal horizons of Europe. *Rec. Geol. Surv. India* 43: 264–326.

Potter and Pettijohn, 1977, Palaeocurrents and Basin Analysis, 2nd ed. Springer, Berlin, Germany, 425p

Selley, Richard C., 1968, A classification of paleocurrent models, Journal Geology, 76: 99-110.

Singh, I. B. 1996, Geological evolution of Ganga plain-an overview, journal of Palaeontological Society of India, 23: 99-137.

Syangbo, D. K. and Tamrakar, N. K., 2013, Lithofacies and depositional environment of the Siwalik Group in Samari-Sukaura River area, Central Nepal, Bulletin of the Department of Geology, Tribhuvan University, 16 (2009): 53-64.

Tamrakar N. K. and Syangbo, D. K., 2014 Petrography and provenance of the Siwalik Group sanstones from the main boundary thrust region, Samiri river area, Central Nepal, Sub-Himalaya, Boletin de Geologia: 36 (2), 1-27.

Tandon, S. K., 1976, Siwalik sedimentation in a part of the Kumaun Himalaya, India Sedimentary Geology, 16: 131-154,

Tandon, S. K., 1991, The Himalayan Foreland: Focus on Siwalik Basin. In Sedimentary Basins of India: Tectonic Context (Eds. S; K; Tondon, C. C. Pant & S. M. Cashyap), Nainital: Gyanodaya Prakashan,: 177-201.

Tauxe and Opdyke, 1982, A time framework based on magnetostratigraphy for the Siwalik sediments of Khaur area, northern Pakistan, palaeogeographhy, palaeoclimatology, palaeoecology, 37: 43-61.

Tewari R. C., 1998 a, Plant fossil orientation in Early Permian Barakar Formation of eastern-central India Gondwana basins. The Palaeobotanists, 47: 32-36.

Tewari R. C., 1998 b, Channel sandstone bodies in fluvial Permian-Triassic Gondwana succession of peninsular India, Journal Geological Society of India, 51: 747-754.

Tokuoka, T. and Yoshida, M., 1984, Some characteristics of the Siwalik (Churia) Group in Chitwan Dun, Central Nepal, Journal of Nepal Geological Society, 4: 63-72.

Ulak, P D, 2009, Lithostratigraphy and late Cenozoic fluvial styles of Siwalik Group along Kankai River section, East Nepal Himalaya, Bulletin of the Department of Geology, Tribhuvan University Vol. 12, 2009, pp. 63-74

Ullah K, Arif M., and Shah M. T, 2009; Petrography of sandstones from Kamakial and Chinji Formations, south-western Kohat Plateau, NW Pakistan: Implications for source lithology and palaeoclimate, J. Him. Earth Sci. V-39, pp 1-13.

Valdiya, K. S., 2010, Making of India: Geodynamic Evaluation, McMillan, New Delhi,

Visser, C.F. & Johnson, G.D., 1978. Tectonic control of late Pliocene molasse sedimentation in a portion of the Jhelum reentrant, Pakistan. Son. Geol. Rund. Band 67. 15-87.

Wynne, A. B. (1878): Notes on the Tertiary zone and underlying rocks in the northwest Punjab, Rec. Geol. Surv. India., v-I(3), pp. 107-132.

Yoshida, M. and Arita, K., 1982, On the Siwaliks observed along some routes in Central Nepal, Journal of Nepal Geological Society, 2: 59-66.